Diversity Strategies for MIMO Communication Systems

Fan Zhang

Wadham College

A thesis submitted for the degree of Doctor of Philosophy at the University of Oxford

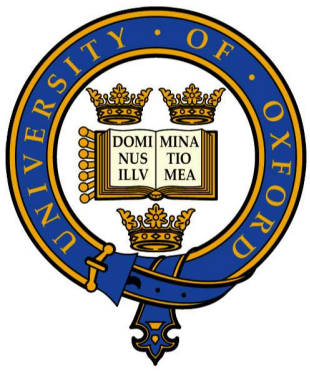

Department of Engineering Science

Parks Road, Oxford, OX1 3PJ

Michaelmas term 2009

Diversity Strategies for MIMO Communication Systems

Doctor of Philosophy Thesis, Michaelmas, 2009

Fan Zhang

The Dept. of Engineering Science and Wadham College

University of Oxford

Abstract

This thesis proposes a joint spatial diversity scheme in MIMO systems in order to improve the transmission reliability of the wireless links, thereby to extend the transmission range and increase the information throughput. Cyclic delay diversity (CDD) and antenna selection are employed here for their low complexity, high flexibility, no spectrum efficiency reduction and high compatibility with many existing standards. A bit error performance bound for CDD system with orthogonal frequency division multiplexing and convolutional coding in multipath Rayleigh fading channel is generated, which renders a fundamental understanding of the mechanism of CDD and can be used instructively for CDD system design. A transmit cyclic delay diversity and receive antenna selection (TCDD/RAS) system is proposed here to achieve a performance gain with lower additional complexity and no data rate reduction compared with a transmit orthogonal space-time block coding (OSTBC) system, which is combined with the optimum receive antenna selection scheme. A hybrid system with both OSTBC and CDD in the transmitter and antenna selection in the receiver is also derived to avoid the high complexity requirement and data rate degradation of the OSTBC system as well as the performance loss of the CDD system. A receive antenna selection criterion for the TCDD/RAS system based on the previous performance analysis results is defined, however it demands high computational complexity. Therefore a much simpler and faster selection rule, named maximum minimum post-processing SNR criterion, is generated for the TCDD/RAS system in flat fading channels and another maximum group minimum post-processing SNR selection principle is developed in frequency selective channels. Both of these two selection rules achieve higher diversity gains with lower additional complexity compared with the traditional norm and capacity selection rules. Two relay systems embedded with the TCDD/RAS scheme are also constructed: the MIMO relay system and the cooperative relay system. The joint diversity scheme in the MIMO relay system obtains a higher diversity gain than in the cooperative relay system. Moreover, these two relay systems could be combined to a system with multiple cooperative relay nodes on which multiple antennas are deployed depending on the practical requirement in the future wireless communication systems.

To my loving Parents

Acknowledgements

I am deeply grateful to my supervisor Professor David J. Edwards, for his guidance, support, encouragement and endless patience. As he said, just come to me when you are depressed with your work. I really appreciate the knowledge, more important the way of thinking and the attitude to research he taught me.

I would also like to thank Dr. Yangyang Zhang for his cooperation in my research and patient to correct my papers. The intellectual discussions with him bring me a lot of new ideas and passion for moving on. Special thanks to Dr. Wasim Q. Malik and Dr. Ben Allen. Dr. Wasim Q. Malik is like my co-supervisor when I newly arrived in Oxford. He is ready to help whenever I go to him. I would like to thank Dr. Ben Allen for his instructive talk about cyclic delay diversity and discussion about the practical issues and simulations problems.

Thank Dr. Nyembezi Nyirongo for introducing me Simulink and basic knowledge about OFDM. Thanks to Riqing Chen for his advice on industrial aspect. Thank Grahame Faulkner for his work solving all my computer problems. Thanks to Dr. Dominic O'brien, Dr. Steve Sheard, Lubin Zeng, Dr. Jingjing Liu, Dr. Tong Hao, Weiliang Wang, Yi Liu, Wei Peng, Dr. Zunnoor Tarique, Dr. Hammad Khan, Dr. Angela Amphawan and all my colleagues for their friendship and support.

Most important, I would like to thank my parents for their trust and support all the time. I could feel they are standing beside me even they are tens of thousands miles far away.

List of Publications

1. F. Zhang, Y. Zhang, W. Q. Malik, B. Allen and D. J. Edwards, "Optimum receive antenna selection for transmit cyclic delay diversity," *Commun., 2008. ICC '08. IEEE Int. Conf.*, pp. 3829 – 3833, May 2008.

2. F. Zhang, D. J. Edwards, Y. Zhang, C. Ji and K. K. Wong, "Low complexity joint spatial diversity scheme in MIMO systems," *ICN 2010: The Ninth International Conference on Networks*, in preparation.

3. F. Zhang, D. J. Edwards, Y. Zhang, C. Ji and K. K. Wong, "Transmit cyclic diversity and receive antenna selection system in frequency selective channels," *Transaction on Wireless Communications*, in preparation.

4. F. Zhang, D. J. Edwards, Y. Zhang, C. Ji and K. K. Wong, "Transmit diversity schemes combined with receive antenna selection in Rayleigh flat fading channels," *Transaction on Wireless Communications*, in preparation.

5. F. Zhang, D. J. Edwards, Y. Zhang, C. Ji and K. K. Wong, "Transmit cyclic delay diversity and receive antenna selection in relay systems," *Transaction on Wireless Communications*, in preparation.

6. R. Chen, F. Zhang and D. J. Edwards, "Cyclic delay diversity in KR orthogonal modulation system," *Transaction on Communications*, in preparation.

Acronyms

ACRONYM	Definition
ADSL	Asynchronous digital subscriber line
AF	Amplify-and-forward
AS	Antenna selection
AWGN	Additive white Gaussian noise
BER	Bit error rate
BPSK	Binary phase-shift keying
CDD	Cyclic delay diversity
CDMA	Code division multiple access
CP	Cyclic prefix
CSI	Channel state information
DAB	Digital audio broadcasting
DF	Decode-and-forward
DVB	Digital video broadcasting
DVB-T	Terrestrial digital video broadcasting
ECK	Exact channel knowledge
FEC	Forward error correction/forward error control
FFT	Fast Fourier transform
GI	Guard interval
ICI	Inter-carrier interference
IFFT	Inverse fast Fourier transform
ISI	Inter-symbol interference

MC-CDMA	Multi-carrier code division multiple access
MIMO	Multiple-input multiple-output
MGMP-SNR	Maximum group minimum post-processing SNR
MMP-SNR	Maximum minimum post-processing SNR
MQAM	M-ary quadrature amplitude modulation
MRC	Maximal ratio combining
OFDM	Orthogonal frequency division multiplexing
OSTBC	Orthogonal space-time block coding
pdf	Probability distribution function
PEP	Pairwise error probability
PDP	Power delay profile
PSK	Phase-shift keying
QAM	Quadrature amplitude modulation
SCK	Statistical channel knowledge
SER	Symbol error rate
SNR	Signal-to-noise ratio
TCDD/RAS	Transmit CDD and receive AS
TCDD-OSTBC/RAS	Transmit CDD combined with OSTBC and receive AS
TOSTBC/RAS	Transmit OSTBC and receive AS
UWB	Ultra wide band
WLAN	Wireless local area network
WMAN	Wireless metropolitan area network
WPAN	Wireless personal area network

List of Figures

List of Tables

Content

Chapter 1

Introduction

1.1 A Brief History of Wireless Communications

There are many early forms of wireless communications in the pre-industrial age, for instance smoke signals, signal flags and the signal flares mainly used in the military or the navigation areas, although the terminology ‘wireless’ had not been used at that time. Between 1861 and 1864, James Clerk Maxwell postulated the theory of electromagnetic waves [1]. This was verified by Heinrich Hertz in 1887. He demonstrated the existence of radio waves by generating a spark and receiving it several meters away, though without the awareness of the practical importance of it [2]. However the young Guglielmo Marconi took over his work and explored the commercial value of radio wave in wireless communications. Marconi made a great effort establish the first radio communication service in the world [3]. Since then, wireless communication had been regarded as synonymous with radio communication for a long time.

In the last century, wireless communications have experienced a flourishing period. In 1916, Reginald Fessenden made the first voice broadcast over North Atlantic. In 1921, shortwave radio, also known as high frequency (HF) radio, was developed, which made long distance wireless transmission available. In 1931, Edwin Armstrong introduced frequency modulation (FM), which has become very important for transmitting digital

signals. In 1946, the first mobile service connected to the public switched telephone network (PSTN) was launched in 25 cities in the United States. The number of subscribers to this mobile radio telephone service was limited because of the inefficient use of the radio spectrum. The introduction of the cellular system by AT&T Bell Laboratories largely solved this problem [4]. The cellular system divided a wide area into smaller cells. Therefore the signals could be transmitted within a cell with lower power. Two cells separated by a sufficient distance could share the same frequency band with little mutual interference, which rendered higher spectrum efficiency and thereby accommodated more users. In 1979, NTT DoCoMo in Japan deployed the first commercial cellular communication system. Analog telecommunications technologies in this time were referred to as the first-generation (1G) of wireless telephone technology. There were many 1G standards applied in different areas of the world, such as Nordic Mobile Telephone (NMT), used in Nordic countries, Switzerland, Netherlands, Eastern Europe and Russia, Advanced Mobile Phone System (AMPS) used in the United States and Australia, and Total Access Communications System (TACS) in the United Kingdom.

In 1982, the European Conference of Postal and Telecommunications Administrations (CEPT) decided to develop a new standard for a digital mobile telephone system that could be used across Europe. In 1989, the Groupe Special Mobile (GSM), also known as the Global System for Mobile communications, was defined as the European digital cellular standard based on a narrowband time division multiple access (TDMA) technology [5]. The first GSM service was available in 1991 by Radiolinja network in Finland with technical support from Ericsson, which indicated the start of the second-

generation wireless telephone technology (2G). The codecs for compressing and multiplexing digital signals in the 2G system rendered higher spectrum efficiency than previous systems [6]. Also the digital encryption of the conversations provided higher security. The ubiquitous standards allowed global roaming for the subscriber without changing the handset. Also data services, such as short message service (SMS) and email, were introduced to mobile devices. A GSM network is deployed in more than 200 countries and serves more than 3.9 billion users nowadays [7] [8]. 2G systems provide a data rate ranging from 9.6 kbit/s to 28.8 kbit/s.

The third-generation mobile telecommunication technology (3G), also named as the International Mobile Telecommunications-2000 (IMT-2000) was defined by the International Telecommunication Union (ITU) in 1999 [9] and also adopted by other standard bodies afterwards. There are several radio interfaces for IMT-2000. The most popular standards include EDGE (which is deployed worldwide), UMTS (which is deployed in Europe and Asia), CDMA2000 (which is deployed in the United States and Asia) as well as DECT (which is deployed in Europe, Asia, Australia and the United States) and WiMAX (which is used worldwide). 3G promised a much higher data rate than 2G systems, “a minimum speed of 2 Mbit/s for stationary or walking users, and 348 kbit/s in a moving vehicle” [10]. Based on high speed transmission, 3G systems are able to provide a variety of multimedia entertainment and infotainment services, including voice conversation, web browsing, video teleconference, sensing and file transferring with lower cost, lighter, smaller and cheaper mobile terminals. 3G also promised seamless global roaming due to its multiple mode-switched techniques [9].

Other wireless communication networks have emerged in the last decade. In 1993, the European Launching Group (ELG) renamed itself as the Digital Video Broadcasting (DVB) project in order to explore a commercial digital television broadcasting network for private users [11]. Among the DVB standard family, the DVB specification for satellite television (DVB-S) was released in 1994; the DVB specification for terrestrial broadcasting (DVB-T) was first broadcast in UK in 1997 [12]; the DVB specification for handheld devices (DVB-H) was ratified in 2004. DVB is used for delivering digital high definition television programs worldwide. The development of digital audio broadcasting (DAB) started even earlier in 1981 at the Institut für Rundfunktechnik (IRT). Currently there are more than 1000 stations broadcasting audio programs using DAB forms all over the world [11]. The original IEEE 802.11, also known as Wireless Fidelity (Wi-Fi) which carries out the wireless local area network (WLAN) computer communications was released in 1997 [13]. In 1999, a competitive technique, Bluetooth 1.0 (IEEE 802.15.1) was released for wireless personal area networks (WPAN) [14]. IEEE 802.16, a standard for wireless metropolitan area networks (WMAN), also called Worldwide Interoperability for Microwave Access (WiMAX) was created in 2001 [15].

1.2 Current Wireless Communication Techniques

Driven by the demand for high fidelity, high speed multimedia wireless communication services, fourth-generation (4G) wireless telecommunication, also defined as IMT Advanced as by the International Telecommunication Union, is currently being developed. The data rate of the fourth generation mobile communication system is elevated to a nominal data rate of 100 Mbit/s while the client physically moves at high

speeds relative to the base station, and 1 Gbit/s while the client and station are relatively stationary as defined by ITU-R [16]. 4G accommodates wireless communication applications in diverse networks such as cellular telephone systems, wireless broadband systems, as well as DVB and DAB networks. It has been developed to deliver high quality multimedia content among different all IP-based wireless components with seamless connectivity and global roaming across these heterogeneous networks [17] [18]. The Long Term Evolution (LTE) standard, which is proposed by the 3rd Generation Partnership Project (3GPP) organization, is an evolution from 3G to 4G. The LTE advanced standard is designed to fulfill the requirements of 4G [19].

Wireless communication by its nature is not as stable and predictable as wired communication systems. The signal suffers from reflection, diffraction, refraction, scattering, shadowing and attenuation while being transmitted through the wireless channel. This complicated process is named fading. Many techniques have been developed to mitigate these random fluctuations and guarantee a decent performance.

After the discrete Fourier transform (DFT) was introduced in multicarrier modulation by Weinstain and Ebert, orthogonal frequency division multiplexing (OFDM) became popular [20]. Nowadays OFDM has been used in many standards including ANSI ADSL standards, ANSI HDSL standards, the original ETSI DVB standards, ETSI DVB-T standards, ANSI VDSL and ETSI VDSL standards, Wi-Fi standards (IEEE 802.11a, g, n), WiMAX standards (IEEE802.16) and wireless personal area network (WPAN) standard (IEEE802.15.3a) [21]-[29].

Multiple-input and multiple-output technique (MIMO), which introduces multiple antennas to both the transmitter and receiver sides, is also attractive [1]. MIMO improves the data throughput and service coverage without sacrificing spectral efficiency or consuming additional transmit power. MIMO is proposed to be combined with 3G techniques and all proposed 4G systems may employ MIMO technology, which supports data rate up to 1 Gbit/s [30]. MIMO is also included in wireless broadband standards such as wireless metropolitan area networks (WMAN, also named WiMAX) standards 802.16e, 802.16m and wireless local area networks (WLAN, also named Wi-Fi) standard 802.11n [15], [31], [32]. The utilization of the MIMO system is divided into two groups: multiplexing (data-rate oriented) and diversity (reliability oriented). For the multiplexing technique, the Bell Laboratories Layered Space-time (BLAST) coding has been proposed, and achieves a spectral efficiency of 42 b/s/Hz compared to spectral efficiencies of 2-3 b/s/Hz in 2G cellular mobile services and current WLAN links [33] [34]. In this thesis, we will explore the diversity branch.

1.3 Diversity Strategies

The technique of obtaining variant versions of the same signal is called diversity [35]. As the wireless link is corrupted by fading, it appears randomly fluctuating and deviating, which makes the radio signal difficult to detect. Diversity schemes are proposed to combat fading and build a reliable communication system with guaranteed performance. As the fading effects exist in the time domain, the frequency domain and the space domain, diversity also can be obtained in these three domains. In this thesis, we are mainly concerned with spatial diversity in MIMO systems. However, diversity scheme in

one domain always renders selectivity in the other two domains as well. For instant, multipath diversity (refer to Chapter 2) utilizes multiple paths in space incurs frequency selectivity which can be exploited by the channel coding.

Equipped with the MIMO technique, many spatial diversity schemes have been derived, which can be deployed both in the transmitter side and the receiver side. There are three common spatial receive diversity techniques: selection diversity, equal gain combining and the well-known optimal SNR approach, maximal ratio combining (MRC) [36]. The maximal ratio combining scheme is designed to combine the received signals with optimum weighting factors which maximize the signal to noise ratio of the processed symbols. Although MRC attains a maximum SNR and hence a full diversity gain, it demands multiple radio frequency (RF) chains (including the low-noise amplifier, up/down converters, and digital-analog converters, etc.) equal to the number of the receive antennas, which cost a lot of space, power and money [1]. Equal gain combining has the same demand for RF chains. Limited by the power consumption, size and the cost of the mobile subscriber unit, the application of MIMO system should be as simple as possible. Thereafter, antenna selection can be utilized to eliminate unnecessary RF chains whilst obtaining the same diversity gain [37] [38]. The application of antenna selection in a MIMO system can be found in [39].

The idea of transmit diversity was originally investigated in [40] and [41] in 1993. The term of “space time coding” was first suggested in 1998, where a space-time trellis code (STTC) is introduced [42]. In the same year, the simple and popular Alamouti space-time

block code is constructed in [43]. The Alamouti scheme has been employed in 802.11n [32]. Subsequently, considerable work has been done in space-time code construction, among which quasi-orthogonal space-time block code (QSTBC) is an important branch [44]. Although the orthogonal space-time block coding (OSTBC) scheme obtains a full diversity gain, it requires the channel to stay constant for two consecutive symbol times or subcarriers. Moreover, OSTBC for complex signals suffers from a data rate reduction when the transmitter number is larger than two [35].

Cyclic delay diversity (CDD) was generated in 1993 to provide a diversity gain with much less complexity and more flexibility, however it suffers a performance degradation comparing to orthogonal space-time block coding [45] [46]. CDD can be employed in arbitrary number of antennas both at the transmitter side and the receiver side. In addition, it does not require any static channel condition and renders no data rate loss [47] [48] [49]. Moreover, cyclic delay diversity has high compatibility to many current wireless communication standards for broadcasting and broadband networks as well as mobile services, such as the DVB-T standards [12], the Wi-Fi standards (IEEE 802.11a, g, n) [13], the WiMAX standards (IEEE802.16) [15] and the wireless personal area network (WPAN) standard (IEEE802.15.3a) [29].

1.4 Transmit Cyclic Delay Diversity and Receive Antenna Selection System

Due to the high performance requirement of wireless links (a data rate of more than 100Mbps and a bit error rate (BER) of 10^{-8} or less [50]), systems with multiple diversity schemes are suggested both at the transmitter side and the receiver side [51] [52]. When channel state information (CSI) is available at the transmitter side, transmit antenna selection outperforms OSTBC (using all the transmit antennas) for a higher coding gain and the same diversity gain [53]. However, in some circumstances the CSI is absent at the transmitter, for instance, a base station with limited feedback from the handset. For these cases, the aforementioned transmit diversity schemes can be combined with receive diversity schemes to obtain higher transmission quality than systems with a single space diversity scheme.

There is a considerable amount of published research concerned with the performance analysis of orthogonal space-time coding with optimum antenna subset selection where antenna selection is executed at either the transmitter side or the receiver side [54], [55], [56], [57], [58], [59]. In [60], antenna selection combined with orthogonal space-time coding techniques was analyzed based both on exact channel knowledge (ECK) and on statistical channel knowledge (SCK). The antenna selection criterion for ECK is based on the instantaneous outage probability of the system, which achieves an equal diversity gain as if all of the antennas provided were employed. On the other hand, the antenna selection criterion for SCK is based on the average error probability of the system, which obtains a diversity order depending on the number of the selected antennas. Some papers

also reported on the investigation of the performance for antenna selection criteria from the perspective of average SNR gain, such as in [54], or the channel capacity, such as in [61]. From the results given in these papers, the norm selection criterion, which selects the antenna subset with the largest Frobenius norm of the MIMO channel matrix, achieves the optimum error probability performance for the antenna selection system combined with OSTBC.

In this thesis, a transmit cyclic delay diversity and receive antenna selection (TCDD/RAS) system will be proposed. This system combines two space diversity schemes, and it significantly improves the error probability performance of the system with low additional complexity and no spectrum efficiency reduction compared with the aforementioned antenna selection system combined with OSTBC. At the same time, as both CDD and antenna selection are applicable to various existing standards, the resulting system is also highly compatible with these standards.

An antenna selection criterion based on the error probability analysis is proposed for the TCDD/RAS system. However, this selection rule is highly computationally demanding. Another much simpler and faster antenna selection criterion, named maximum minimum post-processing signal to noise ratio (MMP-SNR) antenna selection criterion is derived for the TCDD/RAS system in a flat fading channel. For the frequency selective channel, a further new antenna selection rule named maximum group minimum post-processing signal to noise ratio (MGMP-SNR) criterion will be proposed here which offers lower complexity. In addition, in order to make the proposed system simple to be implemented,

a low complexity antenna selection algorithm is presented to supplant the exhaustive search.

From the numerical results based on Monte Carlo simulations, it is shown that the TCDD/RAS system with the MMP-SNR selection rule achieves a diversity order of 8 compared to a diversity order of 9 for the corresponding transmit orthogonal space-time block coding diversity scheme with optimum receiver antenna selection of the same number of antennas, but cyclic delay diversity has the advantages of much lower complexity, as well as higher spectral efficiency and compatibility to existing standards. The MGMP-SNR selection rule performs 3dB better than other traditional antenna selection rules and 2dB better than the principle based on the error probability bound at a bit error rate (BER) of 2×10^{-5} with lower computational complexity. The optimum selection parameter for the MGMP-SNR criterion is demonstrated to be irrespective to the channel coding but dependent on the numbers of the antennas.

1.5 Organization of the Thesis

This thesis continues as follows. Chapter 2 summarizes a variety of background literature that describes a fairly general MIMO-OFDM system model. The statistic characteristics of the multipath fading and operation mechanism of spatial diversity schemes are also presented as a basis for the system design in the following chapters. Chapter 3 presents the BER performance analysis of a cyclic delay diversity system with convolutional coding in a multipath Rayleigh fading channel which provides a mathematical basis for the antenna selection criterion design. In chapter 4 and 5, a MIMO system with cyclic

delay diversity on its transmitter and antenna selection on its receiver (TCDD/RAS) is derived. This system achieves a similar diversity gain as the transmit orthogonal space-time block coding and receive antenna selection system, but renders much lower complexity, no data rate reduction and higher compatibility to existing standards. A combined system with both CDD and OSTBC in the transmitter and antenna selection in the receiver is constructed to balance the complexity requirement of the OSTBC scheme and the performance degradation of CDD. A selection criterion based on the bit error rate analysis bound derived in Chapter 3 is generated which demands high computational complexity. A much less complex MMP-SNR antenna selection rule is generated to achieve the optimum BER performance for flat Rayleigh fading channels. While for the frequency selective channels, a MGMP rule is also proposed. In Chapter 6, the TCDD/RAS scheme is introduced to the relay systems. Cyclic delay diversity is applied in either a single relay station with multiple antennas or cooperative multiple relay nodes, with a single antenna on each node. Assuming a non-regenerative relay with no knowledge of the channel state information, antenna selection plays a more important role in the first system while cyclic delay diversity obtains larger diversity gain in the second. Finally, Chapter 7 summarizes the work and points to areas for future research.

References

[1] James Clerk Maxwell, “A Dynamical Theory of the Electromagnetic Field,” *Philosophical Transactions of the Royal Society of London*, pp. 459-512, 1865.

[2] Eugenii Katz, *Heinrich Rudolf Hertz*, Biographies of Famous Electrochemists and Physicists Contributed to Understanding of Electricity, Biosensors & Bioelectronics, http://chem.ch.huji.ac.il/history/hertz.htm, retrieved in Oct. 2009.

[3] Robert McHenry, "Guglielmo Marconi," in *Encyclopaedia Britannica*, 1993.

[4] Richard H. Frenkiel, *Cellular Radiotelephone System for Different Cell Sizes,* U.S. Patent 4,144,411, Bell Labs, Mar. 1979.

[5] "Brief History of GSM & GSMA," *GSM World*, http://www.gsmworld.com/about-us/history.htm, 2007.

[6] Thierry Turletti, *A brief Overview of the GSM Radio Interface*, Telemedia Networks and Systems Group, Laboratory for Computer Science, Massachussets Institute of Technology, Mar. 1996.

[7] "Two Billion GSM Customers Worldwide," *3G Americas*, Jun. 2006.

[8] "Global GSM and 3GSM Mobile Connections," *http://www.gsmworld.com*, Oct. 2009.

[9] C. Smith and D. Collins, *3G Wireless Networks*, 2nd Edition, McGraw-Hill, 2007.

[10] "Cellular Standards for the Third Generation," ITU, Dec. 2005.

[11] http://www.dvb.org.

[12] "Digital video broadcasting (DVB); Framing structure, channel coding and modulation for digital terrestrial television," European Telecommunications Standards Institute, ETS EN 300 744 v 1.1.2, Tech. Rep., 1997.

[13] IEEE802.11a, "Wireless LAN medium access control (MAC) and physical layer (PHY) specifications: high-speed physical layer in the 5 GHz band," Tech. Rep., Sep. 1999.

[14] "IEEE 802.15 WPAN Task Group 1a (TG1a)," ieee802.org, retrieved in Oct. 2009.

[15] H. Liu and G. Li, *OFDM-based broadband wireless networks*, Wiley-Interscience, 2005.

[16] Y. K. Kim and P. Ramjee, *4G Roadmap and Emerging Communication Technologies*, Artech House, 2006.

[17] S. Hussain, Z. Hamid and N. S. Khattak, "Mobility management challenges and issues in 4G heterogeneous networks," in *ACM Proceedings of the first international conference on Integrated internet ad hoc and sensor networks*, May. 2006.

[18] N. Schmitz, "The path to 4G will take many turns," *Wireless Systems Design*, Mar. 2005.

[19] E. Seidel, "Progress on 'LTE advanced'-the new 4G standard," white paper, Nomor Research GmbH, Munich, Germany, Jul. 2008.

[20] S. C. Draper, *Successive Structuring of Source Coding Algorithms for Data Fusion, Bu_ering, and Distribution in Networks*, PhD thesis, Massachusetts Institute of Technology, Cambridge, MA, Jun. 2002.

[21] M. Gastpar and M. Vetterli, "On the asymptotic capacity of Gaussian relay Networks", in *Proc. IEEE Int. Symp. Information Theory (ISIT)*, pp.195, Lausanne, Switzerland, Jul. 2002.

[22] M. Gastpar and M. Vetterli, "On the capacity of wireless networks: The relay case," in *Proc. IEEE INFOCOM*, New York, NY, Jun. 2002.

[23] A. J. Goldsmith and P. P. Varaiya, "Capacity of fading channels with channel side information," *IEEE Trans. Inform. Theory*, pp. 1986-1992, Nov. 1995.

[24] M. Grossglauser and D. N. C. Tse, "Mobility increases the capacity of ad-hoc wireless networks," *IEEE/ACM Trans. Networking*, pp.181, Mar. 2001.

[25] P. Gupta and P. R. Kumar, “The capacity of wireless networks,” *IEEE Trans. Inform. Theory*, pp. 388-404, Mar. 2000.

[26] Piyush Gupta and P.R. Kumar, “Towards and information theory of large networks: An achievable rate region,” in *Proc. IEEE Int. Symp. Information Theory (ISIT)*, pp.150, Washington DC, Jun. 2001.

[27] S. V. Hanly and D. N. C. Tse, “Multiaccess fading channels-Part II: Delaylimited capacities,” *IEEE Trans. Inform. Theory*, pp. 2816-2831, Nov. 1998.

[28] V. Hayes, *IEEE standard for wireless LAN medium access control (MAC) and physical layer (PHY) specifications*, 1997.

[29] A. Batra, J. Balakrishnan, A. Dabak, R. Gharpurey, P. Fontaine, J. Lin, J. M. Ho, and S. Lee, “Physical layer proposal for IEEE 802.15 task group 3a,” IEEE P802.15-03/142r2, May 2003.

[30] “The WINNER II Air Interface: Refined Spatial-Temporal Processing Solutions,” WINNER II, http://www.ist-winner.org/WINNER2-Deliverables/D3.4.1.pdf, Nov. 2006.

[31] C. B. Chae, K. Huang and T. Inoue, “MIMO technologies for WiMAX systems: present and future,” *WiMAX Evolution: Emerging Technologies and Applications*, Wiley, Jan. 2009.

[32] “802.11n: Next-Generation Wireless LAN Technology,” Broadcom white paper, Apr. 2006.

[33] V. Tarokh, N. Seshadri, and A. R. Calderbank, “Space–time codes for high data rate wireless communication: performance criterion and code construction,” *IEEE Trans. Inform. Theory*, vol. 44, no. 2, pp. 744-765, Mar. 1998.

[34] V. Tarokh, A. Naguib, N. Seshadri and A. R. Calderbank, “Space-time codes for high data rate wireless communication: Performance criteria in the presence of channel estimation errors, mobility, and multiple paths,” *IEEE Trans. Commun.*, vol. 47, no. 2, pp. 199-207, Feb. 1999.

[35] B. Vucetic and J. Yuan, *Space-Time Coding*, Wiley, 2003.

[36] D.G. Brennan, “Linear diversity combining techniques,” in *Proc. IRE*, vol.47, no.1, pp.1075–1102, Jun. 1959.

[37] S. Sanayei and A. Nosratinia, “Antenna selection in MIMO systems,” *IEEE Communications Magazine*, vol. 42, no. 10, pp. 68-73, 2004.

[38] M. A. Jensen and J. W. Wallace, “Antenna selection for MIMO systems based on information theoretic considerations,” *IEEE International Symposium on Antennas and Propagation: URSI North American Radio Science Meeting*, 2003.

[39] A. F. Molisch, *Antenna Selection for Multi-Input Multi-Output System*, patent, Mitsubishi Electric Research Laboratories, Inc., Cambridge, MA, US, 2005.

[40] N. Seshadri and J. H. Winters, “Two signaling schemes for improving the error performance of frequency-division-duplex (FDD) transmission systems using transmitter antenna diversity,” in *IEEE Veh. Tech. Conf. (VTC)*, pp. 508–511, 1993.

[41] A. Wittneben, “A new bandwidth efficient transmit antenna modulation diversity scheme for linear digital modulation,” in *IEEE Int. Conf. on Commun.*, pp. 1630–1634, 1993.

[42] R. Peterson R. E. Ziemer, *Introduction to Digital Communication*, Second edition, 2000.

[43] S. M. Alamouti. “A simple transmit diversity technique for wireless communications,” *IEEE J. on Select. Areas in Commun.*, Vol. 16, no. 8, pp. 1451–1458, Oct. 1998.

[44] A. Sezgin, *Space-time codes for MIMO systems: quasi-orthogonal design and concatenation*, PhD thesis, Fakultat IV-Elektrotechnick und Informatik der, Technischen Universitat Berlin, 2005.

[45] N. Seshadri and J. H. Winters, “Two signaling schemes for improving the error performance of frequency-division-duplex (FDD) transmission systems using transmitter antenna diversity,” *International Journal of Wireless Information Networks*, pp. 49–59, 1994.

[46] A.Wittneben, “A new bandwith efficient transmit antenna modulation diversity scheme for linear digital Modulation,” in *IEEE International Conference on Communications (ICC)*, pp. 1630–1633, May 1993.

[47] Kaiser A. Dammann, “Standard conformable antenna diversity techniques for OFDM and its application to DVB-T system,” in *Proc. IEEE Global Telecommun. Conf. (GLOBECOM 2001)*, San Antonio, USA, pp. 3100-3105, Nov. 2001.

[48] J. Tan and G. L. Stuber, “Multicarrier delay diversity modulation for MIMO systems,” *IEEE Trans. on Wireless Commun.*, pp. 1756–1763, 2004.

[49] F. Schuehlein, H. Haas, E. Costa, M. Bossert and A. Huebner, “On cyclic delay diversity in OFDM based transmission schemes,” technical report, by Department of Telecommunications and Applied Information Theory, University of Ulm, Nov. 2002.

[50] Andrea Goldsmith, *Wireless Communications*, Cambridge University Press, 2005.

[51] B. Badic, P. Fuxjaeger, and H. Weinrichter, “Performance of quasi-orthogonal space-time code with antenna selection”, *Electronics Letters*, pp. 1282–1284, 2004.

[52] C. Lee, *Antenna Selection for Space-Time Block Coded Systems with Imperfect Channel Knowledge*, PhD thesis, Queen’s University, 2006.

[53] Z. Chen, J. Yuan and B. Vucetic, “Analysis of transmit antenna selection/maximal-ratio combining in Rayleigh fading channels,” *IEEE Trans. Veh. Technol.*, vol. 54, no. 4, pp. 1312-1321, Jul. 2005.

[54] D. Gore and A. Paulraj, “Space-time block coding with optimal antenna selection,” in *Proc. Int. Conf. Acoustics, Speech, and Signal Processing*, vol.4, pp. 2441-2444, May 2001.

[55] W. Hamouda and A. Ghrayeb, “Performance of combined channel coding and space-time block coding with antenna selection,” in *Proc. IEEE Veh. Technol. Conf.*, vol. 2, pp. 623-627, May 2005.

[56] X. N. Zeng and A. Ghrayeb, “Performance bounds for combined channel coding and space-time block coding with receive antenna selection,” *IEEE Trans. Veh. Technol.*, vol. 55, no. 4, pp. 1441-1446, Jul. 2006.

[57] K. T. Phan and C. Tellambura, “Capacity analysis for transmit antenna selection using orthogonal space-time block codes,” *IEEE Commun. Let.*, vol. 11, no. 5, pp. 423-425, May 2007.

[58] S. Kaviani and C. Tellambura, “Closed-form BER analysis for antenna selection using orthogonal space-time block codes,” *IEEE Commun. Let.*, vol. 10, pp. 704-706, Oct. 2006.

[59] P. Lan, J. Liu, B. Gu and H. Xu, “A new antenna selection algorithm combined with beam space time block coding transmit scheme,” in *Proc. 8th Int. Conf. Sig. Proc.*, vol. 4, Nov. 2006.

[60] D. A. Gore and A. J. Paulraj, “MIMO antenna subset selection with space-time coding,” *IEEE Trans. Sig. Proc.*,vol. 50, no. 10, pp. 2580-2588, Oct. 2002.

[61] Z. Tang, H. Suzuki and I.B. Collings, “Performance of antenna selection for MIMO-OFDM systems based on measured indoor correlated frequency selective channels,” in *Proc. of the Australian Telecommunications Networks and Applications Conf. (ATNAC),* Melbourne, Australia, pp. 435-439, Dec. 2006.

Chapter 2

Diversity Schemes

2.1 Introduction

Owing to the dynamic and randomly fluctuating nature of wireless channels, when radio signal propagates through the channel, it experience deviation, distortion and attenuation which vary in time, space and frequency. This distortion effect is generally termed as fading. Fading makes it difficult to design a reliable system with guaranteed performance. Therefore, diversity technologies have been derived to combat fading and even make use of it to improve the system performance in terms of the bit error rate.

Diversity scheme is a technique which provides duplicate copies of the same signal in the time, frequency or space domain. As the probability that all of them suffer severe channel fading is much smaller than the probability that one copy suffers fading, the error detection probability is greatly reduced. Diversity schemes are especially important for orthogonal frequency division multiplexing (OFDM) systems which have poor inherent error performance. A well known diversity scheme, space time codes have been derived to eliminate wireless channel fading and improve the transmission reliability [1]. This scheme transmits multiple replicas of the original signal in space and time domain, which are orthogonal with each other and can be detected separately after combination and equalization in the receiver. One of the well known space time codes is the orthogonal space-time block coding (OSTBC) scheme [2] [3]. Another approach, cyclic delay

diversity (CDD) has been adopted, due to its low complexity and flexibility [4]. CDD generates cyclically shifted replicas of the original signal, which can be transferred to fluctuations of the channel transfer functions in the frequency domain by OFDM and utilized by channel error correction coding. The compatibility of CDD with many existing standards, such as the terrestrial digital video broadcasting (DVB-T) standards, wireless local area network (WLAN) standards and wireless metropolitan area (WMAN) standards as well as wireless personal area network (WPAN) standard makes CDD attractive. Antenna selection (AS) is another diversity scheme which selects the antenna subset with the best performance from a large group of antennas, in order to save radio frequency (RF) chains and significantly cut down on the system complexity [5].

In this chapter, the fading characteristics are introduced in Section 2.2. The multiple-input and multiple-output channel model is shown in Section 2.3. The concept of OFDM is presented in Section 2.4. Diversity schemes in time, frequency and space domains are introduced in Section 2.5. In Section 2.6, the features of a simple CDD system with OFDM are analyzed. In Section 2.7, antenna selection is presented in details. Section 2.8 concludes the chapter.

2.2 Channel Parameters and Signal Fading

The wireless communications channel is unstable and unpredictable. It can not be simply described as the ideal additive white Gaussian noise (AWGN) model, in which statistically independent Gaussian noise samples corrupt data samples free of inter symbol interference (ISI), which denotes the interference between the current symbol and

the previous symbols, and inter carrier interference (ICI), which denotes the interference between signals on different carriers. Therefore, channel fading has to be considered, which can be defined as the deviation, distortion and attenuation that a wireless transmitted signal experiences in certain propagation media.

There are two types of fading in wireless communications: large-scale fading and small-scale fading [1]. Large-scale fading occurs when signals are transmitted over large areas, and they can be shadowed, eclipsed or distorted by terrain factors such as hills, forests, buildings, *etc.* Solutions for large scale fading are addressed mostly at the system level (e.g., base station placement, power control). Small-scale fading represents the short-term fluctuations both in signal amplitude and phase that can take place as a result of small changes (as small as a half-wavelength) in the spatial positioning between a receiver and a transmitter. As this thesis focuses on diversity schemes in MIMO systems, small-scale fading is of more interest in this case.

Small-scale fading composes of three main dimensions: time-variance, frequency-variance and space-variance of the channel parameter. Time-variance of the channel can also be called Doppler spreading or time selectivity of the channel, which is caused by the relative movement between the transmitters and the receivers. Frequency-variance of the signals is caused by multipath fading, which is due to that the signals travel from the transmitter to the receiver over multiple propagation paths and experience differences in attenuation and distortion. Space-variance can be defined as the position of the

transmitter or receiver changes, the amplitude, phase and angle of the received signals change.

In this thesis, I will focus on small-scale fading channels and elaborate on the channel properties and their impacts on the system performance with different fading behaviours. The work will be generalized to MIMO channels, which are the basis for the diversity schemes introduced in the following chapters.

2.2.1 Channel Parameters

The channel impulse response (CIR) can be presented by $h_{n_r,n_t}(t,\tau)$ which is a function of time, delay as well as positions of the transmit and receive antennas. It can be regarded as the receive signal which is observed by the n_rth receive antenna at time t, when a unit impulse was transmitted τ time in advance from the n_tth transmit antenna.

Selectivity can be considered as diversity of which particular strategies can be applied to take advantage. For instance, a MIMO system with spatial selectivity provides frequency diversity. With proper combination and equalization schemes, the selectivity helps to improve the system performance. However, sometimes selectivity adds complexity to the system solution. For example, a fast fading channel whose CIR varies rapidly will place heavy demand for a system to response in a real time application.

Frequency Selectivity

In the multipath propagation environment, as stated previously, several versions of the original signal arrive at the receiver which cause time spreading and can make the observed channel coefficients frequency selective. In order to quantify the coherence bandwidth, the RMS delay (square root of the second central moment of the power delay profile of the channel transfer function), τ_{RMS} needs to be introduced [6]

$$\tau_{RMS} = \sqrt{\frac{\int_0^{\tau_{\max}} (\tau - \overline{\tau})^2 \psi_{De}(\tau) d\tau}{\int_0^{\tau_{\max}} \psi_{De}(\tau) d\tau}}, \tag{2.1}$$

where $\psi_{De}(\tau)$ is the power delay profile or spectrum (the average power of the channel output as a function of delay τ), $\tau_{\max}$ is the maximum path delay and $\overline{\tau}$ is the average delay spread given by [6]

$$\overline{\tau} = \frac{\int_0^{\tau_{\max}} \tau \psi_{De}(\tau) d\tau}{\int_0^{\tau_{\max}} \psi_{De}(\tau) d\tau}. \tag{2.2}$$

The coherence bandwidth is the frequency spacing between two subcarriers by which the amplitude of the correlation coefficient for the channel transfer functions reduces to a predetermined value. The coherence bandwidth, B_c, can be approximated by the inverse of the RMS delay [6]

$$B_c \approx \frac{1}{\tau_{RMS}}. \tag{2.3}$$

By comparing of the channel coherence bandwidth and the signal bandwidth, the definition of frequency selectivity is derived. A signal experiences flat or frequency-

nonselective fading when its bandwidth W is smaller than the channel coherence bandwidth, and frequency selective fading if W is equal to or larger than B_c.

Although the time dispersion is an intrinsic property of the channel, its effect varies on signals with different symbol periods. The relative time dispersion becomes more severe as the transmitted symbol period decreases, because a larger number of symbols will be influenced by the same delay spread time when the duration of each symbol decreases. Thereafter, to combat the time spreading, the signal bandwidth should be narrow enough and the symbol duration should be long enough. OFDM is conceived to reduce the symbol bandwidth and use separate uncorrelated narrow bands to carry the signals. Guard intervals are applied to avoid inter symbol interference (ISI) [7].

Time Selectivity

Time selectivity is caused by the phenomenon that the channel changes its propagation characteristics when the signal is in transmission. It is due to Doppler spreading or other frequency dispersion. For the estimation of the signal duration time when time selectivity is noticeable, the concept of coherence time should be introduced. Coherence time indicates the time separation T_c at which the amplitude of the correlation coefficient between two signals falls below a predesigned value.

By comparing the coherence time and the symbol duration, we can define three important terms, slow fading, fast fading and quasi-static channel. If the channel transfer function keeps constant over the whole transmission time, the signal undergoes slow or time-

nonselective fading in transmission. Whereas when symbol period is comparable with the coherence time, the channel transfer function changes within the period that a detection takes place, such as an interleaving depth or an OFDM frame, then it is characterized by fast fading or time-selective fading. Particularly, when the parameter of a channel is static within a block of symbol intervals, which is larger than the period over which one detection takes place, and changes independently from block to block, the channel can be called quasi-static [1] [8]. For instance, assume a 3G system with an interleaving depth of 20ms and a carrier frequency of 900MHz. Then a relative moving speed of 3m/h between the ends of the link generates a Doppler shift of $2.5x10^{-5}$Hz and therefore a channel coherence time of 400s [1]. In this case, the channel can be regarded as a slow fading channel. Whereas a relative moving speed of 3km/h (a walking speed) renders a channel coherence time of 400ms. In this case, the channel can be regarded as a quasi-static fading channel. For a vehicle speed of 300km/h (maglev speed), the channel coherence time is 4ms. In this case, the channel can be regards as a fast fading channel. This thesis is mainly concerned with quasi-static channels.

It should be noticed that since the time variance of the channel is determined by the coherence time (which is the inverse of the relative Doppler shift, but not the absolute Doppler spreading), the time selectivity is determined by two aspects of the system property. One is the relative movement speed between the transmitter and the receiver; the other is the system data rate. When the data rate is low and the mobile unit is moving rapidly, fast fading is generated. Meanwhile, in broadband transmission with a very high data rate, the time selectivity can be negligible.

Space Selectivity

Signals reflected from different scatterers experience different attenuation and delay, therefore the amplitudes and phases of received signals change as the antenna element locations vary. The coherence distance represents the minimum distance in which two antenna elements are separated such that the channel transfer function for each antenna is independent with the other. Space selectivity can also be regarded as angle dispersion. The extension of the fading is dependent on the channel condition as well as the symbol wavelength. Signals with higher frequencies are more sensitive to small distance changes than those of low frequencies.

2.2.2 Statistical Models for Multipath Fading Channels

As small-scale fading was briefly described in the previous section, here we will focus on the mathematical model of multipath fading channels. The characteristics of the received signal, which is a combination of the complex signals propagated through different paths, are very complicated in phase, amplitude and angle. Therefore, we introduce some statistical models to analyze the effects of the multipath channel.

If there is no line-of-sight (LOS) path between the transmitter and the receiver, and we consider the real and imaginary parts of the complex channel coefficient as independent zero-mean Gaussian processes, then the amplitude of the complex channel parameter can be modeled by Rayleigh distribution and its phase is uniformly distributed between 0 and 2π. The probability density function (pdf) of Rayleigh distribution can be written as [9]

$$f(\alpha)=\begin{cases}\dfrac{\alpha}{\sigma^2}e^{-\frac{\alpha^2}{2\sigma^2}}, & \alpha\geq 0\\ 0, & \alpha<0\end{cases}, \tag{2.4}$$

where the mean value of α is $E(\alpha)=\sqrt{\frac{\pi}{2}}\sigma$ and its average power is $E(\alpha^2)=2\sigma^2$.

In some cases, e.g. in rural areas, there exists a LOS path between the transmitter and the receiver. A Ricean distribution is suggested to describe this channel statistical pattern. Its probability density function is given by [9]

$$f(\alpha)=\begin{cases}\dfrac{\alpha}{\sigma^2}e^{-\frac{\alpha^2+A^2}{2\sigma^2}}I_0\left(\dfrac{A\alpha}{\sigma^2}\right), & \alpha\geq 0\\ 0, & \alpha<0\end{cases}, \tag{2.5}$$

where A is the peak amplitude of the dominant signal and $I_0(\bullet)$ is the zeroth first kind modified Bessel function. The Ricean channel is usually described using the K-factor [10]

$$K=\frac{\text{power in the main path}}{\text{power in the scattered paths}}=\frac{A^2}{2\sigma^2}. \tag{2.6}$$

Notice that when K= 0 the Ricean distribution turns to the Rayleigh distribution.

The Nakagami-m distribution is an alternative two-parameter statistical model for describing the amplitude of a complex channel response. This model encompasses Rayleigh fading as a special case and can approximate Ricean fading as well. In addition, it provides a best fit for urban channel fading. However, Rayleigh fading is more popular for its simplicity. The probability density function of Nakagami-m distribution is [11]

$$f(\alpha)=\begin{cases}\dfrac{2}{\Gamma(m)}\left(\dfrac{m}{2\sigma^2}\right)^m \alpha^{2m-1}e^{-\frac{m\alpha^2}{2\sigma^2}}, & \alpha\geq 0\\ 0, & \alpha<0\end{cases}, \tag{2.7}$$

where σ represents the power of the real and imaginary Gaussian components and the fading factor m is

$$m=\frac{\left(2\sigma^2\right)^2}{E\left(\left(\alpha^2-\sigma^2\right)^2\right)},\ m\geq\frac{1}{2}. \tag{2.8}$$

For more detailed generation of the statistical models of multipath fading channels, please refer to [1].

2.3 MIMO Channel

As the demand for transmission reliability and data rate grows, and the limitation of channel bandwidth and power as well as the size of the handheld unit exists, multiple antenna systems have appeared to provide the desired performance.

2.3.1 MIMO Channel Model

In a multiple-input multiple-output (MIMO) system, there are N_t transmit antennas and N_r receive antennas. The signals are transmitted simultaneously through $N_t \times N_r$ largely independent channels. The channel impulse response between the n_tth ($n_t = 1, 2, \cdots, N_t$) transmit antenna and the n_rth ($n_r = 1, 2, \cdots, N_r$) receive antenna is denoted as $h_{n_r, n_t}(t, \tau)$.

This impulse response is applied to a signal transmitted at time $t-\tau$ and received at time *t*. The MIMO channel transfer function matrix can be written as

$$H(\tau,t)=\begin{bmatrix} h_{1,1}(\tau,t) & h_{1,2}(\tau,t) & \cdots & h_{1,N_t}(\tau,t) \\ h_{2,1}(\tau,t) & h_{2,2}(\tau,t) & \cdots & h_{2,N_t}(\tau,t) \\ \vdots & \vdots & \ddots & \vdots \\ h_{N_r,1}(\tau,t) & h_{N_r,2}(\tau,t) & \cdots & h_{N_r,N_t}(\tau,t) \end{bmatrix}. \quad (2.9)$$

The row vector corresponds to the channel impulse responses at the n_rth receiver and the column vector corresponds to the channel parameters from the n_tth transmitter [12].

Combined with error correction coding, the multipath propagation, which was historically a penalty to the performance of the wireless systems, can be transformed into a diversity benefit for improving the signal quality. MIMO takes advantage of the variance of the channel parameters, referred to as fading in Section 2.2, to provide a diversity gain or use multiple channels to transmit different signal streams simultaneously in order to increase the data rate without extra cost of spectrum or power. These features meet the demand of the current wireless communication systems.

Therefore the aims of MIMO system can be divided to two categories: data rate maximization and diversity maximization. In the first scheme, spatial multiplexing technique is used to improve the channel capacity and therefore increase the data rate. The second approach is employed to minimize the outage probability and improve the signal reliability at a given transmission speed.

2.3.2 MIMO Channel Capacity

Shannon defined the channel capacity as the maximum asymptotical error-free transmission rate supported by the communication channel. In this section the capacity property of MIMO channels will be introduced briefly. Here we focus on the channel capacity of single user systems. More general cases for multiuser systems are included in [8] and [13].

The capacity of a single-input single-output (SISO) system is defined as [1]

$$C = \log_2\left(1+\rho|h|^2\right) \text{ b/s/Hz}, \tag{2.10}$$

where h denotes the complex gain of a fixed wireless channel, and ρ is the signal to noise ratio (SNR) observed by the receiver. The capacity of the MIMO channel with static fading is defined by [8]

$$C_{EP} = \log_2\left[\det(\mathrm{I}_{N_r} + \frac{\rho}{N_t}\mathrm{HH}^*)\right] \text{ b/s/Hz}, \tag{2.11}$$

where [•]* means transpose-conjugate, H is a $N_t \times N_r$ channel matrix, and the subscript EP is short for equal power, which means the transmit power is equally spreading over the N_t transmit antennas. The determinant operator $\det(\bullet)$, yields a product of the minimum (N_t, N_r) nonzero eigenvalues of the inner matrix. From (2.11) we can see that the total capacity can be a summation of the individual capacity per channel if proper weighting strategies are applied here.

Calculation of the capacity of various fading MIMO channels can be found in [12], and detailed derivation of performance analysis can be found in [8]. Information theory reveals the potential capacity gain which can be obtained through MIMO techniques. The outstanding features of MIMO make it attractive for current wireless communication systems. In addition, MIMO has already been employed in WiMAX [14], the third generation mobile communication system [15] and Wi-Fi [16].

2.4 Orthogonal Frequency Division Multiplexing

At high data rates, when the bandwidth of the channel is broad, the frequency selectivity distorts the data significantly. Therefore, a very complex receiver structure is needed with computationally extensive equalization and channel estimation algorithm to correctly eliminate the channel distortion and recover the originally transmitted data. With OFDM, we can simplify the equalization by turning a frequency selective channel to multiple flat fading subchannels, so that only simple on-tap equalizers are needed for channel estimation [7].

OFDM achieves a better spectral efficiency than conventional FDM systems. To make it easy to separate the signals at the receiver side, classical FDM inserts guard bands between subchannels, which result inefficient use of spectral resource [17]. The orthogonal nature of the OFDM scheme makes it possible to arrange the subcarriers in such a way that the side-bands of the individual carriers overlap and still the signals are received at the receiver without suffering by inter carrier interference (ICI) [18]. This

orthogonality is achieved by placing the peak signal power in one subband coincident with the zero-crossing points of all other subbands.

Zero-padding (ZP) and Cyclic Prefix (CP) are introduced to maintain the orthogonal characteristics of the transmitted signals and combat inter symbol interference (ISI) and inter carrier interference. The general idea of CP is to use a cyclic extension of OFDM symbols: a copy of the last part of an OFDM symbol is appended to front of the symbol [19]. CP is capable to keep the integrity of the delayed OFDM symbols to prevent ISI and ICI. Meanwhile, zero padding only transmits zeros during the guard interval which is added after an OFDM frame is finished [20]. With the overlap-add (OLA) technique [21], ZP is able to spread the delayed signal parts in the guard interval to the beginning of the OFDM frame in order to make the delayed signals have integral circles and avoid the ICI.

OFDM is highly sensitive to time and frequency synchronization errors, especially to frequency synchronization errors. Demodulation of an OFDM symbol with an offset in the frequency can lead to high bit error rate. In addition, OFDM has a higher peak to average power ratio (PAPR) comparing to the conventional single carrier system, which is proportional to the number of subcarriers used for an OFDM frame. Large PAPR makes the implementation of digital-to-analog converter (DAC) and analog-to-digital converter (ADC) extremely difficult. The design of the RF amplifier also becomes difficult as the PAPR increases.

2.5 Diversity Strategies

As explained in Section 2.3, channel fading leads to the variation and instability of the propagating signals, which may cause system performance degradation. However, this unstable feature of the signals is not necessarily detrimental. Under certain conditions, the varying characteristic can be taken advantage of and can help to detect the transmitted signals more accurately. For instance, if the channel has two paths and the signals transmitted from different paths experiencing independent fading, two copies of the desired signals arrive at the receiver. The probability that both of them are severely degraded is much lower than the case when at least one observation is available. Thus the probability of severe fading is reduced and better detection can be achieved. The technique of obtaining variant versions of the same signal is called diversity. Diversity is used to improve the signal reliability and can be combined with OFDM system which itself lacks inherent diversity.

There are several kinds of diversity schemes corresponding to different channel selectivity in different domains. In this thesis, we are mainly concerned with spatial diversity for MIMO systems. Nevertheless, time, frequency as well as the multipath diversity is introduced for completeness. In practical scenarios, we always combine several diversity schemes together which cooperate with each other and provide essential performance improvement.

2.5.1 Diversity in Different Domains

Space Diversity

The magnitude of the channel fading coefficient varies as a function of the antenna location. A number of independent fading processes exist when the space between two antenna elements is greater than the coherence distance. As space diversity can be obtained with multiple transmit antennas or receive antennas, it can be divided into two categories: transmitter diversity or receiver diversity. Transmitter spatial diversity will be illustrated in detail in the next section. Here we introduce some receiver diversity schemes.

There are three common receiver diversity techniques as stated in Section 1.3: selection diversity, equal gain combining and the well-known optimal SNR approach, maximal ratio combining (MRC) [22]. Antenna selection at the receiver side cuts down the number of the RF chains. However, it requires channel status information, which is usually unavailable in the mobile unites, to carry out the selection schemes. Limited by the size, power and complexity of the mobile units, these diversity schemes are almost exclusively implemented in the base stations. Therefore the transmit diversity schemes become absolutely attractive to current wireless communication research. Two typical transmit space diversity schemes, orthogonal space time block coding and cyclic delay diversity, will be introduced in the following sections.

Frequency Diversity

As described before, in a multipath channel, delay spread causes frequency selectivity. This selectivity can be explained by observing signals transmitted at the different carrier

frequencies experiencing different fading. Thus, diversity can be achieved by sending signals through uncorrelated fading channels on different frequencies. This diversity is termed frequency diversity.

Frequency diversity can be applied with a simple scheme, called frequency-hopping (FH). System using FH modulation periodically changes the carrier frequency of a single transmitter. Therefore, a block of symbols are transmitted during the first dwell time on a carrier frequency and on another carrier frequency during the next time interval. The frequency difference between adjacent symbols should be greater than the coherence bandwidth to produce sufficient selectivity. A more powerful means of exploiting frequency-hopping diversity is to employ forward error correction coding and interleaving so that encoded symbols are spread over multiple independent frequency dwells. Since signals are transmitted on different frequencies as well as in different time intervals, frequency hopping can also be referred to as a frequency-time diversity scheme.

There are also other frequency diversity strategies that are widely used. For instance, the space-frequency diversity, which will be introduced in the next section, is a combination of space diversity and frequency diversity.

Time Diversity

Recalling Section 2.4, time selectivity is caused by the movement of the mobile unit which leads to the channel instability in time. In a time diversity scheme, the samples should be spaced widely to make sure that the time separation of two copies of a sample

is larger than the coherence time of the wireless channel. The same as frequency diversity, channel coding and interleaving can be used to ensure that the adjacent signals are encoded and transmitted in time slots separated far enough so that independent fading takes place in each time slot.

Time diversity with powerful error correction coding and interleaving is already used in all second-generation cellular systems on both down link and up link [23]. However, as the span of the interleaver is fixed, the performance gain of time diversity is limited by the speed of the mobile. The system performance improves when the subscriber unit is moving in high speeds but with little gain when the unit is moving in a speed slower than a threshold at which the time space between two uncorrelated symbols is not small enough for the interleaver to take place.

Space-time coding will be introduced in the following subsection which is a combination of space diversity and time diversity and plays an important role in the future communication systems.

According to the performance analysis results generated in [8], the pairwise error probability upper bound for a space-time coding system in Rayleigh fading channels can be simplified to

$$P_e \approx G_c \gamma^{G_d} \tag{2.12}$$

when γ is large enough, where γ denotes the signal to noise power ratio. The exponent of γ, G_d is defined as the diversity gain of system with diversity schemes. Whereas G_c is

called the coding gain. These two terms will be used frequently in describing the numerical simulation results in the following chapters.

2.5.2 Spatial Diversity Schemes

Although this thesis is primarily concerned with cyclic delay diversity and antenna selection, several other diversity schemes are introduced here for comparison. Further investigation of these schemes can be found in [24], [25] and [26].

Delay Diversity

Delay diversity can be referred as a kind of frequency diversity as well, for it is indeed similar to the structure of a multipath channel [4]. In a delay diversity scheme, multiple copies of the signal are fed to the transmit antennas with different delays, or delayed in the receivers before combination. Figure 2.1 shows the system structures of the transmit delay diversity and the receive delay diversity.

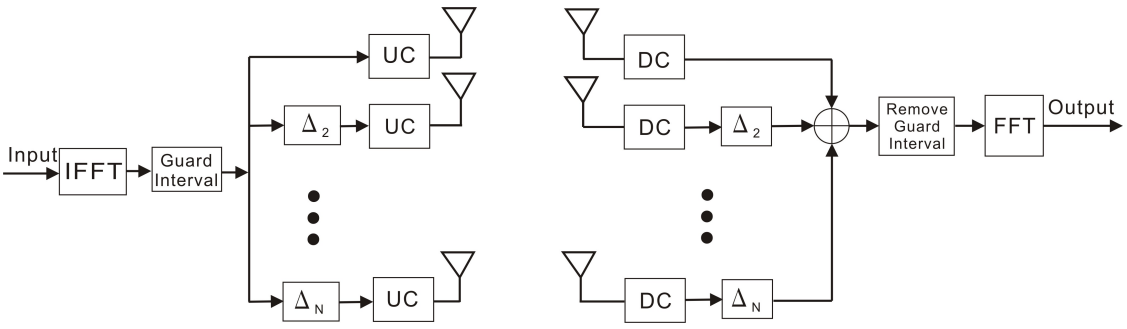

(a) Transmitter Delay Diversity Structure (b) Receiver Delay Diversity Structure

Figure 2.1 Delay diversity Structure

The delay time Δ_n has to fulfill the condition $\Delta_n \geq \frac{1}{B}$, where n $(n=1, \cdots, N-1)$ denotes the antenna index, B is the bandwidth of the transmitted signal. Equalization or rake

receiver should be used in the receiver to recover the overlapped signals. Delay diversity increases the total delay spread and therefore lengthens the guard interval.

Permutation Diversity

The system structure of permutation diversity is similar to the delay diversity. Here we replace the delay block in Figure 2.1 with a permutation block, which is a permutation matrix transforming the original signals to a different order [24]. The permutation block can also be regarded as an interleaver. This diversity strategy does not prolong the total delay spread therefore we do not have to increase the guard interval.

Cyclic Delay Diversity

Defining the permutation matrix as a form

$$P = \begin{pmatrix} 0 & I_m \\ I_{N-m} & 0 \end{pmatrix}, \tag{2.13}$$

which cyclically shifts the last *m* symbols to the front, we generate cyclic delay diversity. Cyclic delay diversity will be explained in detail in Section 2.5.

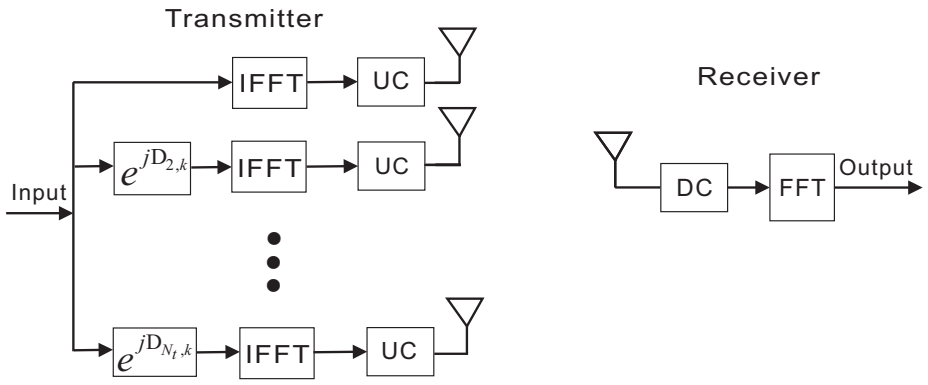

Figure 2.2 Phase diversity Structure

Phase Diversity

In a phase diversity scheme, the signals undergo phase shift $D_{n_t,k}$ on the n_t th transmit antenna and *k*th subcarrier before the OFDM modulation [24]. The block diagram is shown in Figure 2.2.

When the phase shift of each branch is constant during one OFDM symbol but appears time-variant over different OFDM symbols, the system obtains time diversity as well as the frequency and space diversity. This diversity technique can be called as time-variant phase diversity.

Polarization Diversity and Angle Diversity

Polarization diversity uses orthogonally polarized antennas to obtain largely independent fading channels [24]. This strategy is relatively low-cost and small-size that can be used in mobile units. In an angle diversity system, two or more antennas can be pointed in different directions at the receiver site to provide independent replicas of the original signals.

Orthogonal Space-Time Coding

It was in 1998 that the concept of space-time coding was first introduced by Tarokh, Jafarkhani and Calderbank in their pioneering work [2]. The object of space-time diversity coding is to extract the total available spatial diversity in the MIMO channel through appropriate construction of the transmit space-time codewords.

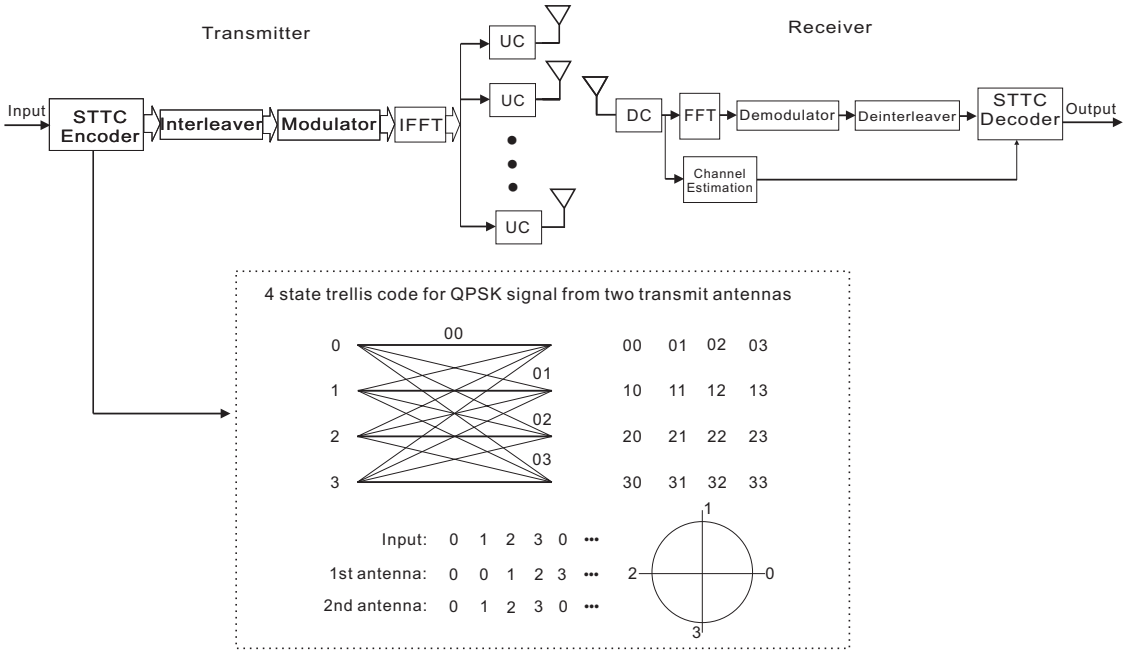

Figure 2.3 A single receiver STTC system

Space-time trellis code (STTC) uses convolutional codes to achieve diversity spreading in temporal and spatial dimensions [2] [3]. STTC combines the functions of error control coding and the diversity scheme, hence achieves maximum diversity gain as well as a high coding gain. But the complexity of the decoder increases exponentially when the numbers of transmit antennas and trellis states become larger. Figure 2.3 shows the structure of a single receiver STTC system.

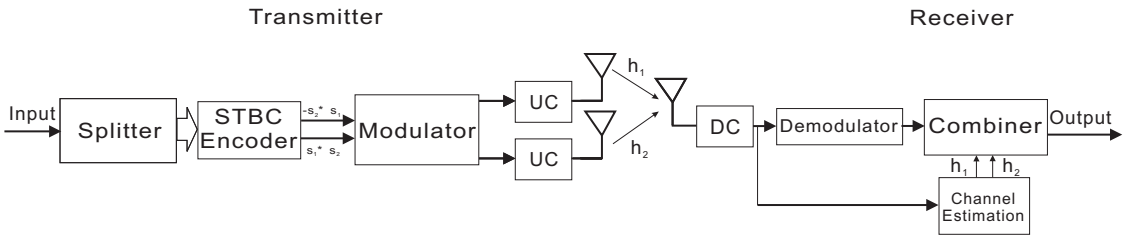

Figure 2.4 A simple Alamouti schemes with one receiver

The Alamouti scheme is a well known orthogonal space-time block code with two transmitters [27]. As shown in Figure 2.4, the information data is divided into two blocks

of symbols. In the first time slot, signal s_1 and s_2 are transmitted simultaneously on separate antennas. In the next time slot, the signals $-s_2^*$ and s_1^* are transmitted. Since we assume that perfect CSI is available in the receiver, a linear combining of received signals weighted by the fading gains is employed. This simple block coding scheme achieves a full diversity gain and renders no loss of the spectrum efficiency. However the orthogonal design of space-time block codes for complex signals suffers a data rate loss when the transmit antenna number is larger than two.

In practical communication systems, two or more different diversity techniques are always employed together, using certain combining schemes, e.g., selection combining or switched combining, to obtain the required performance.

2.6 Cyclic Delay Diversity

In this section the cyclic delay diversity (CDD) scheme will be elaborated from system construction to performance analysis. Numerical results of the CDD system performance are presented compared with the space-time block coding scheme.

2.6.1 CDD fundamentals

Cyclic delay diversity was proposed to provide spatial diversity for multicarrier based transmissions without increasing the decoding complexity. CDD can be referred as a kind of space-time coding. In CDD schemes, normally the signal is transmitted off the first antenna with no delay, while over the second or each additional antenna the signals are

cyclically shifted. According to the location of the diversity scheme, there are two kinds of cyclic delay diversity structures: transmit CDD and receive CDD.

- Transmit CDD

Figure 2.5 shows the block diagram of a communication system with CDD deployed in *M* transmit antennas. The signal bits are modulated after being coded by a forward error control/correction (FEC) block. Then the signals are OFDM modulated, split and transferred to the CDD block where the signal frames for each antenna are cyclically shifted with a specific fractional delay time. Here $\delta_l \ \left(l = 1, \ \cdots, \ N_t - 1\right)$ denotes the cyclic shift for the *l*th antenna. Normally signal on the first antenna is transmitted without additional cyclic shift. After that, an additional cyclic prefix acting as the guard interval is inserted. Then the signals are ready for DA (digital to analog conversion) and UC (up conversion, conversion of signals from base band into RF-band) and transmission from the antennas. At the receiver side, DC (down conversion) and AD (analog to digital conversion) are employed and an OFDM decoder is implemented in reverse.

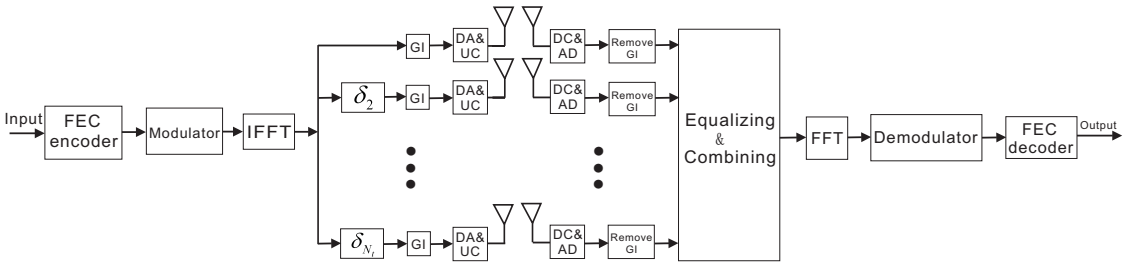

Figure 2.5 Transmit cyclic delay diversity system structure

CDD incorporated with OFDM system can be referred to as a kind of phase diversity (PD). The signal on the first antenna can be denoted as

$$s_1(t) = \frac{1}{\sqrt{N_s}} \sum_{k=0}^{N_s-1} S(k) e^{j\frac{2\pi}{N_s}kt}, \tag{2.14}$$

where N_s, t, k, $s_1(t)$ and $S(k)$ stand for the length of FFT in OFDM, discrete time, the subcarrier index of OFDM, the complex-valued signals in time domain and frequency domain respectively at time t, and frequency k ($k = 1, \cdots, N_s - 1$). While the signal transmitted in another additional antenna is shown as the following format:

$$s_2(t) = \frac{1}{\sqrt{N_s}} \sum_{k=0}^{N_s-1} e^{-j\frac{2\pi}{N_s}k\delta_2} \cdot S(k) \cdot e^{j\frac{2\pi}{N_s}kt}, \tag{2.15}$$

Here δ_2 stands for a cyclic time shift. Theoretically, δ_2 can be any integer, but due to the nature that $(\delta_l + k \cdot N_s) \bmod N_s = \delta_l$ and then $e^{j\frac{2\pi}{N_s}(\delta_2 + k \cdot N_s)} = e^{j\frac{2\pi}{N_s}\delta_2}$, the range of δ_2 can reasonably be constricted to $\delta_2 = 0, \cdots, N_s - 1$.

CDD does not add to the length of cyclic prefix (guard interval) for the reason that it is done within the OFDM symbol duration and does not increase the overall channel delay spread in the sense of ISI occurrence. Therefore CDD keeps the system spectrum efficiency. But it increases the channel delay spread within an OFDM symbol time. Like delay diversity, it adds echoes to the original signal which will cause an increment of frequency selectivity and reduction of the coherence bandwidth of the channel. Examined from the receiver in a transmit CDD system, the cyclically shifted signal streams can be viewed as delayed reflections of the original signal and contribute to the overall channel transfer function:

$$H_{equ,n_r}(k,n) = \frac{1}{\sqrt{N_s}} \sum_{n_t=0}^{N_t-1} e^{-j\frac{2\pi}{N_s}k\delta_{n_t}} H_{n_t,n_r}(k,n). \tag{2.16}$$

Here $H_{equ,n_r}(k,n)$ denotes the equalized channel transfer function at the n_r th receiver and δ_{n_t} stands for cyclic delay time at the n_t th transmitter ($\delta_0 = 0$), *k* denotes the *k*th subcarrier and *n* denotes the *n*th OFDM frame. The increase of the channel frequency selectivity cooperating with channel coding contributes to a diversity gain and improves the bit error rate performance.

As the signal streams transmitted from different antennas are partially correlated and not orthogonal, CDD can not achieve the maximum diversity gain. However, CDD does not impose any additional combination structure at the receiver side than the single antenna system. This feature significantly reduces the receiver complexity compared with orthogonal space-time coding systems. In addition, CDD can be deployed for any arbitrary number of antennas, while the orthogonal space time block codes can only be used in several special numbers of antennas. Moreover, when the transmit antenna number is larger than two, the orthogonal space time block coding for complex signals induces a data rate loss. Last but not least, CDD has good compatibility to many existing standards, such as the terrestrial digital video broadcasting (DVB-T) standards, the wireless local area network (WLAN, also known as Wi-Fi) standards (802.11a, g, n), the wireless personal area network (WPAN) standard (802.15.3a) and the wireless metropolitan area network (WMAN, also known as WiMAX) standards (802.16).

In order to obtain any diversity effects, *i.e.* to get constructive and destructive interference within the OFDM signal bandwidth *B*, the delay δ_{n_t} has to fulfill

$$\delta_{n_t} \geq \frac{1}{B \cdot T_s},\ n_t = 1,\ \cdots,\ N_t - 1, \tag{2.17}$$

where T_s denotes the sampling time of the OFDM time domain signal.

- Receive CDD

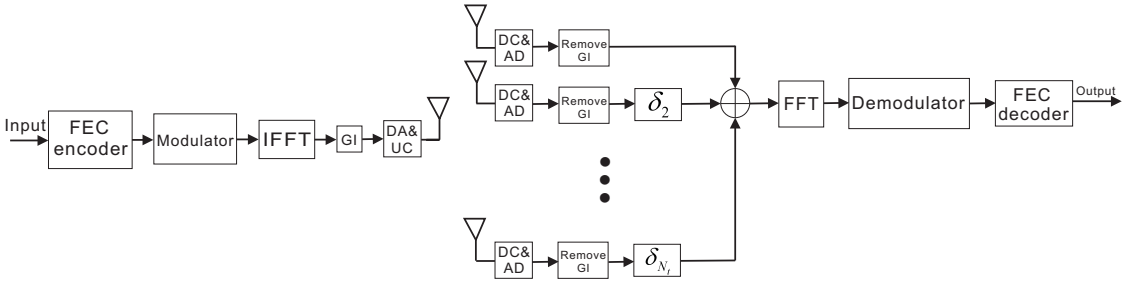

Figure 2.6 Receive cyclic delay diversity system structure

Due to its linearity, CDD can also be implemented at the receiver side [4]. Figure 2.6 shows the structure of a communication system with CDD in the receiver incorporated with OFDM. After DC, the guard interval is removed from the received signal arrays, and then resulting signals are cyclically shifted at δ_{n_r}, $n_r = 1,\ \cdots,\ N_r$ on the n_rth antenna. After that, the signals are summed and demodulated by the FFT transformer. Because of the exact equivalence, all properties of transmit CDD mentioned above are valid for the receive CDD as well.

2.6.2 System Models and Simulation Results

The CDD system combined with OFDM is shown in Figure 2.7, which employs QPSK modulation, ½ rate convolutional coding and interleaving. Perfect channel estimation is assumed here to simplify the simulation. Each block has been tested individually and then assembled together. The simulations results of this system were compared with numerical

results presented in [28] and [29], and found to be identical. This indicates the simulation is operating correctly.

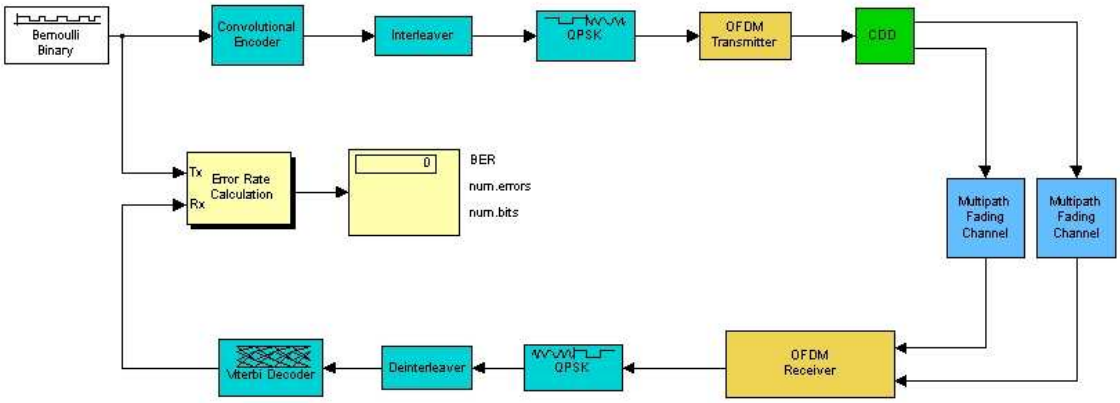

Figure 2.7 CDD system structure

Figure 2.8 shows the channel spectra of a flat Rayleigh fading channel before CDD is implemented and the equalized channel after CDD is utilized. It is clear that the flat fading channel is transformed to a frequency selective channel. Figure 2.9 illustrates how CDD changes the error distribution in the time-frequency-plane. A black spot represents an OFDM symbol error. The number of carriers is N_s = 128 and the cyclic delay on the second antenna is δ = 33. From Figure 2.9, it can be seen that not the total number of errors changes but the error distribution changes when CDD is applied. The error points, which occurred within one OFDM frame before CDD was added, have been largely separated and distributed over different OFDM frames. By virtue of this feature, channel error correction code can take advantage of the dispersed error distribution and obtain a diversity gain.

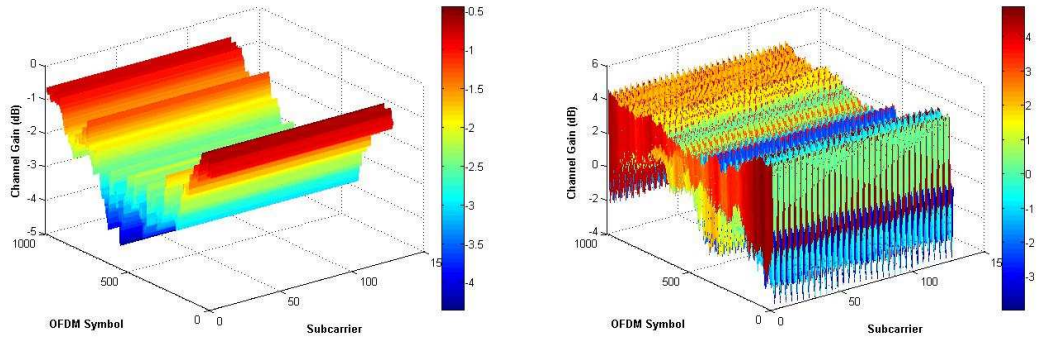

(a) Flat Fading Channel Spectrum (b) Equalized CDD Channel Spectrum

Figure 2.8 Simulated channel spectrum comparison between a flat fading channel and the equalized channel in a 4 transmitter CDD system

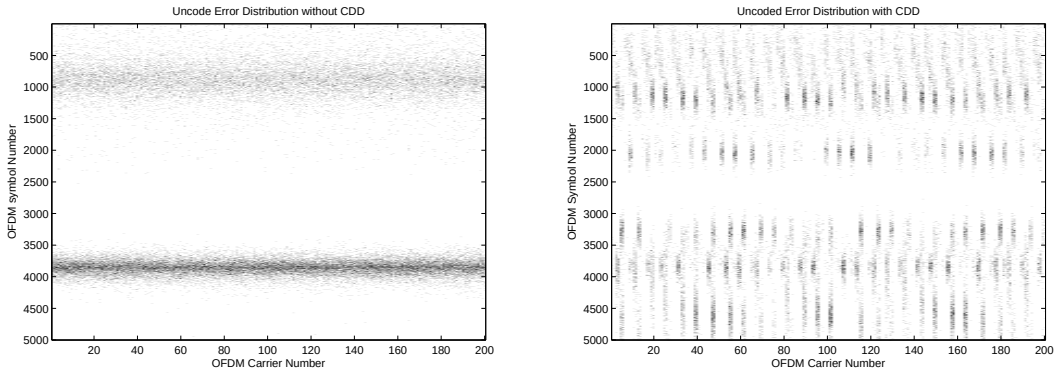

(a) Uncoded error distribution without CDD (b) Uncoded error distribution with CDD

Figure 2.9 Simulated comparison of error distribution between an uncoded single antenna system and an uncoded CDD system

Figure 2.10 shows a performance comparison between a coded CDD system and an uncoded CDD system. It is observed that without the error correction coding, CDD could not change the error performance of the system. But after combined with the error correction coding, CDD achieves the same diversity gain as an orthogonal space time block coding scheme.

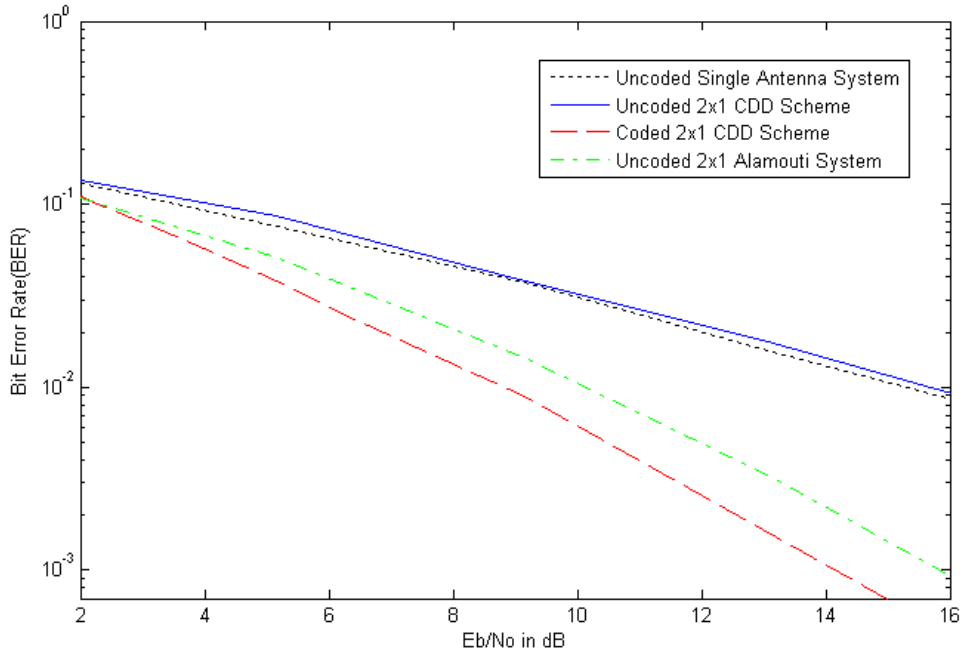

Figure 2.10 Simulated comparison of uncoded and coded CDD systems, a uncoded Alamouti system and a single antenna system

2.7 Antenna Selection

In a MIMO system, it is widely known that the capacity is linearly proportional to the minimum number of the transmit antennas and the receive antennas [13]. However, the complexity of the MIMO system is increasing along with the capacity, and thus the cost is increasing, too. Comparatively, the additional antenna elements and the baseband digital processing units are not expensive. Whereas, the RF chains (including the low-noise amplifier, up/down converters, and digital-analog converters, etc.) are more costly. Normally a MIMO system with N_t transmit antennas and N_r receive antennas requires N_t complete RF chains at the transmitter side, and N_r RF chains at the receiver side

respectively. To reduce this complexity, antenna selection (AS, or a so-called hybrid-selection schemes) is introduced [30]. Antenna selection schemes usually choose L antennas of the best performance, from a cluster of N (N_t at the transmitter and N_r at the receiver) antennas. This scheme reduces the number of the RF chains and consequently saves the cost. If the multiple antennas are used for diversity purpose, the antenna selection scheme can be called as "hybrid selection/maximum-ratio-combining" (H-S/MRC) [31], [32], [33]; if they are used for the purpose of spatial multiplexing, the approach can be referred as "hybrid selection/MIMO" (H-S/MIMO) [34], [35]. In my present research, only the first case is considered.

2.7.1 Antenna Selection Models

Antenna selection can be allocated in the transmitter or the receiver, or both of them. Figure 2.11 shows the block diagrams of these three kinds of antenna selection schemes. Antenna selection located in the transmitter requires feedback of channel knowledge from the receiver, which may lead to inefficiency when the feedback length is limited in some communication circumstances.

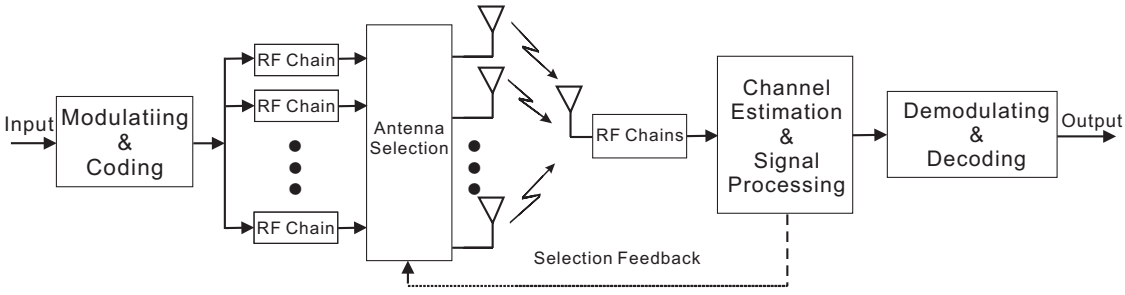

(a) Transmitter antenna selection structure

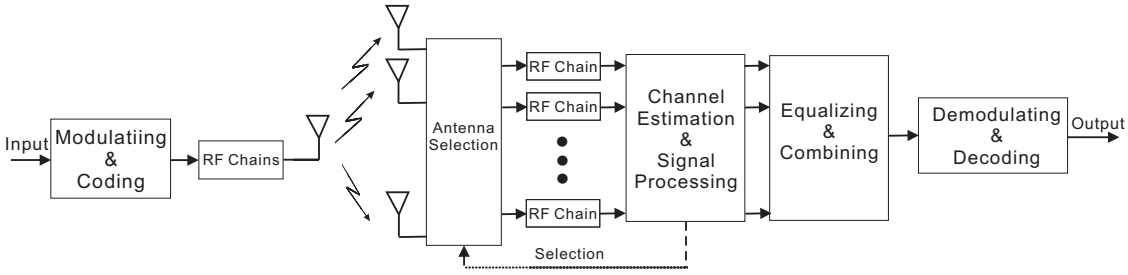

(b) Receiver antenna selection structure

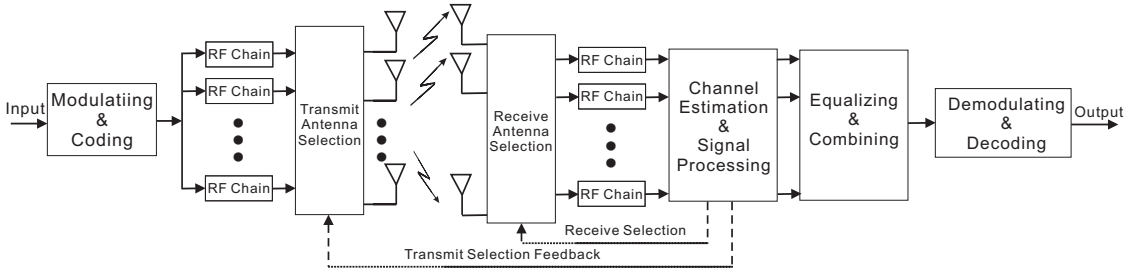

(c) Antenna selection on both sides of MIMO System

Figure 2.11 Antenna selection systems

2.7.2 Antenna Selection Criteria

To select the optimal antenna subset, an exhaustive search takes place of all possible combinations of L antennas from N antennas in order to maximize the SNR (for diversity) or capacity (for multiplexing). There are a variety of antenna selection criteria.

The simplest selection scheme is to choose antenna elements which provide the largest power. This algorithm suffers a great inefficiency when combining with spatial multiplexing strategies. This is because that the selected signal streams with the largest power may suffer high correlation between them, which severely reduces the channel capacity. Another selection algorithm is based on the mutual information (a quantity that measures the mutual dependence of two variables) of the channel [36]. Another approach, which chooses the channels with the largest power gain in a group of highly correlated

channels are suggested in [37]. An opposite criterion is to eliminate the worst antennas in *N-L* passes of loops, which can be found in [38].

2.7.3 Discussion

Antenna selection is a new and valuable concept for the future communication systems using MIMO techniques. The selection algorithms are fast developed within the recent few years. Research on antenna selection schemes is carried out in a large number of transceiver antennas and in various fading environments.

However it is well known that antenna selection operated in highly frequency selective channels obtains low performance gain. It can be inferred from the fact that in highly frequency selective channel, every specific subband calls for a specific optimal selection strategy, which is highly unlikely to be satisfied simultaneously. It can also be considered as, when the number of the multiple paths is large, the channel itself is already highly frequency diverse, therefore the fading in the wireless channel has been mostly eliminated, the channel becomes asymptotic to additive white Gaussian noise (AWGN) channel. The antenna selection is redundant along with such large multipath diversity.

2.8 Conclusions

Firstly, fundamental channel properties have been introduced in this chapter. Because of the fading in the wireless channels, MIMO technology has been developed to improve the signal transmission reliability as well as the data rate. OFDM was introduced to combat the multipath fading in broadband communication links. A number of diversity schemes

have been proposed to enhance the system performance in the perspective of error probability. Cyclic delay diversity has been suggested for its low additional complexity, high flexibility and spectrum efficiency as well as the compatibility to many existing standards. Antenna selection has been introduced to cut down the number of the expensive RF chains and also has the features of high flexibility and compatibility. In the following chapters, cyclic delay diversity, antenna selection and their combination will be discussed thoroughly.

References

[1] J. G. Proakis, *Digital Communications*, McGraw-Hill, 4th Edition, 2000.

[2] V. Tarokh, H. Jafarkhani and A. R. Calderbank, "Space-time block codes from orthogonal designs," *IEEE Trans. Inform. Theory*, vol. 45, no. 5, pp. 1456-1467, Jul. 1999.

[3] V. Tarokh, H. Jafarkhani and A. R. Calderbank, "Space-time block coding for wireless communications: performance results," *IEEE J. Select. Areas Commun.*, vol. 17, no. 3, pp. 451-460, Mar. 1999.

[4] A. Dannabb and S. Kaiser, "Standard conformable antenna diversity techniques for OFDM systems and its application to the DVB-T system," in *Proc. IEEE Globecom*, vol. 5, pp. 3100-3105, Nov. 2001.

[5] R. W. Heath and A. Paulraj, "Antenna selection for spatial multiplexing systems based on minimum error rate," in *Proc. IEEE Int. Conf. Commun. (ICC)*, Helsinki, Finland, p. 2276, June 2001.

[6] D. Gore A. Paulraj, R. Nabar, *Introduction to Space-Time Wireless Communications*, First edition, 2003.

[7] R. Van Nee and R. Prasad, *OFDM for Wireless Multimedia Communications*, Artech House, 2000.

[8] B.Vucetic and J. Yuan, *Space-Time Coding*, John Wiley, 2003.

[9] R. Peterson R. E. Ziemer, *Introduction to Digital Communication*, Second edition, 2000.

[10] A. Sezgin, *Space-time codes for MIMO systems: Quasi-Orthogonal design and concatenation*, PhD thesis, Fakultat IV - Elektrotechnick und Informatik der Technischen Universitat Berlin, 2005.

[11] R. Steele, *Mobile Radio Communications*, First edition, 1996.

[12] A. F. Molisch, M. Z. Win, Y. S. Choi and J. H. Winters, "Capacity of MIMO systems with antenna selection," *IEEE Transactions on Wireless Communications*, vol. 4, no. 4, pp. 1759-1772, 2005.

[13] A. Goldsmith, S. A. Jafar, N. Jindal and S. Vishwanath, “Capacity limits of MIMO channels,” *IEEE Journal on Selected Areas in Communications*, pp. 684–702, 2003.

[14] M. Katz and F. Fitzek, *WiMAX Evolution: Emerging Technologies and Applications*, Wiley, Jan. 2009.

[15] “The WINNER II Air Interface: Refined Spatial-Temporal Processing Solutions,” *WINNER II*, http://www.ist-winner.org/WINNER2-Deliverables/D3.4.1.pdf, Nov. 2006.

[16] “802.11n: Next-Generation Wireless LAN Technology”, Broadcom white paper, Apr. 2006.

[17] R. Prasad, *OFDM for Wireless Communication Systems*, Boston-London: Artech House, 2004.

[18] S. Weinstein and P. Ebert, "Data transmission by frequency-division multiplexing using the discrete Fourier transform," *IEEE Transactions on Communications*, vol. 19, no. 5, pp. 628-634, Oct. 1971.

[19] A. Peled and A. Ruiz, "Frequency domain data transmission using reduced computational complexity algorithms," in *Proc. of the IEEE International Conference on Acoustics, Speech and Signal Processing*, Denver, CO, pp. 964-967, Apr. 1980.

[20] B. Muquet, Z. Wang, G. Giannakis, M. de Courville, and P. Duhamel, "Cyclic prefixing or zero padding for wireless multicarrier transmissions," *IEEE Transactions on Communications*, vol. 50, no. 12, pp. 2136-2148, Dec. 2002.

[21] P. A. Lynn and W. Fuerst, *Digital Signal Processing with Computer Applications*, John Wiley & Sons, 1989.

[22] D.G. Brennan, "Linear diversity combining techniques," *Proc. IRE*, vol.47, no.1, pp.1075–1102, Jun. 1959.

[23] D. TSE and P. Viswanath, *Fundamentals of Wireless Communication*, Cambridge University Press, 2005.

[24] S. Kaiser, "Spatial transmit diversity techniques for broadband OFDM systems," in *Proc. of Global Telecommunications Conference*, San Francisco, CA, USA., pp. 1824-1828, 2000.

[25] A. Wittneben, "A new bandwidth efficient transmit antenna modulation diversity scheme for linear digital modulation," in *Proc. of IEEE International Conference on Communications*, pp. 1630–1634, 1993.

[26]R. Buehrer, T. Rappaport, A. Annamalai and W. Tranter, “Wireless communications: Past events and a future perspective,” *IEEE Communications Magazine*, pp. 148–161, 2002.

[27] S. M. Alamouti, “A simple transmit diversity technique for wireless communications,” *IEEE Journal on Selected Areas in Communications*, pp. 1451–1458, 1998.

[28] M. Bossert, A. Huebner, F. Schuehlein, H. Haas, and E. Costa, “On cyclic delay diversity in OFDM based transmission schemes,” in *Proc. OFDM Workshop*, Sep. 2002.

[29] G. Bauch, J. S. Malik, “Parameter optimization, interleaving and multiple access in OFDM with cyclic delay diversity,” in *proc. VTC 2004*, pp. 505-509, 2004.

[30] T. S. Rappaport, *Wireless Communications*, First edition, 1999.

[31] B. Badic, P. Fuxjager and H. Weinrichter, “Optimization of coded MIMO-transmission with antenna selection,” *In 2005 IEEE 61st Vehicular Technology Conference, VTC2005,* Stockholm, Sweden, pp. 905-909, May 2005.

[32] I. A. Tolochko, *Channel estimation for OFDM systems with transmitter diversity*, PhD thesis, Center for Telecommunications and Micro-Electronics, Victoria University, 2005.

[33] B. Badic, P. Fuxjaeger, and H. Weinrichter, “Performance of quasi-orthogonal space-time code with antenna selection,” *Electronics Letters*, pp. 1282–1284, 2004.

[34] F. H. P. Fitzek, M. I. Rahman and S. S. Das, *OFDM based WLAN systems*, Technical Report, R-04-1002, ISSN 0908-1224, ISBN 87-90834-43-7, Center for TeleInFrastruktur (CTiF), Aalborg University, Denmark, Feb. 2005.

[35] L. Ye, J. C. Chuang, and N. R. Sollenberger, “Transmitter diversity for OFDM systems and its impact on high-rate data wireless networks,” *IEEE Journal on Selected Areas in Communications*, pp. 1233–1243, 1999.

[36] M. A. Jensen and J. W. Wallace, “Antenna selection for MIMO systems based on information theoretic considerations,” in *IEEE International Symposium on Antennas and Propagation: URSI North American Radio Science Meeting*, pp. 515–518, 2003.

[37] Y. S. Choi, A. F. Molisch, M. Z. Win and J. H. Winters, “Fast algorithms for antenna selection in MIMO systems,” in *IEEE 58th Vehicular Technology Conference*, vol. 3, pp. 1733- 1737, 2003.

[38] A. Gorokhov, D. Gore and A. Paulraj, “Receive antenna selection for MIMO flat-fading channels: theory and algorithms,” *IEEE Transactions on Information Theory*, pp. 2687–2696, 2003.

Chapter 3

Performance Analysis of CDD Systems

3.1 Introduction

Because of the benefit of diversity gain that CDD can provide, the performance analysis of a CDD system is now investigated, to obtain a comprehensive understanding of the physical mechanism of the systems and optimum system design. In [1], a performance analysis of space-time trellis coding system for a narrow-band channel is provided, which claims that the system performance is determined by the correlation matrices of pairs of distinct code sequences. This theory also has been applied in the analysis of space-time block coding in [2] and it is fundamental for the analysis of CDD systems as well. In [3], the symbol error rate and outage probability analysis of CDD system in the UWB channel with a repetition code as the channel coding are derived. An approximation is used to simplify the computation based on the mathematical results of [1] and [4]. Meanwhile, in [5] and [6], the performance of CDD in MC-CDMA sensor network is explored. The symbol error probability in these papers is obtained by transferring the multiple-input and multiple-output CDD channel to a single-input and multiple-output Nakagami channel with varied power and fading parameter. This analysis ignores the effect that the cyclic delay times cause and therefore is only applicable to MIMO channel with extensive frequency selectivity.

The optimum delay shift is a very important issue for CDD performance. The research in this area is at early stage, being mainly based on simulation results without sufficient theoretical analysis. For instance, in [7], Bosert showed that the optimum cyclic delay lengths should be the reciprocal of the cardinality of the modulation alphabet. On the other hand, in [8, 9, 10, 11], Bauch showed that the optimum cyclic shifts depend on code rate, channel memory but not on the modulation constellation size. He also derived a condition for full spatial diversity in [12], which is that the free distance of the channel code should be equal to or larger than the number of transmitters. However, the condition in [12] is not enough to guarantee a full diversity gain in CDD, which is indicated by the slopes of the bit error rate (BER) performance curves in [12]. Moreover, Bauch also investigates the performance of CDD systems from a capacity perspective, which indicates CDD performs worse when the cyclic delay shift equals to the maximum factor or other factors of the OFDM length [9]. In fact, the capacity equation should be constructed over a group of subcarriers which are explored by the channel codes, but not over the whole OFDM bandwidth, to obtain the exact effect of the cyclic delay times.

Because of the limitations of the above research, an extensive and general performance analysis of CDD OFDM systems on multipath channel is developed in this chapter. This analysis can be applied to a wide range of channel codes, modulation schemes and multipath or flat fading channels. Although it is based on Rayleigh fading channel, the result can be readily extended to other catalogues of fading channel models. A criterion for selecting the optimum delay shift was investigated. At the end of this chapter, the performance bound of CDD systems with PSK signals and convolutional coding in

Rayleigh fading channel is calculated for a detailed understanding of the analysis methods.

3.2 CDD System Model

Initially, a CDD system with a forward error control/correction (FEC) block, used as the channel coding, and an OFDM block was constructed. The system diagram is as following:

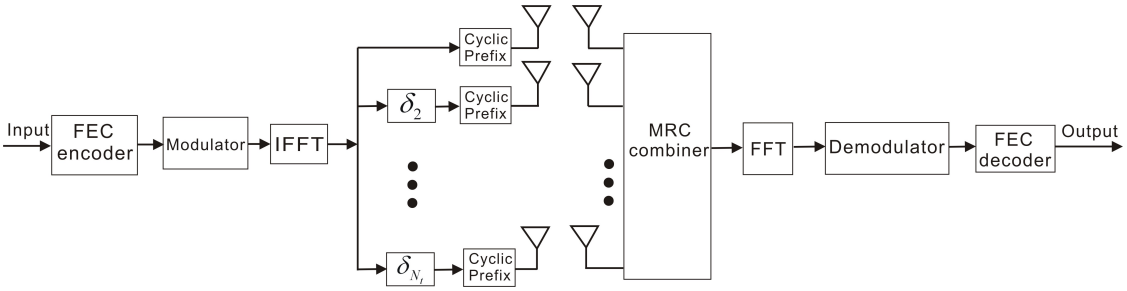

Figure 3.1 A CDD system model

As depicted in Figure 3.1, the signal bits were modulated after being coded by a FEC block. Then OFDM was applied as an inverse fast Fourier transform (IFFT) with length of N_s, which is very important for the CDD scheme to convert the spatial diversity to frequency diversity. Afterwards, the signal vector was transmitted over N_t separate transmit antennas with cyclic delays δ_{n_t}, where n_t denotes the transmitter order. A cyclic prefix was inserted before the signal was transmitted to avoid the inter symbol interference (ISI) and inter carrier interference (ICI). Therefore, if the transmit signal vector at one OFDM frame in the frequency domain is

$$\mathrm{X}' = [X_1, X_2, ...X_{N_s}]. \tag{3.1}$$

The transmit signal matrix after CDD arranging can be expressed as

$$\chi = \begin{bmatrix} X_1 & X_2 e^{j\frac{2\pi}{N_s}\delta_1} & \cdots & X_{N_s} e^{j\frac{2\pi}{N_s}\delta_1(N_s-1)} \\ X_1 & X_2 e^{j\frac{2\pi}{N_s}\delta_2} & \cdots & X_{N_s} e^{j\frac{2\pi}{N_s}\delta_2(N_s-1)} \\ \vdots & \vdots & \ddots & \vdots \\ X_1 & X_2 e^{j\frac{2\pi}{N_s}\delta_{N_t}} & \cdots & X_{N_s} e^{j\frac{2\pi}{N_s}\delta_{N_t}(N_s-1)} \end{bmatrix}, \quad (3.2)$$

where $X_k e^{j\frac{2\pi}{N_s}\delta_{n_t}(k-1)}$ is the signal symbol transmitted by the n_tth transmitter on the kth subcarrier, $n_t = 1,\cdots,N_t, k = 1,\cdots,N_s$, δ_{n_t} is the cyclic delay shift on the n_tth transmitter. The transmitted signals have been normalized so that $E\left(\left|X_k e^{j\frac{2\pi}{N_s}\delta_{n_t}(k-1)}\right|^2\right) = \frac{1}{N_t}$.

On the receiving side, maximal ratio combining (MRC) was used to combine the received symbols over the receive antennas. Following this, a standard OFDM demodulator was applied to recover the signal. By virtue of CDD and Fourier transform, multiple input channels had been converted into equalized single input channels with increased frequency selectivity. Let $\mathrm{H} \in \mathbb{C}^{N_t \times N_r \times N_s}$ denote the original multiple-input multiple-output (MIMO) channel matrix. The equalized channel can be written as

$$H_{equ,k}^{n_r}(i) = \sum_{n_t=1}^{N_t} e^{j2\pi\frac{(k-1)\delta_{n_t}}{N_s}} H_k^{(n_t,n_r)}(i), \quad (3.3)$$

based on [13], where $H_k^{(n_t,n_r)}(i)$ represents the channel transfer function of the channel between the n_tth transmitter and the n_rth receiver on the kth subcarrier in the ith OFDM frame, $H_{equ,k}^{n_r}(i)$ is the equalized channel transfer function as in a single input channel subcarrier.

The received signal at the *k*th subcarrier can be represented as

$$\begin{aligned} \Upsilon_k(i) &= \chi_k(i)'\mathrm{H}_k(i)+\varpi_k(i) \\ &= X_k(i)\mathrm{H}_{equ,k}(i)+\varpi_k(i) \end{aligned}, \tag{3.4}$$

where $(\bullet)'$ denotes the transpose operation, $\Upsilon_k(i)\in\mathbb{C}^{1\times N_r}$ $\chi_k(i)\in\mathbb{C}^{N_t\times 1}$, $\mathrm{H}_k(i)\in\mathbb{C}^{N_t\times N_r}$, $\mathrm{H}_{equ,k}(i)\in\mathbb{C}^{1\times N_r}$ and $\varpi_k(i)\in\mathbb{C}^{1\times N_r}$ denote components of the received signal matrix $\Upsilon(i)\in\mathbb{C}^{N_s\times N_r}$, the transmitted signal matrix $\chi\in\mathbb{C}^{N_t\times N_s}$, the channel coefficient matrix $\mathrm{H}\in\mathbb{C}^{N_t\times N_r\times N_s}$, the equalized channel matrix $\mathrm{H}_{equ}\in\mathbb{C}^{N_s\times N_r}$ and the additive white Gaussian noise vector $\varpi(t)\in\mathbb{C}^{N_s\times N_r}$. As the result of this formulation, the MIMO channel $\mathrm{H}\in\mathbb{C}^{N_t\times N_r\times N_s}$ can be treated as a single-input and multiple-output (SIMO) channel $\mathrm{H}_{equ}\in\mathbb{C}^{N_s\times N_r}$.

Let D(X) be a $N_s\times N_s$ diagonal matrix with the elements of X on its main diagonal. The received signal over one OFDM frame can be stated as

$$\Upsilon(i)=\mathrm{D}(\mathrm{X})\mathrm{H}_{equ}(i)+\varpi(i) \tag{3.5}$$

As the MRC is applied in the receiver, the signal after equalization is

$$\begin{aligned} C_k(i) &= \Upsilon_k(i)\mathrm{H}_{equ,k}(i)^H \\ &= X_k(i)\mathrm{H}_{equ,k}(i)\mathrm{H}_{equ,k}(i)^H+\varpi_k(i)\mathrm{H}_{equ,k}(i)^H \end{aligned}, \tag{3.6}$$

where $(\bullet)^H$ denotes the Hermitian transpose operation. $C_k(i)$ is the *k*th component of the combined signal vector $C(i)\in\mathbb{C}^{N_s\times 1}$. Therefore the effective signal energy per symbol to noise power spectral density ratio, $\frac{E_s}{N_o}$ (where E_s denotes the signal energy per symbol and N_o denotes the noise spectral density), on the *k*th subcarrier is

$$\gamma_k = \frac{E_s \left\| \mathrm{H}_{equ,k} \right\|^2}{N_o}, \tag{3.7}$$

where $\|\bullet\|^2$ denotes the Frobenius norm operation.

In this section, a system model of cyclic delay diversity is constructed combined with OFDM and channel coding in fading MIMO channel. The performance analysis of this system is investigated in the following sections.

3.3 Performance Analysis of CDD system in Rayleigh Fading Channels

In this section, the bit error probability bound for CDD systems with N_t transmit antennas and N_r receive antennas in Rayleigh fading channel is investigated. The derivation is similar as in [3], which is a performance analysis of a CDD system combined with repetition coding in UWB channels and conducted contemporaneously as my work. In next section a new bit error rate performance analysis of CDD system combined with convolutional coding in Rayleigh channels will be generated.

The system structure has been shown in Figure 3.1. The input signals were encoded by a FEC block (which can be any kind of error correction code such as the convolutional code). Then, they were modulated and transferred by the IFFT block. Afterwards, cyclic shift was introduced to map the signal sequence onto different antennas. In the receiver,

the received signal steams were firstly combined with the MRC scheme. After this, they were demodulated and decoded by the error correction decoder.

For a certain kind of channel coding, the detection is normally applied on a specific length of code word but not the whole OFDM frame length. Assume the detection length is *M*. The receiver signals can be presented as

$$\mathrm{R}(i) = \mathrm{D}(\mathrm{S}(i))\mathrm{A}_{equ}(i) + \omega(i), \tag{3.8}$$

where $\mathrm{R}(i) \in \mathbb{C}^{M \times N_r}$, $\mathrm{S}(i) \in \mathbb{C}^{M \times 1}$, $\mathrm{A}_{equ}(i) \in \mathbb{C}^{M \times N_r}$ and $\omega(i) \in \mathbb{C}^{M \times N_r}$ are the received signal matrix, transmitted signal vector, the equalized channel transfer function and the white Gaussian noise matrix over a group of channel subcarriers of length *M*.

Now, we assume the maximum likelihood algorithm is applied in the receiver and the receiver has ideal channel state information. Maximum likelihood detection is used to find the code sequence with the minimum squared Euclidean distance to the received sequence. MRC is applied as stated in (3.6), and FEC is applied to *M* subcarriers, the detection metric can be denoted as

$$\tilde{\mathrm{S}} = \arg\min_{\tilde{\mathrm{S}}} \left\| \mathrm{R} - \mathrm{D}(\tilde{\mathrm{S}})\mathrm{A}_{equ} \right\|^2 = \arg\min_{\tilde{\mathrm{S}}} \sum_{n_r=1}^{N_r} \sum_{k=1}^{M} \left| r_k^{n_r} - \tilde{X}_k H_{equ,k}^{n_r} \right|^2, \tag{3.9}$$

where $r_k^{n_r}$ is a component of the received signal matrix R on the *k*th subcarrier and on the n_rth receiver, $\tilde{\mathrm{S}}$ is the detected signal vector and $\tilde{X}_k$ denotes the *k*th component of $\tilde{\mathrm{S}}$. The index *i* has been eliminated for simplicity.

The pairwise error probability (PEP) is the probability that the detector selects an erroneous sequence $\hat{\mathrm{S}} = (\hat{X}_1, \hat{X}_2, \cdots, \hat{X}_M)$ when the real transmitted signal sequence was $\mathrm{S} = (X_1, X_2, \cdots, X_M)$ [2]. According to Appendix.A and the description in [14], the PEP of our system can be written as

$$\begin{aligned} P_e &= E\left[Q\left(\sqrt{\frac{E_s}{2N_t N_o} \left\| \Delta_S \mathrm{A}_{equ} \right\|^2} \right) \right] \\ &= E\left\{ Q\left[\frac{E_s}{2N_t N_o} \sum_{n_r=1}^{N_r} \sum_{k=1}^{M} \left| (X_k - \hat{X}_k) H_{equ,k}^{N_r} \right|^2 \right] \right\}, \end{aligned} \tag{3.10}$$

where $\frac{E_s}{N_o}$ is the signal to noise power ratio per symbol, $\Delta_S = \mathrm{D(S)\text{-}D}(\hat{\mathrm{S}})$ and $E(\bullet)$ is the expectation operation of the inner function. Let $\eta = \left\| \Delta_S \mathrm{A}_{equ} \right\|^2$ and use the alternative form of Q function: $Q(x) = \int_0^{\pi} \frac{1}{\pi} \exp\left(-\frac{x^2}{2\sin^2\theta} \right) d\theta$, the PEP can be represented as

$$\begin{aligned} P_e &= E\left[\frac{1}{\pi} \int_0^{\pi/2} \exp\left(-\frac{E_s \eta}{4N_o N_t \sin^2\theta} \right) d\theta \right] \\ &= \frac{1}{\pi} \int_0^{\pi/2} E\left[\exp\left(-\frac{E_s \eta}{4N_o N_t \sin^2\theta} \right) \right] d\theta \quad , \\ &= \frac{1}{\pi} \int_0^{\pi/2} \left[\int_0^{\infty} \exp\left(-\frac{E_s \eta}{4N_o N_t \sin^2\theta} \right) p_\eta(\eta) d\eta \right] d\theta \end{aligned} \tag{3.11}$$

where the inner integral is in the form of a Laplace transform with respect to the variable η. As defined in [15] the moment generating function (MGF) of η ($\mathrm{M}_\eta(s) = \int_0^{\infty} e^{s\eta} p_\eta(\eta) d\eta$) is the Laplace transform of $p_\eta(\eta)$ with the exponent reversed in sign. Therefore the PEP equation can be rewritten as

$$P_e = \frac{1}{\pi}\int_0^{\pi/2} \mathrm{M}_\eta\left(-\frac{E_s}{4N_o N_t \sin^2\theta}\right)d\theta. \tag{3.12}$$

Then we consider a simplification of the above equation according to the operation in [4]. We assume the channel is Rayleigh fading channel. Therefore the channel transfer functions $H_k^{(n_t,n_r)}$ are complex Gaussian distributed with zero mean and variance of unit 1. Then $H_{equ,k}^{n_r}$ are also complex Gaussian distributed with zero mean. As both X_k and $\hat{X}_k$ are constant, $(X_k - \hat{X}_k)H_{equ,k}^{n_r}$ are zero-mean complex Gaussian random variables as well. According to [4] and [16], the quadratic form of a zero-mean Gaussian random vector $\boldsymbol{x}$ can be represented by a weighted summation of $|\upsilon_n|^2$, where υ_n are mutually independent standard Gaussian random variables, and the weights are the eigenvalues of the covariance matrix of x. As $\eta = \left\|\Delta_S \mathrm{A}_{equ}\right\|$ is in the quadratic form of the Gaussian random vector x,

$$\begin{aligned} \mathrm{x} &= [I_{N_r} \otimes \Delta_S B_{equ}]' \\ &= \left[\left(X_1-\hat{X}_1\right)H_{equ,1}^1, \left(X_2-\hat{X}_2\right)H_{equ,2}^1, \cdots; \left(X_M-\hat{X}_M\right)H_{equ,M,}^1 \cdots; \left(X_1-\hat{X}_1\right)H_{equ,1}^{N_r}, \cdots; \left(X_M-\hat{X}_M\right)H_{equ,M}^{N_r}\right]' \end{aligned} \tag{3.13}$$

where $B_{equ} = \left[H_{equ,1}^1, H_{equ,2}^1, \cdots H_{equ,M}^1, \cdots, H_{equ,1}^{N_r}, H_{equ,2}^{N_r}, \cdots, H_{equ,M}^{N_r}\right]'$, I_{N_r} is an identity matrix with size N_r and $\otimes$ is a Kronecker product operation. Then we have

$$\eta \approx \sum_{n_r}^{N_r}\sum_{k=1}^{M} eig_n^{n_r}(\Phi)\left|\mu_n^{n_r}\right|^2, \tag{3.14}$$

where $\mu_n^{n_r}$ are independent identically distributed standard complex Guassian random variables, and

$$\Phi = E\left[I_{n_r} \otimes \Delta_S B_{equ} \left(I_{n_r} \otimes \Delta_S B_{equ} \right)^H \right] = I_{n_r} \otimes \Delta_S R_M^{N_r} \left(I_{n_r} \otimes \Delta_S \right)^H, \quad (3.15)$$

where $R_M^{N_r} = E\left(B_{equ} B_{equ}^H \right)$ is the covariance matrix of B_{equ}. From [4], by Ostrowski's theorem [17], the eigenvalues of Φ can be given by

$$eig_n\left(\Phi\right) = eig_n\left[I_{n_r} \otimes \Delta_S R_M^{N_r} \left(I_{n_r} \otimes \Delta_S \right)^H \right] = v_n eig_n\left(R_M^{N_r} \right), \quad (3.16)$$

where v_n are nonnegative real numbers that satisfy

$$eig_M\left[I_{n_r} \otimes \Delta_S \left(I_{n_r} \otimes \Delta_S \right)^H \right] \geq v_n \geq eig_1\left[I_{n_r} \otimes \Delta_S \left(I_{n_r} \otimes \Delta_S \right)^H \right] \text{ for } n = 1, 2, ...M. \quad (3.17)$$

As $\mu_n^{n_r}$ are of Rayleigh distribution (complex Gaussian distribution), $\left|\mu_n^{n_r}\right|^2$ follow a Gamma distribution or Chi-square distribution of freedom degree 2. The probability density function of $\left|\mu_n^{n_r}\right|^2$ can be denoted as

$$P(\alpha) = \frac{1}{\bar{\alpha}} e^{-\frac{\alpha}{\bar{\alpha}}} \quad (\alpha \geq 0), \quad (3.18)$$

where $\bar{\alpha}$ is the mean value of the variable α. The MGF of this distribution is

$$\mathrm{M}(-s) = \frac{1}{1 + s\bar{\alpha}}. \quad (3.19)$$

For a Rayleigh distribution $\bar{\alpha} = 1$, the MGF can be written as $\mathrm{M}(-s) = \frac{1}{1+s}$.

Therefore the PEP of equation (3.11) can be represented as

$$
\begin{aligned}
P_e &= \frac{1}{\pi}\int_0^{\pi/2} E\left[\exp\left(-\frac{E_s\eta}{4N_oN_t\sin^2\theta}\right)\right]d\theta \\
&\approx \frac{1}{\pi}\int_0^{\pi/2} E\left\{\exp\left[-\frac{E_s\sum_{n_r=1}^{N_r}\sum_{n=1}^{M}\nu_n eig_n^{n_r}\left(R_M^{N_r}\right)\left|\mu_n^{n_r}\right|^2}{4N_oN_t\sin^2\theta}\right]\right\}d\theta \\
&= \frac{1}{\pi}\int_0^{\pi/2} E\left\{\prod_{n_r=1}^{N_r}\prod_{n=1}^{M}\exp\left[-\frac{E_s\nu_n eig_n^{n_r}\left(R_M^{N_r}\right)\left|\mu_n^{n_r}\right|^2}{4N_oN_t\sin^2\theta}\right]\right\}d\theta. \qquad (3.20) \\
&= \frac{1}{\pi}\int_0^{\pi/2}\prod_{n_r=1}^{N_r}\prod_{n=1}^{M} E\left\{\exp\left[-\frac{E_s\nu_n eig_n^{n_r}\left(R_M^{N_r}\right)\left|\mu_n^{n_r}\right|^2}{4N_oN_t\sin^2\theta}\right]\right\}d\theta \\
&= \frac{1}{\pi}\int_0^{\pi/2}\prod_{n_r=1}^{N_r}\prod_{n=1}^{M}\frac{1}{1+\frac{E_s\nu_n eig_n^{n_r}\left(R_M^{N_r}\right)}{4N_oN_t\sin^2\theta}}d\theta
\end{aligned}
$$

This analysis is a prediction of the pairwise error probability of a CDD system with various kinds of channel codes and modulation schemes in multipath Rayleigh fading channels with arbitrary numbers of transmitters and receivers. It also can be readily extended to other classes of fading channels. The bit error probability or symbol error probability can be developed for any specific catalogue of channel codes. As for convolutional coding, the bit error probability is generated according to (A.15).

For the correlation matrix $R_M^{N_r}$, let $R(n,n')$ be the (n,n')th entry of the matrix $R_M^{N_r}$, $0 \le n,n' \le MN_r$.

Firstly, assume the channel transfer function is flat fading Rayleigh distributed. According to (3.3), $H_{equ,k}^{n_r}(i)=\sum_{n_t=1}^{N_t} e^{j2\pi\frac{k\delta_{n_t}}{N_s}} H_k^{(n_t,n_r)}(i)$, the elements on the main diagonal of the correlation matrix are given by

$$R(n,n)=E\left[H_{equ,k}^{n_r}{H_{equ,k}^{n_r}}^*\right]=\sum_{n_t=1}^{N_t}E\left[\left|H_k^{(n_t,n_r)}\right|^2\right]=N_t, \tag{3.21}$$

where $n=(n_r-1)*M+k$. The correlations of the channel transfer functions from different transmitters are zero-mean, so they can be eliminated.

For the off-diagonal elements, the correlations of channel transfer functions from different receivers or transmitters can be eliminated. Therefore, $R(n,n')$ can be denoted as

$$R(n,n')=\begin{cases}\sum_{n_t=1}^{N_t}E\left[\left|H^{(n_t,n_r)}\right|^2\right]e^{j2\pi\frac{(k-k')\delta_{n_t}}{N_s}}=\sum_{n_t=1}^{N_t}e^{j2\pi\frac{(k-k')\delta_{n_t}}{N_s}} & n_r=n_r'\\ 0 & n_r\neq n_r'\end{cases}. \tag{3.22}$$

For multipath Rayleigh fading channel, a common non-line-of-sight channel model can be written as

$$h(t)=\sum_{L=0}^{L}\alpha(l)\delta(t-\tau_l). \tag{3.23}$$

The multipath gain coefficient $\alpha(l)$ is modeled as a zero-mean, complex Gaussian random variable on the *l*th path. Its absolute value follows Rayleigh distribution and its phase is uniformly distributed between 0 and 2π . The variance of $\alpha(l)$ is given as

$$\Omega_l = E\left[\left|\alpha(l)\right|^2\right] = \Omega_0 e^{-\frac{\tau_l}{\lambda}}, \tag{3.24}$$

where Ω_0 is the mean energy of the first path, and λ is the decay factor. The powers of the multipath components are normalized such that $\sum_{l=0}^{L}\Omega_l = 1$.

The elements on the main diagonal of the equalized channel covariance matrix are given by

$$R(n,n) = E\left[H_{equ,k}^{n_r} H_{equ,k}^{n_r\ *}\right] = \sum_{n_t=1}^{N_t}\sum_{l=0}^{L}\left|\alpha^{(n_t,n_r)}(l)\right|^2 = N_t. \tag{3.25}$$

For the off-diagonal elements, $R(n,n')$ can be denoted as

$$R(n,n') = \begin{cases} \sum_{n_t=1}^{N_t}\sum_{l=0}^{L} E\left[\left|\alpha^{(n_t,n_r)}(l)\right|^2\right] = \sum_{n_t=1}^{N_t}\sum_{l=0}^{L}\Omega_0 e^{j2\pi\frac{(k-k')(\delta_{n_t}+l)}{N_s}+\frac{\tau_l}{\lambda}} & n_r = n_r' \\ 0 & n_r \neq n_r' \end{cases}. \tag{3.26}$$

At this point, the optimum delay times for the CDD system need to be considered. To optimize the performance of the CDD system is to minimize the error probability, or equally the pairwise error probability. According to (3.10) and (3.20), the optimum delay time can be obtained by

$$\begin{aligned} \{\delta_{n_t}\}_{opt} &= \arg\min_{\{\delta_{n_t}\}}\{P_E\} \\ &= \arg\min_{\{\delta_{n_t}\}}\left\{E\left[Q\left(\sqrt{\frac{E_s}{2N_tN_o}\left\|\Delta_S \mathrm{A}_{equ}\right\|^2}\right)\right]\right\} \\ &\approx \arg\min_{\{\delta_{n_t}\}}\left\{\frac{1}{\pi}\int_0^{\pi/2}\prod_{n_r=1}^{N_r}\prod_{n=1}^{M}\frac{1}{1+\frac{E_s\nu_n eig_n^{n_r}\left(R_M^{N_r}\right)}{4N_oN_t\sin^2\theta}}d\theta\right\} \end{aligned}. \tag{3.27}$$

From the PEP equation (3.20), only the terms of $eig_n^{n_r}\left(R_M^{N_r}\right)$ depend on the delay time in CDD. Therefore, to minimize PEP is to maximize $eig_n^{n_r}\left(R_M^{N_r}\right)$. According to the analysis in [3], with relative high $\frac{E_s}{N_o}$, the PEP of (3.20) can be written as

$$P_e \approx \left(\prod_{n_r=1}^{N_r}\prod_{1}^{\hat{M}_{n_r}}\varphi_n^{n_r}\right)^{-1}\frac{1}{\pi}\int_0^{\frac{\pi}{2}}\left(\frac{E_s\nu_n}{4N_oN_t\sin^2\theta}\right)^{-1}d\theta, \tag{3.28}$$

where $\varphi_n^{n_r}$ are the nonzero eigenvalues of $R_M^{N_r}$, and $\hat{M}_{n_r}$ is the number of nonzero eigenvalues of $R_M^{N_r}$ for the n_rth receiver. Therefore the optimum delay time can be determined by

$$\{\delta_{n_t}\}_{opt} = \arg\max_{\{\delta_{n_t}\}}\prod_{n_r=1}^{N_r}\prod_{n=1}^{\hat{M}_{n_r}}\varphi_n^{n_r}\ . \tag{3.29}$$

If $R_M^{N_r}$ has a full rank then $\prod_{n_r=1}^{N_r}\prod_{1}^{\hat{M}_{n_r}}\varphi_n^{n_r} = \det\left(R_M^{N_r}\right)$, where $\det(\bullet)$ denotes the determinant operation. Then the optimum criteria can be represented similarly to [3]

$$\{\delta_{n_t}\}_{opt} = \arg\max_{\{\delta_{n_t}\}}\left[\det\left(R_M^{N_r}\right)\right]. \tag{3.30}$$

However, according to simulation results, when the number of the transmitters is large enough, normally equal to or greater than four, the maximum division criterion can be applied:

$$\delta_n = \delta_{n-1} + \frac{N_s}{N_t}. \tag{3.31}$$

This selection principle is much simpler, and therefore is more applicable when the transmit antenna number is large enough.

In this section, a general pairwise error analysis of CDD system in a multipath Rayleigh fading channel has been derived. This PEP can be applied to any specific class of channel coding such as a convolutional coding and any kind of modulation schemes. This PEP is also extendable to fading channels obeying statistic models other than Rayleigh distribution. The MIMO channel is investigated with MRC at the receiver side to combine the received signals. Finally, a principle for the selection of the optimum cyclic delay time has been derived in (3.29) basing on the PEP in (3.20).

3.4 Performance Analysis of a 2x1 CDD system with Convolutional Coding in Rayleigh Fading Channels

A new bit error probability bound for a CDD system with two transmit antennas and one receive antenna (2x1 CDD system) combined with convolutional coding is investigated in this section. As shown in Figure 3.2, input signals were encoded by a convolutional coding block, and then modulated as BPSK signals. IFFT transferred the signals from frequency domain to time domain. Afterwards, cyclic shift was introduced to map the signal sequence onto two different antennas. In the receiver, signals were transferred to the frequency domain again. After this, they were demodulated to binary signals and decoded by the Viterbi trellis decoder.

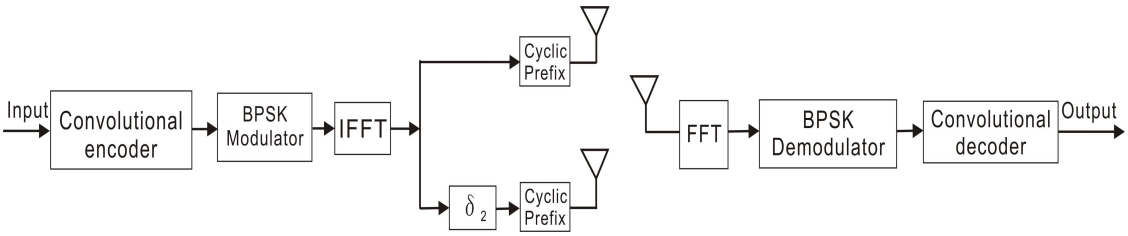

Figure 3.2 Structure of a 2x1 CDD system with convolutional coding

According to (3.20), the pairwise error probability of this simple CDD system can be denoted as

$$P_2(d) \approx \frac{1}{\pi} \int_0^{\pi/2} \prod_{n=1}^{d} \frac{1}{1+\frac{E_s \nu_n eig_n(R_d)}{4N_o N_t \sin^2\theta}} d\theta, \tag{3.32}$$

where d is the Hamming distance between the erroneous codeword and the transmitted codeword. In this system, ν_n=4 for BPSK signals, N_t=2, N_r=1, so N_r and n_r have been eliminated for simplicity, and $\frac{E_s}{N_o} = \frac{E_b}{N_o} R_c$ ($\frac{E_b}{N_o}$ is the signal to noise power ratio per bit). Therefore (3.32) can be represented as

$$P_2(d) \approx \frac{1}{\pi} \int_0^{\pi/2} \prod_{n=1}^{d} \frac{1}{1+\frac{E_b R_c eig_n(R_d)}{2N_o \sin^2\theta}} d\theta, \tag{3.33}$$

where R_d can be calculated from (3.21) and (3.22).

Using (A.15), a newly derived bit error rate bound for CDD system combined with convolutional coding can be written as

$$
\begin{aligned}
P_b &< \sum_{d=d_{free}}^{\infty} \beta_d P_2(d) \\
&< \sum_{d=d_{free}}^{\infty} \beta_d \frac{1}{\pi} \int_0^{\pi/2} \prod_{n=1}^{d} \frac{1}{1+\frac{E_b R_c eig_n(R_d)}{2N_o \sin^2\theta}} d\theta,
\end{aligned}
\tag{3.34}
$$

where d_{free} is the free distance of the convolutional trellis code and β_d is the weight of each $P_2(d)$.

This calculation is an approximation of the error probability bound because of using the approximation of (3.14). The exact bound can be generated with the original form of the PEP equation (3.10). The pairwise error probability of (3.10) can be denoted as

$$
P_2(d) = E\left\{ Q\left(\frac{E_c}{N_0} \left[\sum_{l=1}^{d} \left(|H_l^{(1)}|^2 + |H_l^{(2)}|^2 \right) + 2\,\mathrm{Re}\left(\sum_{l=1}^{d} H_l^{(1)} \bullet H_l^{(2)*} e^{j\frac{2\pi\Delta k_0}{N_s}} e^{j\frac{2\pi\Delta k_l}{N_s}} \right) \right] \right) \right\}, \tag{3.35}
$$

where $\Delta = \delta_1 - \delta_2$, is the relative cyclic shift between signals mapped onto two different transmit antennas. As the transfer functions $H_l^{(1)}$ and $H_l^{(2)}$ are complex numbers, they can be presented as: $H_l^{(1)} = h_1(l)e^{j\phi_1}$ and $H_l^{(2)} = h_2(l)e^{j\phi_2}$, where $\{h_n(l)\}$ and $\{\phi_n\}$ are the absolute values and the phase shifts of the channel transfer functions $\{H_l^{(n)}\}$ respectively. Let $\phi = \phi_1 - \phi_2$. Because both of the channel transfer functions are i.i.d. Rayleigh distributed, phases ϕ_1 and ϕ_2 should be two random variables that are uniformly distributed between *0* and 2π. Then ϕ is also a random variable uniformly distributed between -2π and 2π. Assume the channel is a flat Rayleigh fading channel. Therefore the index of OFDM subcarrier *l* for the channel transfer functions can be omitted. Then the pairwise error probability for a possible erroneous path can be expressed as

$$
\begin{aligned}
P_2(d) &= E\left\{Q\left(\frac{E_c}{N_0}\left[d\bullet\left(h_1^{\,2}+h_2^{\,2}\right)+2\,\mathrm{Re}\left(h_1\bullet h_2 e^{\,j(\frac{2\pi\Delta k_0}{N_s}+\phi)}\sum_{l=1}^{d}e^{\,j\frac{2\pi\Delta k_l}{N_s}}\right)\right]\right)\right\} \\
&= E\left\{Q\left(\frac{E_c}{N_0}\left[d\bullet\left(h_1^{\,2}+h_2^{\,2}\right)+2\,\mathrm{Re}\left(h_1\bullet h_2 e^{\,j(\frac{2\pi\Delta k_0}{N_s}+\phi+\omega)}\left|\sum_{l=1}^{d}e^{\,j\frac{2\pi\Delta k_l}{N_s}}\right|\right)\right]\right)\right\}. \qquad (3.36) \\
&= E\left\{Q\left(\frac{2E_c}{2N_0}\left[d\bullet\left(h_1^{\,2}+h_2^{\,2}\right)+2h_1h_2\left|\sum_{l=1}^{d}e^{\,j\frac{2\pi\Delta k_l}{N_s}}\right|\cos(\varphi)\right]\right)\right\}
\end{aligned}
$$

where $\varphi=\frac{2\pi\Delta k_0}{N_s}+\phi+\omega$. Because k_0 can be any integer between *0* and N_s-1, ω is a real constant if the convolutional coding trellis is fixed, and ϕ is a random variable uniformly distributed between - 2π and 2π. Considered the symmetric feature of function cos(x), φ can be regarded as a random variable which is also uniformly distributed between *0* and 2π.

Because the absolute values of the channel transfer functions, $\{h_{n_t}\}$, obey identically independent distributed Rayleigh distributions, so we can integrate the pairwise error probability (3.36) over their distributions:

$$
\begin{aligned}
P_2(d)=&\int_0^{+\infty}2h_1\exp(-h_1^{\,2})\int_0^{+\infty}2h_2\exp(-h_2^{\,2})\int_0^{2\pi}\frac{1}{2\pi} \\
&Q\left(\frac{E_c}{N_0}\left[d\bullet\left(h_1^{\,2}+h_2^{\,2}\right)+2h_1\bullet h_2\bullet\left|\sum_{l=1}^{d}e^{\,j\frac{2\pi\Delta k_l}{N_s}}\right|\cos(\varphi)\right]\right)dh_1dh_2d\varphi
\end{aligned}
\qquad (3.37)
$$

The previous pairwise error probability can also be expressed as:

$$P_2(d) = \int_0^{+\infty} 2h_1 \exp(-h_1^2) \int_0^{+\infty} 2h_2 \exp(-h_2^2) \int_0^{2\pi} \frac{1}{2\pi} \int_0^{\pi/2} \frac{1}{\pi} \bullet$$
$$\exp\left(-\frac{E_c}{N_0} \frac{\left[d \bullet \left(h_1^2 + h_2^2 \right) + 2h_1 \bullet h_2 \bullet \left| \sum_{l=1}^{d} e^{j\frac{2\pi\Delta k_l}{N_s}} \right| \cos(\varphi) \right]}{2\sin^2\theta} \right) d\theta d\varphi dh_1 dh_2 \quad . \qquad (3.38)$$

Substitute (3.38) into (A.15), the bit error probability can be expressed as

$$\begin{aligned} P_b \; < \; & \sum_{d=d_{free}}^{\infty} \beta_d P_2(d) \\ & \sum_{d=d_{free}}^{\infty} \beta_d \{ \int_0^{+\infty} 2h_1 \exp(-h_1^2) \int_0^{+\infty} 2h_2 \exp(-h_2^2) \int_0^{2\pi} \frac{1}{2\pi} \int_0^{\pi/2} \frac{1}{\pi} \bullet \\ < \; & \exp\left(-\frac{E_b R_c}{N_0} \frac{\left[d \bullet \left(h_1^2 + h_2^2 \right) + 2h_1 \bullet h_2 \bullet \left| \sum_{l=1}^{d} e^{j\frac{2\pi\Delta k_l}{N_s}} \right| \cos(\varphi) \right]}{2\sin^2\theta} \right) d\theta d\varphi dh_1 dh_2 \} \end{aligned} \quad . \qquad (3.39)$$

This performance bound is much more complex than (3.34), however it provides a more exact analysis. The comparison of these two error probability bounds is provided in the following section along with the numerical results.

3.5 Numerical Results

3.5.1 The Computations of Convolutional Coding

For the exact bound (3.37), the only component which cyclic delay times have an effect on is the sum of the phase shifts over the possibly erroneously decoded symbols between

the original path and the error path with a Hamming distance of d: $\left|\sum_{l=1}^{d} e^{j\frac{2\pi\Delta k_l}{N_s}}\right|$. Meanwhile for the performance bound with the approximation (3.34), only the correlation matrix R_M is influenced by the cyclic shifts. Both $\left|\sum_{l=1}^{d} e^{j\frac{2\pi\Delta k_l}{N_s}}\right|$ and R_M depend on the codewords constructed by the channel coding, which we assume as convolutional coding here.

As the convolutional codes are symmetric codes [14], the difference of two arrays of uncoded signals determines the difference of two sequences of coded signals. Such as the encoded codeword of signal sequence '000000' is '000000000000'. '100000' (which differs with '000000' on the first bit) generates a codeword '111011000000'. The two codewords differ on the 1st, 2nd, 3rd, 5th and 6th symbols. Meanwhile the signal sequence '111111' generates '110110101010' and '011111' generates '001101101010'. The two codewords differ on the 1st, 2nd,3rd, 5th and 6th symbols as well. Because the probable erroneously decoded information bits are decided by the transmitted signal and the convolutional codes, every possible allocation of the error bits has to be included in the error probability calculation except the duplicated ones. (This case will be discussed in the following paragraph.) Therefore, when the trellis structure of a convolutional code is fixed, the probable error bits in each erroneous signal sequence are fixed and are unchanged for whatever the transmitted information bits are. That indicates the error symbols for each erroneously decoded codeword are the same for all possibly transmitted codewords. For instance, if the transmitted codeword is all zero, the erroneously decoded

codeword is '111011000000', which differs with the correct codeword on the 1st, 2nd, 3rd, 5th and 6th symbols. Then for any other transmitted codeword there is one probable erroneous codeword with errors on the 1st, 2nd, 3rd, 5th and 6th symbols.

As stated in Appendix A, whether the information signal $C_l = 0$ or 1, the pairwise error probability is the same for a BPSK signal. Therefore, the pairwise error probability only depends on the places of the symbols where two codewords differ, or, the absolute difference of the two codewords, which is independent of the exact phases of the BPSK signals. Therefore, codewords of all-zero signals can be assumed without loss of generality. The numerical calculation is based on all-zero signals in the following section. However for other modulation schemes, the pairwise error probability is dependent on the Euclidean distance of the two symbols.

All error paths that may cause an error at the first information bit (which is the one being decoded accounting for a sequence of signal bits of a certain traceback length) must be included for the calculation of error probability bound whereas the duplicate codewords should be excluded. We assume the convolutional coding for a constraint length of 3, the octal form of the generator polynomial of [7 5], and the trace back length of 5. The Viterbi decoding traces back to 5/coderate (coderate = 1/2) symbols for the detection of the first bit. As all-zero signals are assumed to be transmitted, only codewords which may introduce a '1' in the first bit should be calculated. In addition, repetitive codeword must be avoided. For example, '110011' has to be excluded because this case has already been

counted in with ‘110000’. Therefore, all signal arrays with two or more continuous ‘0’ should be excluded from the calculation.

To save time, the Viterbi decoding always records the merits, pre-states and input symbol of the previous bits. Therefore the merits cumulate from the first bit to the one being decoded. This mechanism causes a continuous feature. Although only the previous bits within a trace back length are recorded, the decision is based on all information bits that are transmitted beforehand. Therefore, the error probability (3.5.14) is not exactly the real case as in the practical world. However, this state merits left by the previous detection have little effect on the current detection as shown by the simulation results.

3.5.2 Simulation Results

The CDD system is shown in Figure 3.1. Firstly we considered a 2x1 CDD system, which had two transmit antennas and one receive antenna. The channels were quasi-static Rayleigh flat fading channels (quasi-static means the channel transfer functions keep static over a block of signals and vary block by block). BPSK signals were coded by convolutional coding. Two convolutional codes were considered. For the first case, the constraint length was 3, the octal form of the generator polynomial was [7 5], and the traceback length was 5 or 7. The other case had a constraint length of 5, a trellis generation code [23 35], and a traceback length of 5 or 7. On the receiver, the signals were decoded by Viterbi soft decision detection. For an OFDM system with frame length of 16, the comparison of the exact performance analysis bound produced by (3.39) and

the approximate performance analysis bound (3.34) as well as the simulation results at an E_b/N_o of 20dB is shown in Figure 3.3.

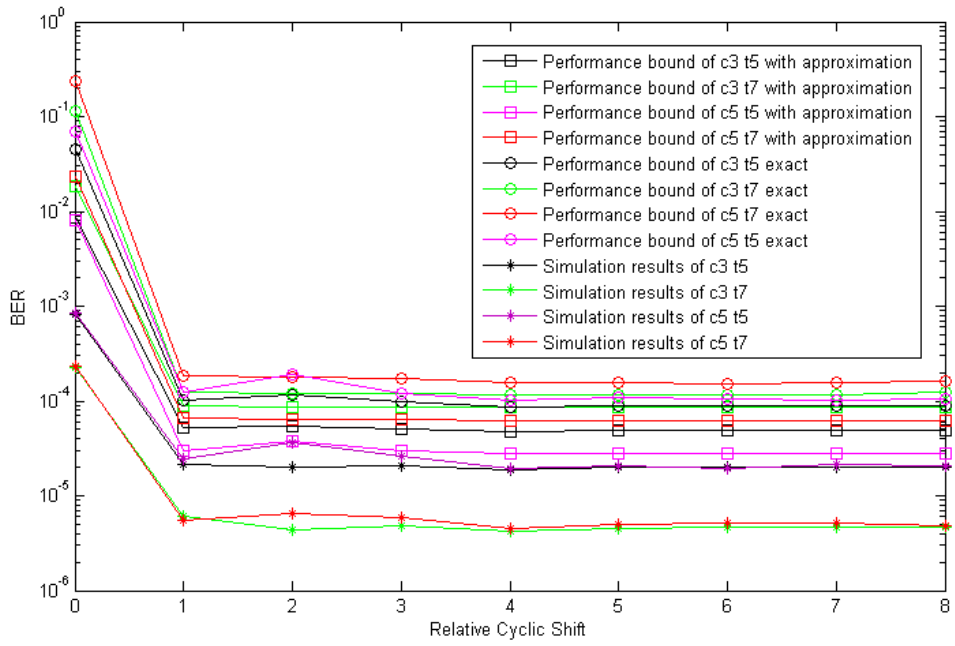

Figure 3.3 Comparison between the performance bounds and simulation results of the bit error probability of a 2x1 CDD system with varying cyclic delay time and an OFDM frame length of 16 in Rayleigh flat fading channels

From Figure 3.3, it can be seen both the exact BER performance bound and the approximated one yield the same varying shapes as the simulation results for different cyclic delay shifts. This feature demonstrated that the performance bounds provide a valuable prediction of the BER performance of CDD system with varying cyclic delay shift. Therefore, the performance bound, especially the one with approximation, can be used to calculate the optimum cyclic delay time for a minimum error probability. Compared to the exhaustive simulation or experimental search, this performance analysis saves a lot of time and is more efficient. In addition, performance analysis renders a

fundamental understanding of the mechanism of cyclic delay diversity and is instructive for CDD system design.

For an OFDM system with frame length of 64, the comparison of the BER between performance bounds and simulation results at an E_b/N_o of 20dB is shown in Figure 3.4. It can be observed that for both convolutional codes the approximated performance analysis bounds lays lower than the simulation results, while the exact performance analysis bounds lays upper than the simulation results. This error loss is because of the approximation scheme used in (3.34). However, the simulation results have the same shape as predicted by both of the performance analysis bounds.

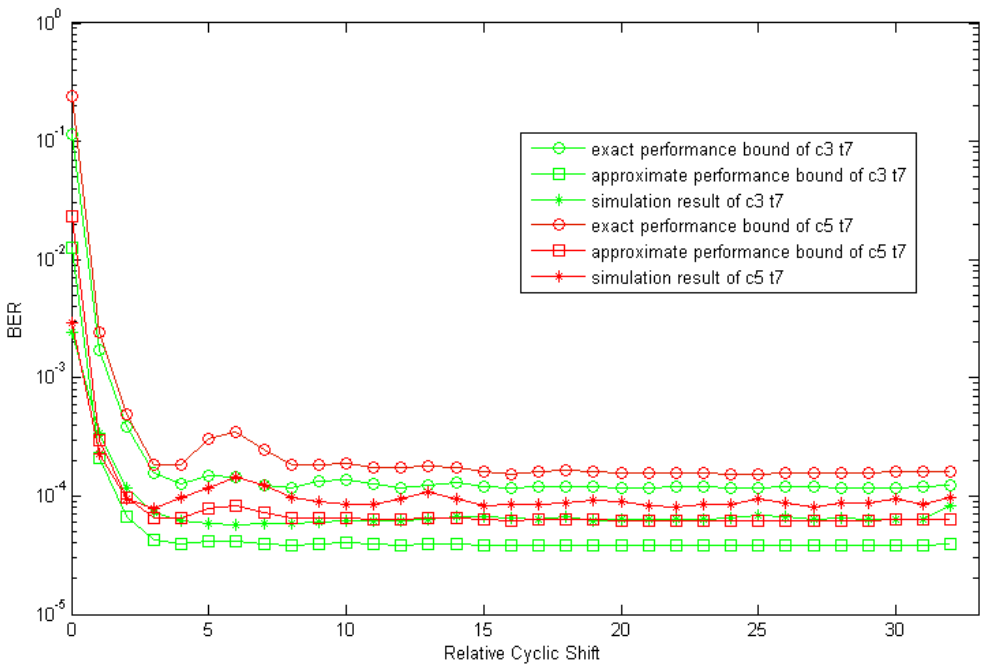

Figure 3.4 Comparison between the performance bounds and simulation results of bit error probability of 2x1 CDD systems with cyclic delay time varying and OFDM frame length of 64 in Rayleigh flat fading channels

3.6 Conclusions

For this chapter, based on the error probability analysis of CDD system with repetition coding in UWB channel in [3], a new bit error probability analysis bound for a cyclic delay diversity system combined with OFDM and convolutional coding in multipath Rayleigh fading channels has been derived. An approximation method has been used to reduce the computational complexity. These performance analysis results can be readily extended to any other kind of channel codes and fading channels. From the numerical results presented in Section 3.5 it can be observed that performance bounds provide a valuable prediction of the BER performance of a CDD system with varying cyclic delay shift. Therefore, the performance bound especially that developed with an approximation method can be used to calculate the optimum cyclic delay time for a minimum error probability. Compared to the exhaustive simulation or experimental search, this performance analysis saves a significant amount of time and is less computationally complex hence more efficient. In addition, the performance analysis renders a fundamental understanding of the mechanism of cyclic delay diversity and is instructive for CDD system design. This aspect will be utilized in the following chapters.

References

[1] V. Tarokh, N.Seshadri and R.A. Calderbank, “Space-time codes for high data rate wireless communication: Performance criterion and code construction,” *IEEE Trans. Inform. Theory*, vol.44, pp. 744-765, Mar. 1998.

[2] B.Vucetic and J. Yuan, *Space-Time Coding*, John Wiley, 2003.

[3] P. Tarasak, K. Png, X. Peng and F. Chin, “Design and performance of cyclic delay diversity in UWB-OFDM systems,” *Eurasip Journal Wireless Communication and Networking*, doi:10.1155/2008/541478, 2007.

[4] W. P. Siriwongpairat, W. Su and K. J. R. Liu, “Performance characterization of multiband UWB communication systems using Poisson cluster arriving fading paths,” *IEEE J. on Select. Areas in Commun.*, vol. 24, no. 4, pp. 745-751, 2006.

[5] L. Guerrero, F. Said, A. Lodhi and A. H. Aghvami, “Performance analysis of distributed CDD MC-CDMA sensor networks with frequency-correlated subcarriers over Nakagami-m fading channels,” in *Proc. of IEEE VTC*, pp. 81-85, 2008.

[6] A. Lodhi, F. Said, M. Dohler and A. H. Aghvami, “Closed-form symbol error probabilities of STBC and CDD MC-CDMA with frequency-correlated subcarriers over Nakagami-m fading channels,” *IEEE Transactions on Vehicular Technology*, Vol. 57, Issue 2, pp. 962-973, Mar. 2008.

[7] M. Bossert, A. Huebner, F. Schuehlein, H. Haas, and E. Costa, “On cyclic delay diversity in OFDM based transmission schemes,” in *Proc. OFDM Workshop*, Sep. 2002.

[8] G. Bauch, “Design of cyclic delay diversity with adaptive coding based on mutual information,” in *Proc. of the 10th International OFDM-Workshop*, Hamburg, Germany, pp. 184-188, Aug. 31st –Sep. 1st 2005.

[9] G. Bauch, “Capacity optimization of cyclic delay diversity,” *Proc. of IEEE VTC-Fall, Los Angeles, CA*, vol. 3, pp. 1820–1824, Sep. 2004.

[10] G. Bauch, “Aspects of delay diversity in OFDM,” *African Journal of Information & Communication Technology*, vol. 2, no. 1, pp. 12, 2006.

[11] G. Bauch, J. S. Malik, “Parameter optimization, interleaving and multiple access in OFDM with cyclic delay diversity,” in *proc. VTC 2004*, pp. 505-509, 2004.

[12] G. Bauch and J. S. Malik, “Cyclic delay diversity with bit-interleaved coded modulation in orthogonal frequency division multiple access,” *IEEE Transactions on Wireless Communications*, vol. 5, no. 8, pp. 2092-2100, 2006.

[13] A. Dammann and S. Kaiser, “Standard conformable antenna diversity techniques for OFDM and its application to the DVB-T sytem,” in *Proc. IEEE Global Telecommun. Conf. (GLOBECOM 2001)*, pp. 3100-3105, Nov. 2001.

[14] J. G. Proakis, *Digital Communications*, McGraw-Hill, 4th Edition, 2000.

[15] M. K. Simon and M. S. Alouini, *Digital Communication over Fading Channels*, Wiley-IEEE Press, 2nd Edition, Jan. 2005.

[16] A. M. Mathai and S.B. Provost: *Quadratic Forms in Random Variables: Theory and Applications*, Marcel Dekker, New York, 1992.

[17] R. A. Horn and C.R. Johnson, *Matrix Analysis*, Cambridge University Press, New York, 1985.

Chapter 4

Transmit CDD and Receive Antenna Selection

4.1 Introduction

Antenna selection is another diversity scheme which saves radio frequency (RF) chains and therefore significantly cuts down on the system complexity [1]. When channel state information (CSI) is available at the transmitter, transmit antenna selection outperforms OSTBC (using all the transmit antennas) for a better bit error rate performance [2]. However in some scenarios CSI is absent at the transmitter, e.g. in the mobile unit for a up link, in this case, transmitter diversity schemes can be combined with receiver antenna selection to obtain higher transmission quality rather than the systems with a single space diversity scheme.

There is a considerable amount of published research concerned with the performance analysis of orthogonal space-time coding with MIMO antenna subset selection and the optimum selection criteria. In [3], antenna selection combined with the orthogonal space-time coding techniques was analyzed based both on exact channel knowledge (ECK) and on statistical channel knowledge (SCK). The antenna selection principle for ECK is based on the instant outage probability of the system, which provides an equal diversity gain as if all of the antennas provided were employed. On the other hand, the antenna

selection criterion for SCK is based on the average probability of error, which offers a diversity order which depends on the number of the selected antennas. Some papers also report on the investigation of the performance for antenna selection criteria from the perspective of average SNR gain, such as in [4], or the channel capacity, such as in [5].

In this chapter, we investigate a new system with transmit cyclic delay diversity and receive antenna selection (TCDD/RAS). This system combines two space diversity schemes therefore it significantly improves the error probability performance of the system with very low additional complexity. At the same time, as both CDD and antenna selection are applicable to a variety of existing standards, so the resulting system is also practical. A novel antenna selection criterion, the maximum minimum post-processing signal to noise ratio (MMP-SNR) antenna selection rule for this system in a flat fading channel has been derived. A performance comparison is presented in the last section for different selection principles, which illustrates the advantage of the MMP-SNR criterion over the other selection criteria. The performance of TCDD/RAS system in frequency selective channels is investigated in the next chapter.

4.2 System Models

Firstly, the transmitter cyclic delay diversity and receiver antenna selection system are introduced in Figure 4.1. For comparison, another transmitter orthogonal space-time block coding and receiver antenna selection system is also provided. Furthermore, a new hybrid system which combines CDD and OSTBC in the transmitter as well as antenna selection in the receiver is also proposed to compensate the performance loss of CDD,

and to avoid the data rate reduction and the high decoding complexity incurred by OSTBC.

In order to isolate the diversity effect of the CDD transmitter, we assume i.i.d. quasi-static flat Rayleigh fading channels plus additive white Gaussian noise all through this chapter. As proved in [6], [7], CDD can retain a substantial diversity gain even in relatively strong frequency-selective channels. Therefore, our method can be further generalized to frequency selective channels, which will be introduced in the next chapter. However, the cyclic delays have to be large enough to be distinguished from the existing resolvable taps in the multipath channel as indicated in [8].

A. TCDD/RAS System

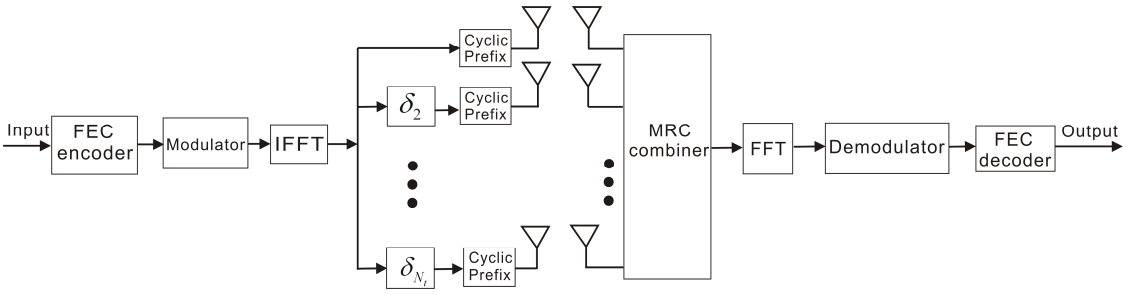

Figure 4.1 Transmit CDD and receive antenna selection system model

First, we consider the TCDD/RAS system as depicted in Figure 4.1. The signal bits were modulated after being coded by a forward error control/correction (FEC) block. OFDM was applied as an inverse fast Fourier transform (IFFT) with length of N_s. Afterwards, the signal vector was transmitted over N_t separate transmit antennas with cyclic delays δ_{n_t}, where n_t denotes the transmitter order. A cyclic prefix was inserted before the signal was transmitted to avoid the inter symbol interference (ISI) and inter carrier interference(ICI).

Antenna selection was implemented at the receiver side to choose L_r optimum receive antennas from N_r available receive antennas. Let $\mathrm{H} \in \mathbb{C}^{N_t \times N_r \times N_s}$ denote the original MIMO channel matrix, $\hat{\mathrm{H}} \in \mathbb{C}^{N_t \times L_r \times N_s}$ is the channel submatrix selected. Afterwards, maximal ratio combining (MRC) was used to combine the received symbols over the selected antennas. Following this, a standard OFDM demodulator was applied to recover the signal.

B. TOSTBC/RAS System

Figure 4.2 shows a traditional diversity system with OSTBC at the transmitter and antenna selection at the receiver side (TOSTBC/RAS).

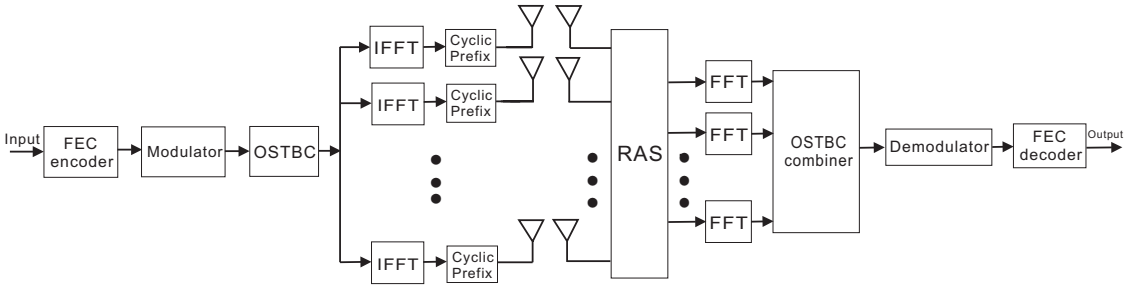

Figure 4.2 Transmit OSTBC and receive antenna selection system model

After the modulation, the signal streams were coded by the orthogonal space-time bock code and assigned to parallel IFFT blocks. Also a cyclic prefix was inserted as in a normal OFDM system. At the receiver side, antenna selection was carried out to select L_r antennas from N_r. After the FFT modulation, a STBC decoder was applied to combine the signals from the L_r receivers. It can be seen that the STBC scheme induces more complexity than CDD.

C. TCDD-OSTBC/RAS System

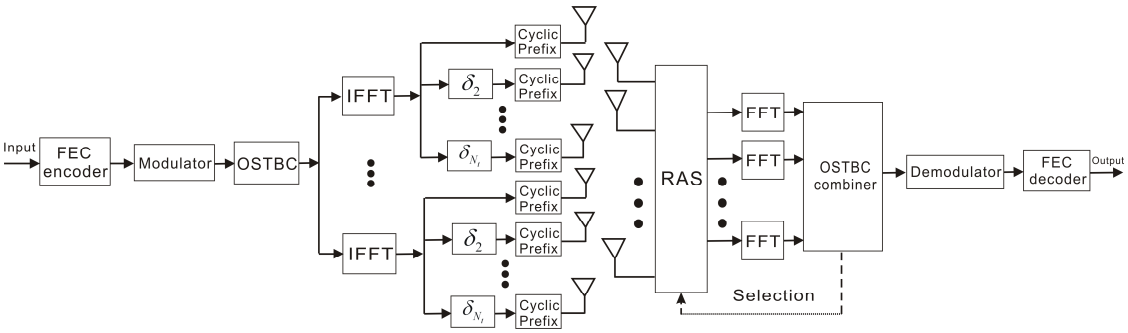

Figure 4.3 Transmit OSTBC-CDD and receive antenna selection system model

A new system with both orthogonal space time block coding and cyclic delay diversity in the transmitter is presented in [9], to obtain more diversity gain. Figure 4.3 shows a TCDD-OSTBC/RAS system with both OSTBC and CDD in the transmitter and antenna selection applied in the receiver as a comparison. After the channel coding and modulation, signals were firstly fed to an Alamouti encoder to map each two consecutive symbols onto two parallel signal streams. Then these two streams were modulated by an IFFT separately. Afterwards, CDD was employed to assign these two symbol arrays onto N_t transmit antennas. CDD usually ensures the channel coefficients for two neighbouring subcarriers to be uncorrelated, and this may result in total failure of the Alamouti scheme. Therefore, an interleaver should be introduced to make sure that the channel parameters on two successive subcarriers are highly correlated. Channel estimation should be applied for each group of transmit antennas which send out the same signal array coded by OSTBC but shifted and mixed by CDD.

This concatenated CDD-STBC transmitter diversity is derived to compensate the performance loss of CDD, and meanwhile reduce the complexity demand compared with the OSTBC schemes. Moreover, it does not decrease the data rate when the transmit antenna number is larger than two for transmitting complex signals.

The TCDD/RAS system will be investigated in the following sections. The optimum antenna selection criterion of TCDD/RAS will be analyzed. The performance of the TOSTBC/RAS system and the TCDD-OSTBC/RAS system will be provided for comparison.

4.3 TCDD/RAS System Analysis

4.3.1 Receive Antenna Selection Criterion Based on System Performance Analysis

A novel antenna selection criteria based on the system performance analysis can be designed according to either statistical channel knowledge (SCK) or exact channel knowledge (ECK).

1) SCK Based

In the TCDD/RAS system, the optimum antenna selection principle, to minimize the error probability, is based on the BER performance analysis generated in Chapter 3. As stated in (3.20),

$$P_e = \frac{1}{\pi}\int_0^{\pi/2}\prod_{n_r=1}^{N_r}\prod_{n=1}^{M}\frac{1}{1+\dfrac{E_s \nu_n eig_n^{n_r}\left(R_M^{N_r}\right)}{4N_o N_t \sin^2\theta}}d\theta, \tag{4.1}$$

to minimize the error probability is to maximize the eigenvalues $eig_n^{n_r}\left(R_M^{N_r}\right)$. Let $\mathrm{H}_{equ}^{n_r} = [H_{equ,1}^{n_r}, H_{equ,2}^{n_r}, \cdots, H_{equ,M}^{n_r}]'$. The covariance matrix of $\mathrm{H}_{equ}^{n_r}$ is $r_M^{n_r} = E\left(\mathrm{H}_{equ}^{n_r}\mathrm{H}_{equ}^{n_r\ H}\right)$. According to (3.22), the elements of the covariance matrix of B_{equ}, $R(n,n')$ are equal to zero when $n_r \neq n_r'$. Therefore,

$$eig_n^{n_r}\left(R_M^{N_r}\right) = eig_p(r_M^{n_r}), \tag{4.2}$$

where $eig_p(r_M^{n_r})$ is the pth eigenvalue of the covariance matrix $r_M^{n_r}$. Now, to minimize the pairwise error probability of the TCDD/RAS system, it is necessary to select the receiver antennas with the largest eigenvalues $eig_n(r_M^{n_r})$. The selection criterion based on the pairwise error probability can be presented as

$$\varpi_{pe\_SCK}^{*} = \arg\max_{L_r \le N_r}\left\{\prod_{n_r=1}^{L_r}\prod_{n=1}^{M}\left(1+\frac{E_s \nu_n eig_n\left(r_M^{n_r}\right)}{4N_o N_t \sin^2\theta}\right)\right\}, \tag{4.3}$$

where $\varpi_{pe\_SCK}^{*}$ denote the selected channel subset indices. The integral can be eliminated for simplification. However, not only one pairwise error probability has to be considered but the pairwise error probability for every possibly erroneous codeword of a practical channel coding scheme, such as convolutional coding, has to be taken into account. Therefore, the selection criterion based on bit error rate probability can be represented as

$$\varpi_{pe\_SCK}^{*} = \arg\min_{L_r \le N_r}\left\{\sum_{d=d_{free}}^{\infty}\beta_d\prod_{n_r=1}^{L_r}\prod_{n=1}^{M_d}\frac{1}{1+\frac{E_s \nu_n eig_n\left(r_{M_d}^{n_r}\right)}{4N_o N_t \sin^2\theta}}\right\}, \tag{4.4}$$

where $r_{M_d}^{n_r}$ denotes the covariance matrix of the equalized channel for the dth codeword and the n_rth receiver.

2) ECK Based

As in Chapter 3, the pairwise error probability for a CDD system with forward error correction (FEC) in a MIMO channel is given in (3.11)

$$P_e = E\left[\frac{1}{\pi}\int_0^{\pi/2}\exp\left(-\frac{E_s\left\|\Delta_S \mathrm{A}_{equ}\right\|^2}{4N_oN_t\sin^2\theta}\right)d\theta\right] \quad . \tag{4.5}$$

Because the antenna selection is applied on exact channel information, the expectation operator can be elimitated. According to (A.15), the bit error probability bound for convolutional code as the FEC code can be written as

$$P_b < \sum_{d=d_{free}}^{\infty}\beta_d\frac{1}{\pi}\int_0^{\pi/2}\exp\left(-\frac{E_s\left\|\Delta_S \mathrm{A}_{equ}\right\|^2}{4N_oN_t\sin^2\theta}\right)d\theta \ . \tag{4.6}$$

For a certain modulation scheme, Δ_S can be denoted as a constant v, then (4.6) can be rewritten as

$$\begin{aligned} P_b &< \sum_{d=d_{free}}^{\infty}\beta_d\frac{1}{\pi}\int_0^{\pi/2}\exp\left(-\frac{E_s v\left\|\mathrm{A}_{equ}\right\|^2}{4N_oN_t\sin^2\theta}\right)d\theta \\ &< \sum_{d=d_{free}}^{\infty}\beta_d\frac{1}{\pi}\int_0^{\pi/2}\exp\left(-\frac{E_s v\sum_{n_r=1}^{N_r}\sum_{k=1}^{M}\left|H_{equ,k}^{n_r}\right|^2}{4N_oN_t\sin^2\theta}\right)d\theta \quad . \end{aligned} \tag{4.7}$$

The bit error probability over one OFDM frame can be written as

$$P_f < \frac{1}{N_s-M+1}\sum_{n=0}^{N_s-M}\sum_{d=d_{free}}^{\infty}\beta_d\frac{1}{\pi}\int_0^{\pi/2}\exp\left(-\frac{E_s v\sum_{n_r=1}^{N_r}\sum_{k=0}^{M-1}\left|H_{equ,k+n}^{n_r}\right|^2}{4N_oN_t\sin^2\theta}\right)d\theta, \tag{4.8}$$

where N_s is the OFDM frame length.

Therefore, the antenna selection scheme based on the bit error probability can be written as

$$\varpi_{P_f}^{*} = \arg\min_{L_r \le N_r} \left\{ P_f \left| L_r \right. \right\}$$

$$= \arg\min_{L_r \le N_r} \left\{ \frac{1}{N_s - M + 1} \sum_{n=0}^{N_s - M} \sum_{d=d_{free}}^{\infty} \beta_d \frac{1}{\pi} \int_0^{\pi/2} \exp\left(- \frac{E_s v \sum_{n_r=1}^{L_r} \sum_{k=0}^{M-1} \left| H_{equ,k+n}^{n_r} \right|^2}{4 N_o N_t \sin^2 \theta} \right) d\theta \right\}, \qquad (4.9)$$

where $\varpi_{P_f}^{*}$ indicate the selected channel subset indices.

Even if (4.4) and (4.9) are the ideal optimum antenna selection criteria for TCDD/RAS systems, it is difficult to obtain because of the high complexity. Therefore, in the following sections, alternative antenna selection principles are introduced to minimize the error probability at the same time with reasonable computation complexity.

4.3.2 An Optimum Receiver Antenna Selection Criterion

In this section, we apply antenna selection based on the exact channel knowledge (ECK) as discussed in Section 4.3.1. The best antenna subset is selected with maximum post processing SNR and therefore the lowest BER.

1) Norm Selection Criterion

The norm selection was proposed for antenna selection combined with the OSTBC schemes. Extensive work has been done with respect to combining transmit orthogonal space-time block coding diversity with antenna selection, where the antenna selection is executed at either the transmitter side or the receiver side. The antenna selection methods in these papers are mostly based on the post-processing SNR, [3], [4], [5], [12], [13], [14], [15], except [16] which is based on a capacity perspective. From the simulation results in

these papers, it can be seen that the selection criterion based on post-processing SNR achieves a better performance. As indicated in [16], [17], the post processing SNR for OSTBC is

$$\gamma_{OSTBC} = \gamma_0 \left\| \mathrm{H} \right\|^2, \tag{4.10}$$

where γ_0 is the average SNR at one receiver from one transmit antenna, H is the $N_t \times N_r$ channel matrix between the transmit and receive antennas and $\left\| \bullet \right\|^2$ denotes the Frobenius norm operation. The relationship between the symbol error probability and the post-processing SNR has been presented in [11]. Therefore, the selection criterion for OSTBC and antenna selection system is to select the antenna subset with the largest Frobenius norm. This selection rule is denoted as the norm selection criterion here. Let $\hat{\mathrm{H}}$ denote the channel matrix of the selected antenna subset, so the antenna selection principle can be represented as

$$\omega_{Norm}^{*} = \arg\max_{L_r \le N_r} \left\{ \left\| \hat{\mathrm{H}} \right\|^2 \right\}, \tag{4.11}$$

where ϖ_{Norm}^{*} denote the optimal selection indices of $\hat{\mathrm{H}}$ from H with the norm selection criterion.

2) Optimized Selection Criteria for the TCDD/RAS System

TCDD/RAS system means the system with transmit CDD and receive antenna selection. After selecting L_r antennas from N_r at the receiver, MRC was applied to combine the signal streams over the selected antennas. It has been proven in [18] that the post-processing SNR after MRC is just the sum of the SNRs from all receive antennas. Therefore, in the TCDD/RAS system, the post-processing SNR at the *k*th subcarrier can be denoted as

$$\gamma_{k,TCDD/RAS} = \gamma_0 \sum_{n_r=1}^{L_r} \left| H_{equ,k}^{n_r} \right|^2 \quad , \tag{4.12}$$

where $H_{equ,k}^{n_r}$ denotes the equalized channel transfer function defined in Chapter 3. As denoted in Section 4.2, because we assume the channels are flat-fading, the channel transfer functions $H_k^{n_t,n_r}$ can be simplified as H^{n_t,n_r} without loss of the generality. Hence the average post-processing SNR over the whole spectrum will be

$$\begin{aligned}
\overline{\gamma}_{TCDD/RAS} &= E\left\{\gamma_{k,TCDD/RAS}\right\} \\
&= \frac{1}{N_s}\gamma_0 \sum_{k=0}^{N_s-1}\sum_{n_r=1}^{L_r}\left|H_{equ,k}^{n_r}\right|^2 \\
&= \frac{1}{N_s}\gamma_0 \sum_{k=0}^{N_s-1}\sum_{n_r}^{L_r}\left\{\left[\sum_{p=1}^{N_t} H^{(n_t,n_r)} e^{j\frac{2\pi}{N_s}\delta_p k}\right]\left[\sum_{l=1}^{N_t}\left(H^{(n_t,n_r)}\right)^* e^{-j\frac{2\pi}{N_s}\delta_l k}\right]\right\} \\
&= \frac{1}{N_s}\gamma_0 \sum_{n_r=1}^{L_r}\left(\sum_{k=0}^{N_s-1}\sum_{n_t=1}^{N_t}\left|H^{(n_t,n_r)}\right|^2 + \underbrace{\sum_{k=0}^{N_s-1}\sum_{\substack{p=1,l=1 \\ p\neq l}}^{N_t} H^{(p,n_r)}H^{(l,n_r)} e^{j\frac{2\pi}{N_s}(\delta_p-\delta_l)k}}_{=0}\right), \\
&= \frac{1}{N_s}\gamma_0 \sum_{n_r=1}^{L_r} N_s \sum_{n_t=1}^{N_t}\left|H^{(n_t,n_r)}\right|^2 \\
&= \gamma_0 \left\|\mathrm{H}\right\|^2
\end{aligned} \tag{4.13}$$

which is the same as in the TOSTBC/RAS system, where $E\{\bullet\}$ denotes the expectation operation over all of the subcarrier orders k, $(\bullet)^*$ denotes conjugation operation. However, in the TCDD/RAS system, as indicated in (4.12), the post-processing SNRs on different subcarriers are not equal. The correlations between the channels from different transmit antennas have an effect on $\left|H_{equ,k}^{n_r}\right|^2$ and thereafter make $\gamma_{k,TCDD/RAS}$ frequency selective [10]. Therefore, the norm selection criterion for TOSTBC/RAS systems cannot be applied to the TCDD/RAS system directly.

As we know, $\gamma_{k,TCDD/RAS}$ has a lower bound $\gamma_0 \min_k \left\{ \sum_{m=1}^{L_r} \left| H_{equ,k}^{n_r} \right|^2 \right\}$. The performance of the selected transmit CDD and receive MRC system will be improved as the smallest possible post-processing SNR increases, since the BER is mostly determined by relatively small SNRs where most errors occur. However, the impairment of SNRs on a small number of subcarriers can be combated by channel coding. As stated in Chapter 3, for a system with more than four transmit antennas, the cyclic delay shift selection criterion (3.31) can be applied. In this case, the sum of equalized channel parameters $H_{equ,k}^{n_r}$ only has N_t distinct states. When $N_t \ll N_s$, the channel parameters at each state will have a significant influence on the BER performance. Hence, if we select a receiver subset to have the maximum value of the quantity $\min_k \left\{ \sum_{m=1}^{L_r} \left| H_{equ,k}^{n_r} \right|^2 \right\}$, the possible lowest $\gamma_{k,TCDD/RAS}$ will be maximized, and consequently, the error probability will be reduced. Therefore a new maximum minimum post-processing SNR (MMP-SNR) criteria can be represented as

$$\varpi_{MMP-SNR}^{*} = \arg\max_{L_r \le N_r} \left\{ \min_k \left\{ \sum_{n_r=1}^{L_r} \left| H_{equ,k}^{n_r} \right|^2 \right\} \right\}, \qquad (4.14),$$

where $\varpi_{MMP-SNR}^{*}$ are the optimal indices of selected receivers from the N_r receive antennas with the MMP-SNR selection criterion.

3) Optimized Selection Criterion for the TCDD-OSTBC/RAS System

Assuming the serial signals before OSTBC in the frequency domain as S_k, the parallel signals encoded by OSTBC in the frequency domain are $S_k^{n_{st}}$, where n_{st} denotes the order

of the encoded OSTBC signals and *k* denotes the subcarrier index. As shown in Figure 4.3, after the IFFT block, the parallel signals were shifted by CDD. The cyclic delay shift was applied within the n_{st}th signal array. The received signal at the n_rth receive antenna in the frequency domain can be presented as

$$R_k^{n_t,\,n_r} = \sum_{n_t=1}^{N_t} S_k^{n_{st}} e^{j\frac{\delta_{n_t}^{n_{st}} k}{2\pi N_s}} H_k^{n_t,\,n_r} + n_k^{n_r} = \sum_{n_{st}=1}^{N_{st}} S_k^{n_{st}} H_{equ,\,k}^{n_{st},\,n_r} + n_k^{n_r}, \tag{4.15}$$

where $\delta_{n_t}^{n_{st}}$ denotes the cyclic delay time on the n_tth transmit antenna for the n_{st}th OSTBC signal array, $n_k^{n_r}$ denotes the additive white Gaussian noise at the n_rth receiver on the *k*th subfrequency, $H_{equ,\,k}^{st,\,n_r}$ denotes the equalized channel for the n_{st}th OSTBC signal array at the n_rth receive antenna, $H_{equ,\,k}^{n_{st},\,n_r} = \sum_{n_{cdd}=1}^{N_{cdd}} e^{j\frac{\delta_{n_t}^{n_{st}} k}{2\pi N_s}} H_k^{n_t,\,n_r}$ ($n_t = n_{cdd} + (n_{st} - 1) \times N_{cdd}$, $N_{cdd} = \frac{N_t}{N_{st}}$), n_{cdd} denotes the order of CDD transmit antenna for the n_{st}th OSTBC signal array, and N_s denotes the OFDM frame length. Channel estimation is employed to estimate each $H_{equ,\,k}^{st,\,n_r}$ for the n_{st}th signal array, and the separate channel estimation for each transmit antenna using specific cyclic delay time can be eliminated. Then the combination scheme for OSTBC mentioned in [17] is implemented. Here we assume that a 2 transmitter Alamouti scheme is employed. Then the detected signal after combination and MRC can be written as

$$\begin{aligned} \hat{S}_{k_1} &= \sum_{n_r=1}^{N_r} \left(\left| H_{equ,k_1,k_2}^{n_1,n_r} \right|^2 + \left| H_{equ,k_1,k_2}^{n_2,n_r} \right|^2 \right) S_{k_1} + \sum_{n_r=1}^{N_r} \left(H_{equ,k_1,k_2}^{n_1,n_r} * n_{k_1}^{n_r} + H_{equ,k_1,k_2}^{n_2,n_r} n_{k_2}^{n_r} * \right) \\ \hat{S}_{k_2} &= \sum_{n_r=1}^{N_r} \left(\left| H_{equ,k_1,k_2}^{n_1,n_r} \right|^2 + \left| H_{equ,k_1,k_2}^{n_2,n_r} \right|^2 \right) S_{k_2} + \sum_{n_r=1}^{N_r} \left(H_{equ,k_1,k_2}^{n_1,n_r} n_{k_2}^{n_r} * + H_{equ,k_1,k_2}^{n_2,n_r} * n_{k_1}^{n_r} \right) \end{aligned} . \tag{4.16}$$

As an interleaver is applied here to guarantee that the channel coefficients on consecutive subcarriers stay as a constant, it is assumed that $H_{equ,k_1,k_2}^{n_t,n_r} = H_{equ,k_1}^{n_t,n_r} = H_{equ,k_2}^{n_t,n_r}$. Therefore the signal power gains achieved by the joint OSTBC and CDD scheme can be presented as $\sum_{n_r=1}^{N_r}\left(\left|H_{equ,k_1,k_2}^{n_1,n_r}\right|^2+\left|H_{equ,k_1,k_2}^{n_2,n_r}\right|^2\right)$ or $\sum_{n_r=1}^{N_r}\left(\left|H_{equ,k_1,k_{21}}^{n_1,n_r}\right|^2+\left|H_{equ,k_1,k_2}^{n_2,n_r}\right|^2\right)$. Compared with the TCDD/RAS system, a new receive antenna selection rule similar to the MMP-SNR rule can be generated as

$$\varpi_{MMP-norm}^{*} = \arg\max_{L_r \le N_r}\left\{\min_{k_1,k_2}\left\{\sum_{n_r=1}^{N_r}\left(\left|H_{equ,k_1,k_2}^{n_1,n_r}\right|^2+\left|H_{equ,k_1,k_2}^{n_2,n_r}\right|^2\right),\ \sum_{n_r=1}^{N_r}\left(\left|H_{equ,k_1,k_{21}}^{n_1,n_r}\right|^2+\left|H_{equ,k_1,k_2}^{n_2,n_r}\right|^2\right)\right\}\right\}, \tag{4.17}$$

where $\varpi_{MMP-norm}^{*}$ denote the selected antenna subset indices. This antenna selection criterion is a combination of the MMP-SNR rule and the norm selection rule so that it can be simply called as MMP-norm criterion.

4) Capacity Selection Criterion

A capacity selection criterion should also be introduced here for comparison. It is designed to select the antenna subset with the maximum possible channel capacity [16]. The selection principle can be denoted as

$$\varpi_{Cap}^{*} = \arg\max_{L_r \le N_r}\left\{\frac{1}{N_s}\sum_{k=1}^{N_s}\log\left[\det\left(\mathrm{I}_{N_r}+\frac{\gamma_0}{N_t}\hat{\mathrm{H}}\hat{\mathrm{H}}^{H}\right)\right]\right\}, \tag{4.18}$$

where ϖ_{Cap}^{*} denote the selected antenna subset indices, $\det(\bullet)$ stands for the determinant operation, $(\bullet)^{H}$ denotes the Hermitian transpose operation and I_{N_r} is a $N_r \times N_r$ identity matrix.

4.3.3 Receive Antenna Selection Algorithm with Cross Entropy Optimization Method

To further optimize the computation of the selection criteria and reduce the calculation complexity, a cross entropy optimization method is introduced in this section (the algorithm is developed by Y. Zhang [23]).

In order to execute these selection criteria efficiently, we transform the antenna selection problem into a combinatorial optimization problem, which can be solved by the cross entropy optimization (CEO) method. The CEO algorithm has been proved to be a global random search procedure in [19] and [20]. It was firstly presented by Rubinstein as a principled adaptive importance sampling to estimate the probabilities of rare events in the complex stochastic networks [21]. It has also been adopted to solve complicated combinatorial optimization problems, such as the nondeterministic polynomial time (NP) problems [19]. In order to apply the CEO method to the antenna selection schemes, we have to formulate the antenna selection problem as a combinatorial optimization problem:[22]

$$\varpi^* = \arg\max_{\omega_q \in \Omega} S\left(\omega_q\right), \tag{4.19}$$

where ϖ^* denotes the indicator corresponding to the global optimum of the objective function $S\left(\omega_q\right)$, which is used for evaluating the potential solutions, ω_q, and chosen according to the specific selection criteria, such as the norm and the capacity selection

criteria. Ω is the set of receive antenna subset selection indicators $\{\omega_1, \omega_2, \cdots \omega_Q\}$. Herein, ω_q is defined as

$$\omega_q = \{I_{n_r}\}_{n_r=1}^{N_r},\ I_{n_r} \in \{0,1\};\ q = 1,2,\cdots,Q, \tag{4.20}$$

where I_{n_r} indicates whether the n_r*th* receive antenna is selected or not. For example, if the first, fourth, fifth and eighth receive antennas are selected out of eight receive antennas, then ω_q will be equal to $\{1,0,0,1,1,0,0,1\}$. Q is the number of all possible antenna subsets and is equal to $\binom{N_r}{L_r}$, where $\binom{x}{y}$ denotes the binomial coefficient, $\frac{x!}{y!(x-y)!}$. The flow of the receive antenna selection algorithm based on the CEO method is described as follows: [22]

Step 1: Start with an initial $P^{(0)} = \{p_{n_r}^{(0)}\}_{n_r=1}^{N_r}$, $p_{n_r}^{(0)} = \frac{1}{2}$. Set the iteration counter $t := 1$;

Step 2: Generate samples $\{\omega_q^{(i)}\}_{i=1}^{N_{CEO}}$ from the density function $f\left(\bullet, P^{(t-1)}\right)$, where N_{CEO} is the total number of the samples;

Step 3: Calculate the performance functions $\left\{S\left(\omega_q^{(i,t)}\right)\right\}_{i=1}^{N_{CEO}}$ and order them from largest to smallest, $S^{(1)} \geq \cdots \geq S^{(N_{CEO})}$. Let $r^{(t)}$ be $(1-\rho)$ the sample quantile of the performances: $r^{(t)} = S^{(\lceil (1-\rho)N_{CEO} \rceil)}$, where $\lceil \bullet \rceil$ is the ceiling operation.

Step 4: Update the parameter $P^{(t)}$ via

$$p_{n_r}^{(t)} = \frac{\sum_{i=1}^{N_{CEO}} I_{\{S(\omega_q^{(i,t)}) \geq r(t)\}} I_{n_r}\left(\omega_q^{(i,t)}\right)}{\sum_{i=1}^{N_{CEO}} I_{\{S(\omega_q^{(i,t)}) \geq r(t)\}}}. \tag{4.21}$$

Step 5: If stopping criterion is satisfied, then stop; otherwise set $t := t+1$ and go back to step 2. Here, the stopping criterion is the predefined number of iterations.

Due to space restriction, the detailed description about the antenna selection algorithm with the CEO method will not be presented in this thesis, but reader can refer to [23]. The algorithm converges without requiring a particular starting point, but for simplicity we set $p_{n_r}^{(0)} = \frac{1}{2}$.

Now, two antenna selection criteria are produced and an optimization algorithm with cross entropy optimization method is also introduced. In the following section, the numerical results of these selection criteria and the performance with other selection principles are presented.

4.4 Numerical Results

In this section, Monte Carlo simulation results of the TCDD/RAS system with multiple receive antenna selection criteria are presented. Performances of the TCDD-OSTBC/RAS system and the TOSTBC/RAS system are also provided for comparison.

Firstly we consider the performance comparison of the TCDD/RAS system with three different antenna selection rules, and the TOSTBC/RAS system with two selection criteria as well. Here we set $N_t = 4$, $L_r = 4$ and $N_r = 8$. The cyclic delay is chosen according to (3.31). The OSTBC code in [24] is adopted to form a 4 transmitter OSTBC

scheme with a code rate of ¾, which indicates a data rate reduction to 3/4. The signals are mapped to 16QAM constellation and coded by a half rate convolutional code with a constraint length of 3 and a free distance of 5.

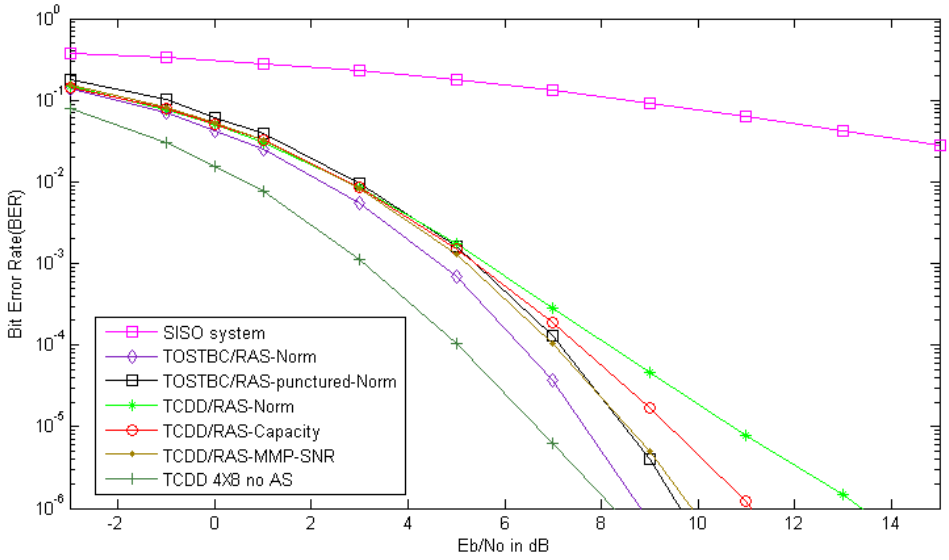

Figure 4.4 Performance comparison of a TCDD/RAS system with three antenna selection criteria and a TOSTBC/RAS system with norm selection criterion, $N_t = 4$, $L_r = 4$, $N_r = 8$.

From Figure 4.4, it can be seen that the MMP-SNR selection criterion yields the best BER performance among the three antenna selection criteria for the TCDD/RAS system, where E_b/N_o denotes the signal energy per bit to noise power spectral density ratio. The norm criterion for the TCDD/RAS system performs 3dB worse at a BER of 10^{-6} than the MMP-SNR selection rule. The capacity criterion obtains a better diversity gain (which is indicated by the slope of the curve) than the norm selection rule but still suffers 1.2dB loss at a BER of 10^{-6} compared with the MMP-SNR. On the other hand, the TCDD/RAS system using the MMP-SNR criterion achieves a diversity gain of 8 compared to a diversity gain of 9 for the corresponding transmit orthogonal space-time block coding diversity scheme combined with optimum receive antenna selection of the same number

of antennas. The diversity gain is calculated according to (2.12) and normalized by the diversity gain of a single antenna system with no diversity scheme neither in the transmitter or the receiver. The diversity gain of the reference single antenna system is defined as 1 unit. However the TCDD/RAS system requires much lower additional complexity, suffers no data rate loss and offers compatibility to many existing standards.

Since for the four transmitter system, the OSTBC code suffers from a data rate loss to a rate of 3/4, we can puncture the convolutional code from a rate of 1/2 to a rate of 2/3 to retain the full data rate as in the CDD system, which has been suggested in [18]. The free distance of the punctured convolutional code is 3. The performance curve of this punctured STBC system is inferior to our TCDD/RAS system when E_b/N_o is smaller than 8dB as depicted in Figure 4.3. It is predictable that with a more powerful channel coding scheme, the spatial diversity provided by CDD can be exploited more efficiently, and the performance gap between the TCDD/RAS system and the TOSTBC/RAS system can be further reduced. But the performance is already acceptable even with our simple channel coding scheme.

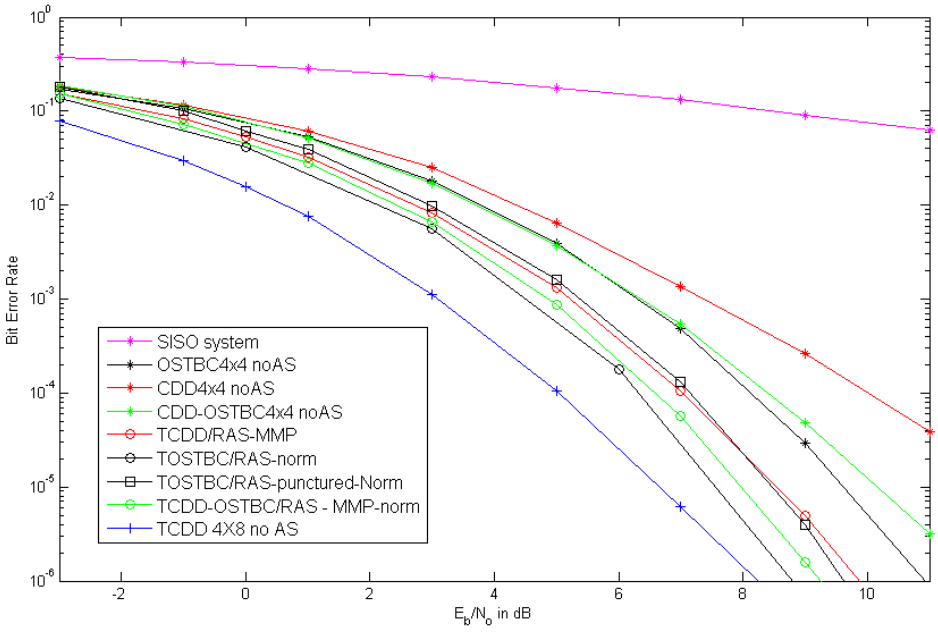

Figure 4.5 Performance comparison of a TCDD/RAS system, a TOSTBC/RAS system and a TCDD-OSTBC/RAS system with a convolutional code of a constraint length of 3, $N_t = 4$, $L_r = 4$, $N_r = 8$.

Figure 4.5 shows the performance of a TCDD-OSTBC/RAS system compared with the TCDD/RAS system and the TOSTBC/RAS system. It is observed that without antenna selection in the receiver, the CDD-OSTBC scheme, which has both CDD and OSTBC employed in the transmitter, performs 1.5dB better than the CDD system but only 0.2dB worse than the OSTBC system at a BER of 10^{-4}, but the CDD-OSTBC scheme incurs no data rate degradation and requires much lower additional complexity compared with the OSTBC system. For the TCDD-OSTBC/RAS system with antenna selection in the receiver, the antenna selection criterion can be a combination of the norm selection for the OSTBC scheme and the MMP-SNR selection for the CDD scheme. The only difference is to apply the MMP-SNR selection after the combination of the signal powers from the equalized parallel channels which carry the OSTBC signals. It can be seen that

the TCDD-OSTBC/RAS system appears 0.6dB better than the TCDD/RAS system and 0.5dB better than the punctured TOSTBC/RAS system at a BER of 10^{-5}. Even it still performs 0.4dB worse at a BER of 10^{-5} than the TOSTBC/RAS system, it suffers no spectral efficiency reduction and is of much lower complexity.

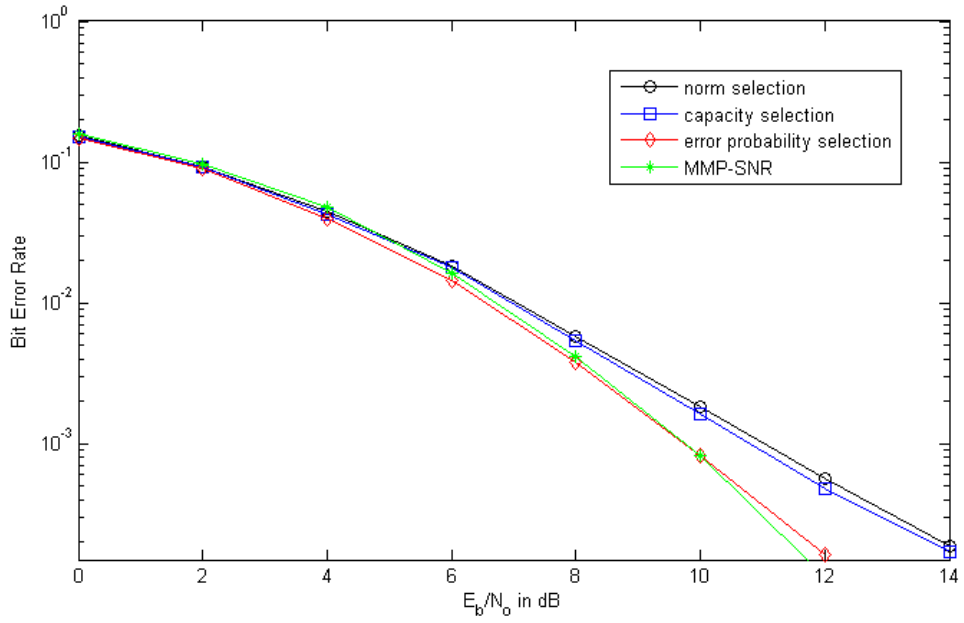

Figure 4.6 Performance of a TCDD/RAS system with four antenna selection criteria, with convolutional coding, $N_t = 4$, $L_r = 2$, $N_r = 4$.

Figure 4.6 shows BER performance of a TCDD/RAS system with four antenna selection criteria. The FEC code is a convolutional code with a constraint length of 3. The number of the transmit antennas is 4, the number of the selected receive antennas is 2 and the total available receive antenna number is 4. The MMP-SNR selection rule performs 2.5dB better than the norm selection principle and 2.3dB better than the capacity selection rule at a BER of 2×10^{-4}. It even performs 0.3dB better at a BER of 2×10^{-4} than the error probability selection criterion.

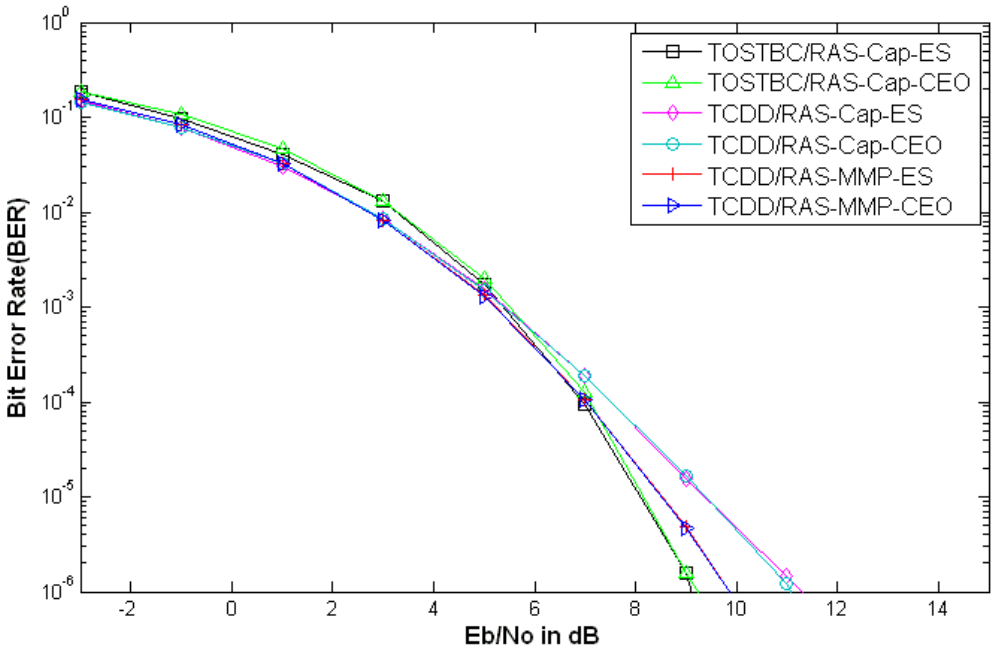

Figure 4.7 Performance comparison between exhaustive search and CEO, N_t =4, L_r = 4, N_r = 8.

(N_r, L_r)	N_{CEO}	t	*O(CEO)*	*O(ES)*	ϑ
(8, 2)	5	3	15	28	≤1%
(8, 4)	10	3	30	70	≤1%
(8, 6)	5	3	15	28	≤1%

Table 4.1 Complexity comparisons between the CEO algorithm and ES method with N_t = 4. [22]

Table 4.1 presents a computational complexity comparison between antenna selection schemes based on the CEO and the exhaustive search (ES) algorithms. The complexity is measured by the number of function evaluations *O*(*CEO*) and *O*(*ES*). In this table, *t* and N_{CEO} are parameters of the CEO algorithm, standing for the numbers of algorithm

iterations and samples, respectively. ϑ(equals to $\frac{S_{CEO} - S_{optim}}{S_{optim}}$, S_{CEO} and S_{optim} denote the BER obtained by the CEO algorithm and the ES method) is the performance difference ratio of the bit error rate produced by the CEO algorithm. From Table.4.1, we find that the CEO algorithm only requires approximately 50% of the computational complexity required by the exhaustive search strategy. From the performance difference ratio, ϑ, it can be observed that the performance difference in terms of BER between the CEO algorithm and the ES method is less than 1%. Figure 4.7 shows the performance comparison between the CEO and the ES algorithms. From it, we find that the BER performance obtained by the CEO algorithm is very close to the optimum performance obtained by the ES method for a wide range of SNR values.

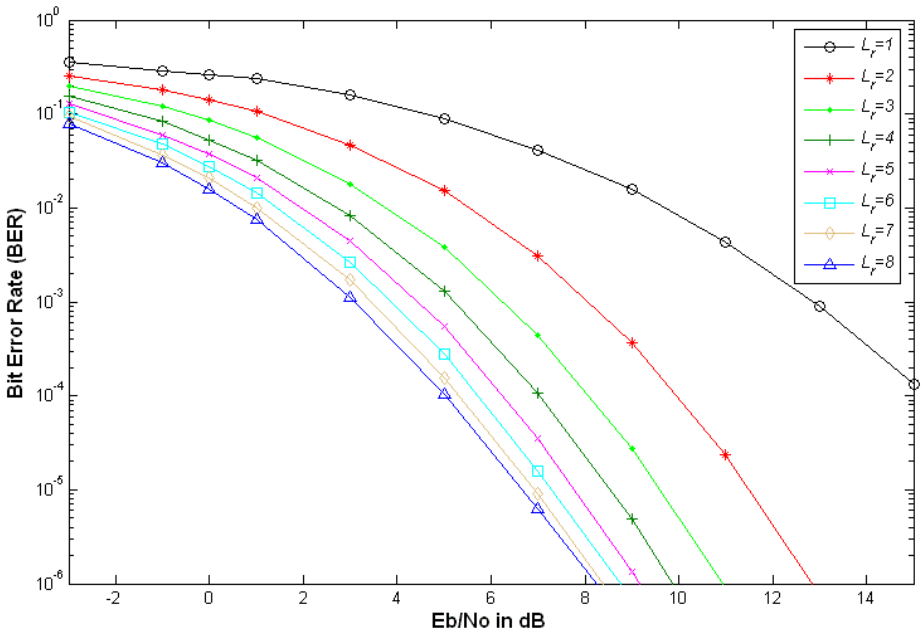

Figure 4.8 Performance comparison between TCDD/RAS systems with the receive antenna array size L_r varying. N_t =4, N_r = 8.

Figure 4.8 shows the performance of the TCDD/RAS system with different numbers of selected antennas L_r. Here the simulated system is similar as that of Figure 4.4, except that L_r varies between 1 and 8. It is seen that when L_r increases, the diversity gain of TCDD/RAS system does not change but the coding gain is enhanced. This feature implies that the diversity order is retained through our antenna selection scheme as if all the receive antennas are used. The result is similar to that described in [6], [11] for OSTBC systems.

4.5 Conclusions

In conclusion, an original system with joint cyclic delay diversity in the transmitter and antenna selection scheme in the receiver, named TCDD/RAS system has been proposed. This system provides significant performance improvement with very low additional complexity, high compatibility and no data rate reduction compared to the TOSTBC/RAS system. Another new system, the TCDD-OSTBC/RAS system is also proposed, to avoid the disadvantages of OSTBC and utilize the high flexibility of CDD to provide a balanced BER performance without sacrificing the complexity and data rate.

A novel receive antenna selection criterion based on bit error rate performance analysis has been derived. However this antenna selection rule is of high computational complexity. Therefore, a further new MMP-SNR antenna selection criterion is derived for the proposed TCDD/RAS system in flat fading channel. The MMP-SNR rule obtains a better BER performance compared with norm selection principle and capacity criterion with much lower complexity. With the MMP-SNR rule, the TCDD/RAS system achieves

a similar diversity gain compared with the corresponding transmit orthogonal space-time block coding diversity scheme combined with optimum receive antenna selection of the same number of antennas, but the TCDD/RAS system requires much lower additional complexity, suffers no data rate loss and offers compatibility to many existing standards. Diversity gain is retained by the antenna selection scheme with the MMP-SNR criterion in the TCDD/RAS system as if all the provided receive antennas are used. In addition, with another novel selection rule, the MMP-norm selection criterion, the TCDD-OSTBC/RAS system achieves better performance than the TCDD/RAS system and the punctured TOSTBC/RAS system. Even it still performs slightly inferior to the TOSBC/RAS system, it suffers no spectral efficiency reduction and is of much lower complexity.

In the newly published IEEE standard 802.11n, two transmitter structures have been proposed. In the first system only CDD (named cyclic shift diversity in 802.11n) is adopted in the transmitter in the same way as in Figure 4.1. In the second system, both CDD and STBC are applied in the transmitter before the inverse Fourier transform block, to achieve an even higher diversity gain by increasing the system complexity.

References

[1] R. W. Heath and A. Paulraj, "Antenna selection for spatial multiplexing systems based on minimum error rate," in *Proc. IEEE Int. Conf. Commun. (ICC)*, Helsinki, Finland, pp. 142-144, Jun. 2001.

[2] Z. Chen, J. Yuan and B. Vucetic, “Analysis of transmit antenna selection/maximal-ratio combining in Rayleigh fading channels,” *IEEE Trans. Veh. Technol.*, vol. 54, no. 4, pp. 1312-1321, Jul. 2005.

[3] D. A. Gore and A. J. Paulraj, “MIMO antenna subset selection with space-time coding,” *IEEE Trans. Sig. Proc.*,vol. 50, no. 10, pp. 2580-2588, Oct. 2002.

[4] D. Gore and A. Paulraj, “Space-time block coding with optimal antenna selection,” *Proc. Int. Conf. Acoustics, Speech, and Signal Processing*, vol.4, pp. 2441-2444, May 2001.

[5] Z. Tang, H. Suzuki and I.B. Collings, “Performance of antenna selection for MIMO-OFDM systems based on measured indoor correlated frequency selective channels,” in *the Proc. of the Australian Telecommunications Networks and Applications Conf. (ATNAC)*, Melbourne, Australia, pp. 435-439, Dec. 2006.

[6] G. Bauch, “Design of cyclic delay divesity with adaptive coding based on mutual informtion,” in *Proc. 10th International OFDM Workshop*, Hamburg, Germany, pp. 184-188, Aug. 2005.

[7] G. Bauch, “Aspects of delay diversity in OFDM,” *African Journal of Information & Communication Technology*, vol. 2, no. 1, pp. 12, 2006.

[8] G. Bauch and J. S. Malik, “Cyclic delay diversity with bit-interleaved coded modulation in orthogonal frequency division multiple access,” *IEEE Trans. Wireless Commun.*, vol. 5, no. 8, pp. 2092-2100, Aug. 2006.

[9] R. Kawauchi, K. Takeda and F. Adachi, “Space-time cyclic delay transmit diversity for a multi-code DS-CDMA signal with frequency-domain equalization,” *IEICE Trans. Commun.*, vol. E90-B, no. 3, pp. 591-596, Mar. 2007.

[10] G. Bauch and J. S. Malik, “Cyclic delay diversity with bit-interleaved coded modulation in orthogonal frequency division multiple access,” *IEEE Trans. Wireless Commun.*, vol. 5, no. 8, pp. 2092-2100, Aug. 2006.

[12] W. Hamouda and A. Ghrayeb, “Performance of combined channel coding and space-time block coding with antenna selection,” in *Proc. IEEE Veh. Technol. Conf.*, vol. 2, pp. 623-627, May 2005.

[13] X. N. Zeng and A. Ghrayeb, “Performance bounds for combined channel coding and space-time block coding with receive antenna selection,” *IEEE Trans. Veh. Technol.*, vol. 55, no. 4, pp. 1441-1446, Jul. 2006.

[14] K. T. Phan and C. Tellambura, “Capacity analysis for transmit antenna selection using orthogonal space-time block codes,” *IEEE Commun. Let.*, vol. 11, no. 5, pp. 423-425, May 2007.

[15] S. Kaviani and C. Tellambura, “Closed-form BER analysis for antenna selection using orthogonal space-time block codes,” *IEEE Commun. Let.*, vol. 10, pp. 704-706, Oct. 2006.

[16] P. Lan, J. Liu, B. Gu and H. Xu, “A new antenna selection algorithm combined with beam space time block coding transmit scheme,” *Proc. 8th Int. Conf. Sig. Proc.*, vol. 4, pp. 2476-2479, Nov. 2006.

[17] S. M. Alamouti, “A simple transmitter diversity technique for wireless communications,” *IEEE J. Select. Areas Commun*., vol. 16, pp. 1451-1458, Oct. 1998.

[18] J. G. Proakis, *Digital Communications*, 4th ed. McGraw-Hill, 2001.

[19] J. L. Vicario, C. Anton-Haro, “Joint exploitation of spatial and multi-user diversity via space-time block-coding and antenna selection,” in *Proc. IEEE Intl. Conf. on Commun. (ICC), Seoul, South Korea*, pp. 2911-2915, May 2005.

[20] M. Caserta and M. C. Nodar, “A cross-entropy based algorithm for combinatorial optimization problems,” *Eur. J. of Operational Research*, accepted, 2008.

[21] R. Y. Rubinstein, “Optimization of computer simulation models with rare events,” *Eur. Journal of Operations Research*, vol. 99, pp. 89-112, May 1997.

[22] F. Zhang, Y. Zhang, W. Q. Malik, B. Allen and D. J. Edwards, “Optimum receive antenna selection for transmit cyclic delay diversity,” *Commun., 2008. ICC '08. IEEE Int. Conf.*, pp. 3829 – 3833, May 2008.

[23] Y. Zhang, C. Ji, W. Q. Malik, D. O’Brien and D. J. Edwards, “Cross entropy optimization of MIMO capacity by transmit antenna selection,” *IEE Proc. Microwaves, Antennas & Propagation* (to be published), 2008.

[24] V. Tarokh, H. Jafarkhani and A. R. Calderbank, “Space-time block codes from orthogonal designs,” *IEEE Trans. Commun.*, vol. 45, pp. 1456-1467, Jul. 1999.

Chapter 5

Receive Antenna Selection for Transmit Cyclic Delay Diversity over Multipath Rayleigh Fading Channels

5.1 Introduction

The Transmit cyclic delay diversity and receive antenna selection system is introduced in the last chapter. This provides significant performance improvement with low additional complexity and high compatibility to the existing standards with OFDM. Receive antenna selection criteria for transmit cyclic delay diversity over flat fading channel have been investigated in last chapter. Antenna selection for a flat fading channel is much simpler than for a frequency selective channel, because with cyclic delay diversity at the transmitter, the channel transfer function varies following certain regular patterns. However for multipath channel, the channel transfer function varies greatly for different subcarriers, and the optimum antenna for a specific subcarrier may not be the optimum antenna for another subcarrier. Therefore the antenna selection scheme should be redesigned for selective channel parameters.

Many papers explore the antenna selection scheme in multipath channels based on the channel capacity, such as in [1, 2, 3]. Although this capacity selection scheme guarantees a high diversity order for the system, it may not provide the lowest error probability. Other papers propose a selection scheme to maximize the minimum SNR, which is similar as the MMP-SNR criterion derived in the last chapter, such as in [4]. However, this selection rule does not work well when the number of the multiple paths for each channel is large.

This chapter proposes two new receiver antenna selection criteria for transmit CDD system over multipath Rayleigh fading channels. The first one is based on the error probability analysis of the system. However it is highly computationally demanding. A further new antenna selection rule named maximum group minimum post-processing signal to noise ratio (MGMP-SNR) criterion is proposed here which offers lower complexity. The numerical results show that these two selection rules provide much better BER performance than the traditional norm selection and capacity selection criteria. In addition, the MGMP-SNR criterion also performs 2dB better at a BER of 10^{-5} than the error probability selection rule.

5.2 System Model and Channel Model

As the receive antenna selection for transmit cyclic delay diversity in a flat fading channel has already been discussed in the last chapter, here we extend the channel to a more practical case of independent identically distributed quasi-static multipath Rayleigh fading channel with additive white Gaussian noise (AWGN). The multipath channel

model is based on [5]. Here we adopt p paths each having a fixed delay τ_p. The decay of each path is defined in an exponential profile

$$\alpha_p = \begin{cases} Ke^{-\frac{\tau_p}{\sigma}}, 0 \le \tau_p \le \tau_{\max}, \\ 0, elsewhere \end{cases} \tag{5.1}$$

where σ is the standard deviation of the delays around the mean value, and K is a constant. The delay spread depends on the environment where fading takes place. In our study, we mainly focus on a typical urban area where σ is 1μs [5]. Therefore the transfer function between the n_tth transmit antenna and the n_rth receive antenna can be written as

$$h_p^{(n_t,n_r)} = \begin{cases} Ke^{-\frac{\tau_p}{\sigma}} h_p^{(n_t,n_r)}, 0 \le p \le p_{\max}, \\ 0, p_{\max}+1 \le p \le N_s \end{cases} \tag{5.2}$$

where $h_p^{(n_t,n_r)}$ is the i.i.d quasi-static Rayleigh fading channel impulse response of the pth path between the n_tth transmit antenna and the n_rth receive antenna, p_{max} is the order of the max delay path.

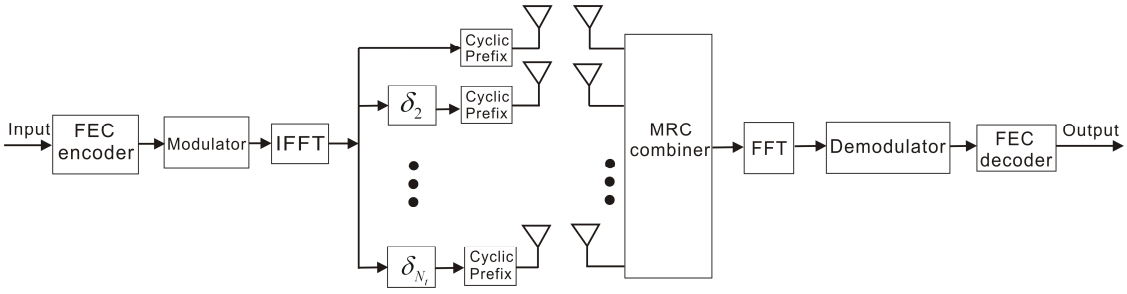

Figure 5.1 System diagram of a TDD/RAS system

We consider a system with transmit cyclic delay diversity and receive antenna selection (TCDD/RAS). As depicted in Figure 5.1, the signal bits were modulated after being coded by the forward error correction (FEC) block, using a convolutional coding. OFDM was applied as an inverse fast Fourier transform (IFFT) afterwards with a length of N_s.

Then the signal arrays were transmitted over N_t separate transmit antennas after being shifted cyclically. A cyclic prefix was inserted as a guard interval (GI) before the signal was transmitted to avoid the inter symbol interference (ISI) and inter carrier interference (ICI).

At the receiver side, antenna selection was implemented to choose L_r optimum receive antennas from N_r available receive antennas. After that, maximal ratio combining was used to combine the receive symbols over the selected antennas. Following this, a standard OFDM demodulator was applied to recover the signals. By virtue of the FFT in the demodulator, CDD was able to convert the multiple input channels into equalized single input channel with increased frequency selectivity as denoted in (3.3)

$$H_{equ,k}^{n_r}(i) = \sum_{n_t=1}^{N_t} e^{j2\pi \frac{k\delta_{n_t}}{N_s}} H_k^{(n_t,n_r)}(i), \tag{5.3}$$

where $H_k^{(n_t,n_r)}(i)$ represents the channel transfer function of the channel between the n_tth transmitter and the n_rth receiver on the kth subcarrier in the ith OFDM frame, and $H_{equ,k}^{n_r}(i)$ is the equalized channel transfer function as in a single input channel. As a cyclic prefix was applied in the system, despite the interference of the noise, $H_k^{(n_t,n_r)}(i)$ can be denoted as

$$H_k^{(n_t,n_r)}(i) = \sum_{p=1}^{p_{\max}} Ke^{-\frac{\tau_p}{\sigma}+j2\pi\frac{kp}{N_s}} H_p^{(n_t,n_r)}(i), \tag{5.4}$$

where $H_k^{(n_t,n_r)}(i)$ is the Fourier transform of the channel impulse response $h_p^{(n_t,n_r)}(i)$ in the time domain.

The following analysis and simulation are both based on this system.

5.3 Optimum Antenna Selection Criterion

5.3.1 Error Probability Selection Criterion

Extensive research has been performed on antenna selection schemes for frequency selective channels from a capacity perspective. The selection rules are the same as the capacity selection rule in flat fading channels given in (4.18). However the capacity selection criterion obtaining the largest possible data throughput capacity may not provide lowest error rate performance. In this section, an antenna selection rule based on the error probability analysis is investigated.

As stated in Chapter 4, a new antenna selection scheme based on the bit error probability for exact channel state knowledge can be denoted as

$$\begin{aligned} \varpi_{P_f}^{*} &= \arg\min_{L_r \le N_r} \left\{ P_f \,|\, L_r \right\} \\ &= \arg\min_{L_r \le N_r} \left\{ \frac{1}{N_s - M + 1} \sum_{n=0}^{N_s - M} \sum_{d=d_{free}}^{\infty} \beta_d \frac{1}{\pi} \int_0^{\pi/2} \exp\left(- \frac{E_s v \sum_{n_r=1}^{L_r} \sum_{k=0}^{M-1} \left| H_{equ,k+n}^{n_r} \right|^2}{4 N_o N_t \sin^2 \theta} \right) d\theta \right\}, \end{aligned} \tag{5.5}$$

where $\varpi_{P_f}^{*}$ indicate the selected channel subset indices, L_r denotes the number of the selected receive antennas, N_r denotes the number of the available receive antennas, N_t denotes the number of the transmit antennas, N_s denotes the OFDM frame length, M denotes the trace back length of the convolutional coding, d_{free} denotes the free distance

of the convolutional code, β_d denotes the weighting factor for each codeword, v is a constant determined by the modulation scheme, E_s denotes the transmit energy per symbol, N_o denotes the noise spectral density and $H_{equ,k+n}^{n_r}$ denotes the equalized channel transfer function observed by the n_r th receive antenna on the $(k+n)$ th subcarrier.

In this chapter, a 16QAM modulation scheme is adopted rather than PSK as it is more commonly used in the existing standards. For this reason, the error bound (4.8)

$$P_f < \frac{1}{N_s - M + 1} \sum_{n=0}^{N_s - M} \sum_{d=d_{free}}^{\infty} \beta_d \frac{1}{\pi} \int_0^{\pi/2} \exp\left(- \frac{E_s v \sum_{n_r=1}^{N_r} \sum_{k=0}^{M-1} \left| H_{equ,k+n}^{N_r} \right|^2}{4 N_o N_t \sin^2 \theta} \right) d\theta , \tag{5.6}$$

has to be modified slightly for 16QAM modulation scheme.

The average symbol error probability of 16QAM signal over AWGN channel is given as [7]

$$P_s \approx \frac{3}{2} erfc\left(\sqrt{\frac{E_s}{N_o}} \right), \tag{5.7}$$

where $erfc(\bullet)$ is the complementary error function and $Q(x) = \frac{1}{2} erfc\left(\frac{x}{\sqrt{2}} \right)$. However this average symbol error probability gives the total probability of error for a signal symbol. For a system with channel coding, the specific pairwise error probability for each pair of codewords should be taken into account.

Consider a typical 16QAM constellation pattern as given in [7]. The alphabet is given as $X_{16QAM} = \sqrt{\frac{E_s}{10}} \begin{Bmatrix} 1\pm j, & 1\pm 3j \\ 3\pm 3j, & 3\pm j \end{Bmatrix}$. Therefore the average energy per symbol is normalized to E_s. The constellation is shown in Figure 5.2:

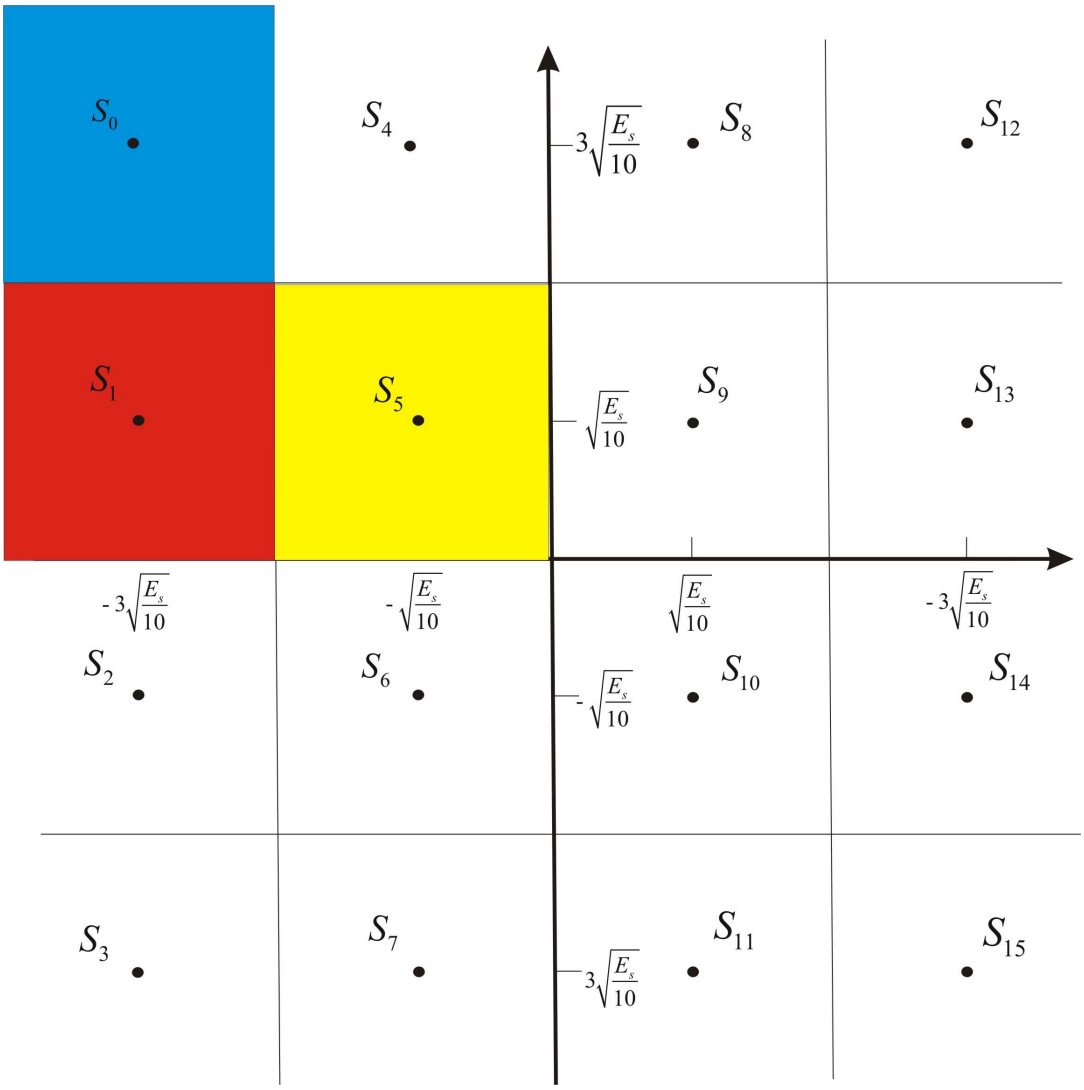

Figure 5.2 16QAM constellation

Assuming that all the symbols are of equal likelihood, there are three main cases of symbol error probability. The first case includes four symbols in the corner, such as S_0; the second case includes four symbols in the middle, such as S_5; and the third case

includes the other eight symbols, such as S_1. Symbols in each case has the same pairwise error probability. The pairwise error probability of symbols for each case is generated in Table.B.1 (see Appendix B).

Therefore the bit error probability bound (5.6) for 16QAM can be rewritten as

$$P_f < \frac{1}{N_s - M + 1} \sum_{n=0}^{N_s - M} \sum_{d=d_{free}}^{\infty} E_{S_x} \left[\prod_{k=0}^{M-1} P\left(S_{y_d} \middle| S_x \right) \right] . \tag{5.8}$$

where $P\left(S_{y_d} \middle| S_x \right)$ denotes the probability that S_{y_d} is detected whereas S_x was transmitted, $E_x\left(f(x) \right)$ denotes the expectation of $f(x)$ over the distribution of *x*, S_{y_d} denotes the erroneously decoded symbol and S_x is the transmitted symbol. The effective SNR can be denoted as

$$\gamma = \frac{E_s}{N_0 N_c} \sum_{n_r=1}^{N_r} \left| H_{equ,k+n}^{n_r} \right|^2 . \tag{5.9}$$

The antenna selection criterion based on this error probability analysis can be expressed as

$$\begin{aligned} \varpi_{P_f}^* &= \arg \min_{L_r \le N_r} \left\{ P_f \middle| L_r \right\} \\ &= \arg \min_{L_r \le N_r} \left\{ \frac{1}{N_s - M + 1} \sum_{n=0}^{N_s - M} \sum_{d=d_{free}}^{\infty} E_{S_x} \left[\prod_{k=0}^{M-1} P\left(S_{y_d} \middle| S_x \right) \right] \right\}, \end{aligned} \tag{5.10}$$

where $\varpi_{P_f}^*$ indicate the selected channel subset indices.

Then the issue remaining is to calculate the expectation of the error probability over the distribution of the transmitted symbol S_x. As stated in Chapter 3, when the convolutional

code has been fixed, the probable differences between the erroneously decoded codewords and the transmitted codewords are fixed. In addition, the error probability is determined only by the absolute difference between the error codewords and the transmitted codewords. With 16QAM, four encoded information symbols are transformed to one 16QAM symbol. For a given absolute difference, such as '1000' (which means the erroneously decoded 16QAM symbol differs with the transmitted 16QAM symbol only on the first signal position), there are three possible computations of error probability which belong to the three cases as mentioned previously and shown in Figure 5.2. Considering this feature, the calculation of the expectation of the error probability over the distribution of the transmitted symbol S_x can be simplified to these three cases. Each codeword can be transformed to a combination of symbols from three cases, so consequently the number of combination is $3^{\frac{L_{codeword}}{4}}$, where $L_{codeword}$ is the length of the unmodulated codeword. In addition, each combination has to be weighted by its probability. Therefore, (5.8) can be represented as

$$P_f < \frac{1}{N_s - M + 1} \sum_{n=0}^{N_s - M} \sum_{n_c=1}^{N_c} \left[\sum_{c=1}^{3^{\frac{L_{tb}+1}{4R_c}}} p_c(x_c) \prod_{k=0}^{M-1} P\left(S_{y_{n_c}}(k) \middle| S_{x_c}(k) \right) \right], \tag{5.11}$$

where n_c denotes the order of the erroneously decoded codeword (there are N_c probable error codewords constricted by the traceback length), L_{tb} and R_c denote the traceback length and the code rate of the convolutional code respectively. $S_{y_{n_c}}(k)$ and $S_{x_c}(k)$ denote the *k*th erroneously decoded symbol and the *k*th transmitted symbol for the *c*th

kind of combination of S_x respectively. $p_c(x_c)$ stands for the probability of the cth combination of $S_{x_c}(k)$.

The antenna selection criterion of (5.10) can be represented as

$$\varpi_{P_f}^{*} = \arg\min_{L_r \le N_r} \left\{ \frac{1}{N_s - M + 1} \sum_{n=0}^{N_s - M} \sum_{n_c=1}^{N_c} \left[\sum_{c=1}^{3^{\frac{L_{tb}+1}{4R_c}}} p_c(x_c) \prod_{k=0}^{M-1} P\left(S_{y_{n_c}}(k) \middle| S_{x_c}(k) \right) \right] \right\}. \tag{5.12}$$

This new selection criterion is based on the error probability analysis, and should provide an optimum performance in the respect of error probability. However, this selection rule demands high computational complexity and therefore simpler and more applicable antenna selection rules will be proposed in the following sections.

5.3.2 Maximum Group Minimum Post-Processing SNR Selection

A selection criterion for TCDD/RAS system in flat-fading channel has been discussed in Chapter 4, which is denoted as maximum minimum post-processing SNR (MMP-SNR) criterion. It can be presented as

$$\varpi_{MMP-SNR}^{*} = \arg\max_{L_r \le N_r} \{ \min_{k} \{ \sum_{m=1}^{Lr} |H_{equ,k}^{m}|^2 \} \}. \tag{5.13}$$

As stated in Chapter 4, the channel between each pair of transmitter and receiver is flat fading and the relative cyclic delay time is chosen by dividing N_s by N_t. Consequently, the equalized channel only has several states which are independent of each other. Therefore, the state with the lowest amplitude of channel transfer function determines the

error probability of the whole system. However, in frequency-selective channels, the channel will have a number of $p_{max}*N_t$ states at least. This leads to a large spacing between the subcarriers in the same state. For a normal FEC scheme, such as the convolutional code we adopted here, two errors separated by several subcarriers can be easily corrected. In this case, the MMP-SNR criterion, which only considers the minimum channel coefficient on one subcarrier has to be modified for multipath channel to its advantage.

To select the optimum antennas in a frequency-selective channel, the MMP-SNR criterion has to be modified slightly. As discussed in Chapter 4, the mean value of the power of the equalized channel transfer function over the whole bandwidth is equal to the Frobenius norm of the exact channel transfer function matrix. Norm selection is the optimum antenna selection criterion for systems with orthogonal space-time block coding in the transmitter, but it does not perform that well in cyclic delay diversity systems. But if we consider the mean power of a group of subcarriers with the minimum amplitudes for the channel transfer function, the results will be different. There are two approaches to find the minimum group. The first way is to find channel coefficients below a certain threshold; the other one is to find a certain number of subcarriers with the lowest channel coefficients. In the first case, if a threshold is chosen, the number of channel coefficients below it varies in time. When this number is too small, it will not have a determinant effect on the error probability even when the coefficients themselves are of very low amplitudes (referring to the property of the FEC code). Therefore in this section, we

choose the second method. A novel maximum group minimum post-processing SNR (MGMP-SNR) selection rule can be denoted as

$$\varpi^*_{MGMP-SNR} = \arg\max_{L_r \le N_r}\{\frac{1}{g_{num}}\sum_{k_i}^{g_{num}}\{\sum_{n_r=1}^{Lr}|H^{n_r}_{equ,k_i}|^2\}\}, \tag{5.14}$$

where $\varpi^*_{MMP-SNR}$ stand for the selected antenna subset indices, k_i subjects to the subcarrier index for the ith minimum value of $\sum_{m=1}^{Lr}|H^m_{equ,k}|^2$, g_{num} is the number of subcarriers with minimum amplitudes considered in this rule.

5.4 Numerical Results

In this section, the simulation results of the TCDD/RAS system with various receive antenna selection criteria are presented for comparison.

Simulation results of the TCDD/RAS system with MGMP-SNR criterion in frequency-selective channel are presented. A typical urban channel model is applied in Figure 5.1, in which σ is 1μs and K is chosen in order to normalize the total transmitting power. The time spacing between two paths, which can be denoted as $\tau_{p+1}-\tau_p$, is equal to one symbol time. In our simulation there are 128 symbols per OFDM frame.

Firstly, we consider the TCDD/RAS system with two transmit antennas and eight receive antennas amongst which four of them are selected for further decoding ($N_t = 2,\ N_r = 8,\ L_r = 4$). The signals are mapped onto a 16QAM constellation and encoded by a half rate convolutional code with a constraint length of 7. Figure 5.3 shows

the simulation results for the TCDD/RAS system with MGMP-SNR antenna selection rule compared with the capacity selection and norm selection rules. The number of the subcarriers, g_{num}, which have the minimum post-processing SNRs, varies. It can be seen that the bit error rate decreases when g_{num} increases from 10 to 25, but becomes higher when g_{num} varies from 25 to 128 (The MMP-SNR selection rule with $g_{num}=128$ equals to the norm selection rule). That means the system performs best on a certain value of g_{num}. With the optimum g_{num}, MGMP-SNR selection rule performs 0.5dB better than the capacity selection rule and 1dB better than norm selection rule at a BER of 10^{-5}. In addition, The MGMP-SNR selection criterion requires lower computational complexity than the capacity selection rule and the norm selection rule. The next task is to determine the optimum g_{num}.

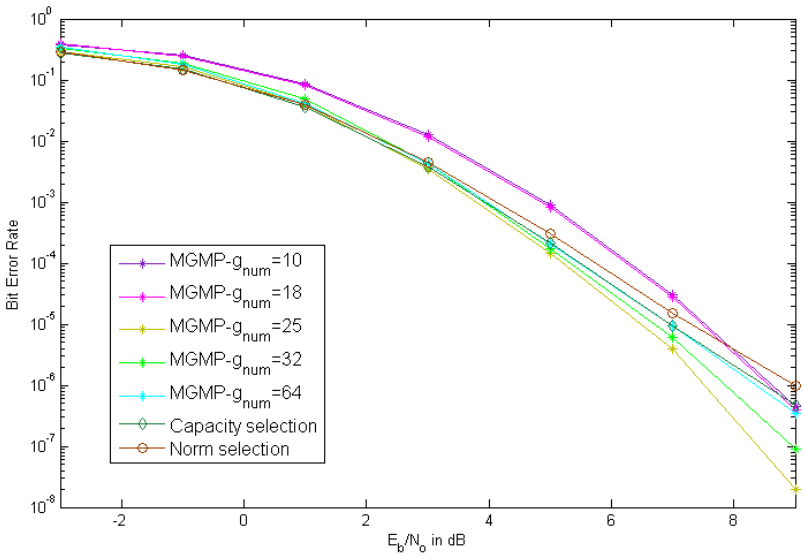

Figure 5.3 Simulation results for a TCDD/RAS system with the MGMP-SNR selection criterion of a varying g_{num}, compared with the capacity selection rule and the norm selection rule. The constraint length for the convolutional code is 7. $N_t=2, N_r=8, L_r=4$.

If g_{num} varies for the above system with an E_b / N_o of 7dB, it is observed that the bit error rate of the system approaches to the lowest value when g_{num} is around 25 in Figure 5.4. In Figure 5.5, if we change the constraint length of the convolutional code to 3, it can be seen 25 is still approximately the optimum choice. It indicates that the optimum g_{num} does not depends on the constraint length of the convolutional code. Figure 5.6 shows the performance of a TCDD/RAS system with 4 transmit antennas and varying g_{num}. The optimum g_{num} is 2 in this case. Therefore, it seems that the optimum g_{num} is becoming smaller when the number of the transmitters increases. In addition, considering the complexity, g_{num} should be chosen to be as small as possible.

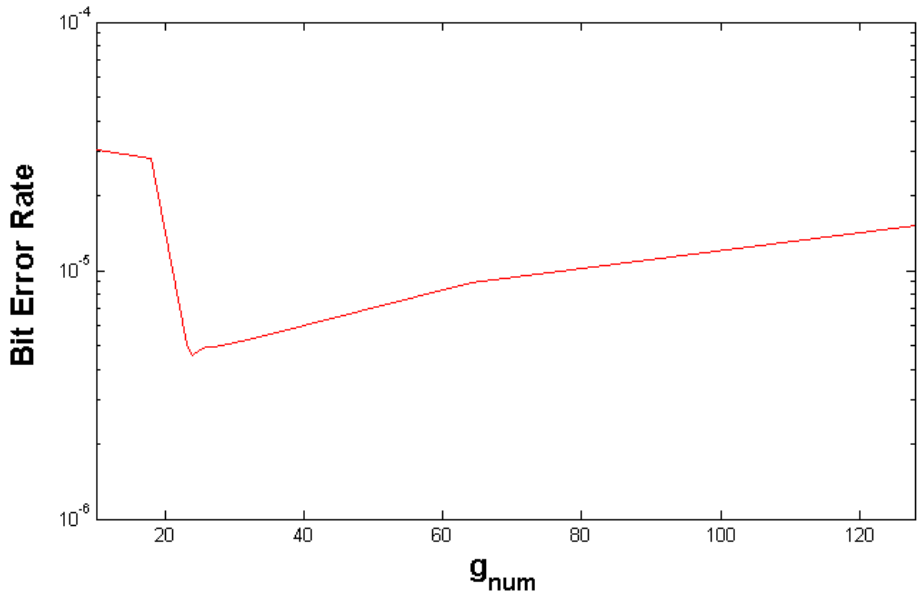

Figure 5.4 Simulation results of the MGMP-SNR selection criterion with a varying g_{num} at an Eb/No=7dB. The constraint length of the convolutional code is 7. $N_t = 2, N_r = 8, L_r = 4$

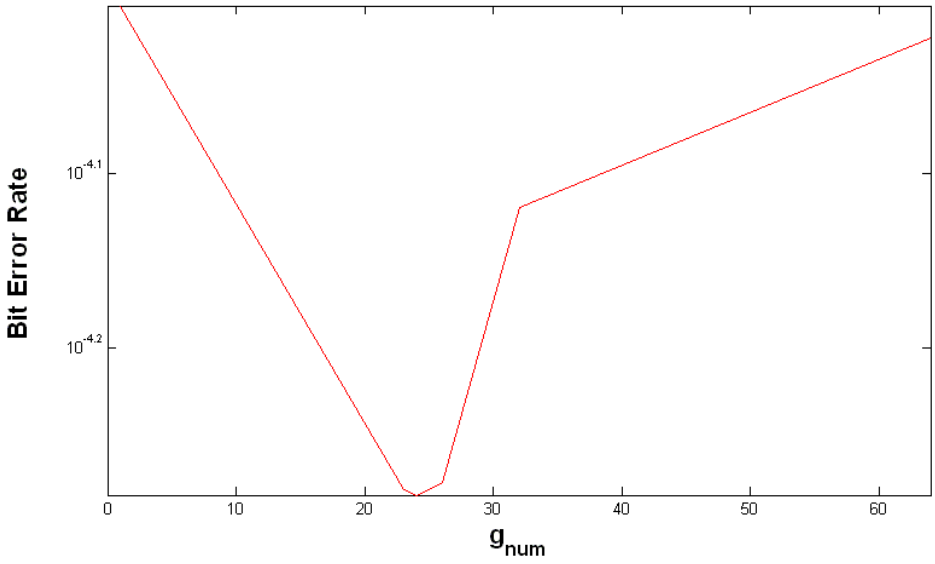

Figure 5.5 Simulation results of the MGMP-SNR selection criterion with a varying g_{num} at an Eb/No=7dB. The constraint length of the convolutional code is 3. $N_t = 2, N_r = 8, L_r = 4$

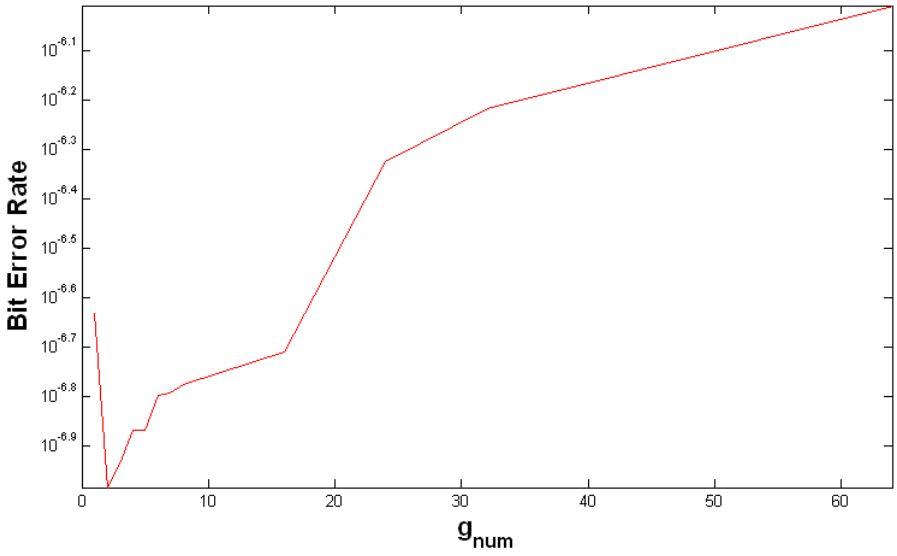

Figure 5.6 Simulation results of the MGMP-SNR selection criterion with a varying g_{num} at an Eb/No=7dB. The constraint length of the convolutional code is 3. $N_t = 4, N_r = 8, L_r = 4$

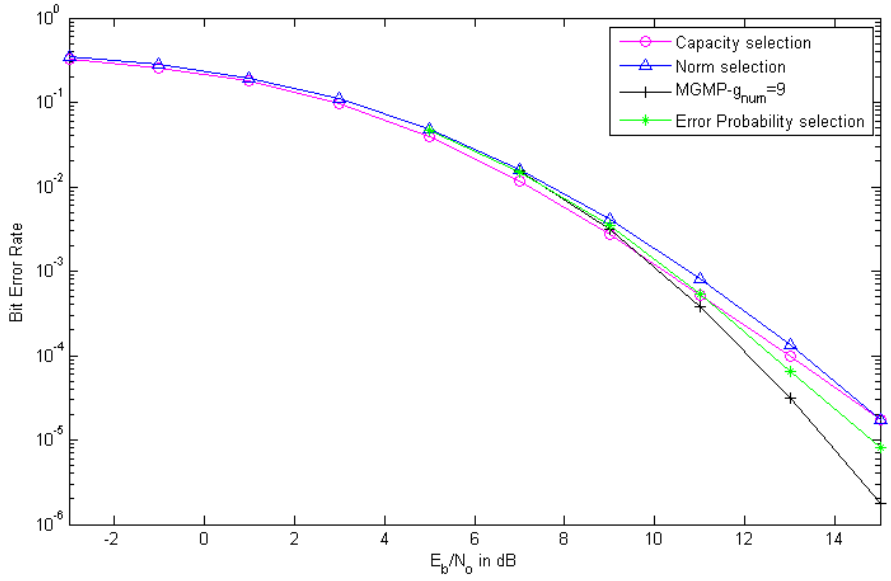

Figure 5.7 Comparison of the simulation results of the error probability selection criterion, the MGMP-SNR selection criterion and also other selection rules. The constraint length of the convolutional code is 3. g_{num}=9, $N_t = 2, N_r = 4, L_r = 2$

The simulation results for the receive antenna selection criterion based error probability are shown in Figure 5.7. Compared to the capacity selection criterion and the norm selection criterion, the error probability selection rule performs much better with respect to the bit error rate. However, the performance of MGMP-SNR selection criterion appears 2dB better at a BER of 10^{-5} than the error probability selection rule, for the reason that the error probability selection is based on the error probability upper bound, but not the exact bit error probability. This approximation renders a reduction on the performance of the error probability selection rule. Moreover, the MGMP-SNR criterion is of much lower complexity than the error probability selection rule. Therefore, for a

given the optimum g_{num}, the MGMP-SNR selection criterion is more applicable than the error probability selection rule.

5.5 Conclusions

In conclusion, a transmit cyclic delay diversity and receive antenna selection system is constructed which achieves significant high diversity gain and is compatible with many existing standards with very low additional complexity and no data rate reduction compared to the system of transmit orthogonal space time block coding combined with receive antenna selection. A new antenna selection criterion based on bit error probability analysis has been generated for this system. However, this rule demands high computational complexity. Therefore another novel maximum group minimum post-processing signal to noise ratio (MGMP-SNR) selection criterion is proposed for the receive antenna selection scheme in frequency selective channels, which is much simpler and faster. The optimum selection parameter for the MGMP-SNR criterion is demonstrated to be independent of the channel coding but dependent on the numbers of the antennas. The MGMP-SNR selection rule achieves a better performance than other traditional antenna selection rules and even the principle based on the error probability analysis with much lower computational complexity, for the reason that the BER performance analysis only generates an upper bound of the system BER performance but not the exact BER performance.

References

[1] Z. Tang, H. Suzuki and I. Collings, “Performance of antenna selection for MIMO-OFDM system based on measured indoor correlated frequency selective channels,” in *the Proc. of the Australian Telecommunications Networks and Applications Conf. (ATNAC)*, Melbourne, Australia, pp. 435-439, Dec. 2006.

[2] A. Wilzeck and T. Kaiser, “Antenna subset selection for cyclic prefix assisted MIMO wireless communications over frequency selective channels,” *EURASIP Journal on Advances in Signal Processing*, pp. 1-14, Article ID 716826, 2008.

[3] H. Zhang and R.U Nabar, “Transmit Antenna Selection in MIMO-OFDM Systems: Bulk Versus Per-Tone Selection Communications,” in *Proc. of ICC '08. IEEE Int. Conf.*, pp. 4371-4375, May 2008.

[4] E. Kurniawan, A. S. Madhukumar and F. Chin, “Antenna selection technique for MIMO-OFDM systems over frequency selective Rayleigh fading channel,” *IET - Communications*, IEE, UK, Vol. 1, No. 3, pp. 458-463, Jun 2007.

[5] R. Prasad, *OFDM for Wireless Communications Systems***,** Artech House, Inc. Norwood, MA, USA, 2004.

[6] F. Zhang, Y. Zhang, W. Q. Malik, B. Allen and D. J. Edwards, “Optimum receive antenna selection for transmit cyclic delay diversity,” *in proc. of ICC '08. IEEE Int. Conf.*, pp. 3829 – 3833, May 2008.

[7] J. G. *Proakis, Digital Communications* , McGraw-Hill, 4th Edition, 2000.

Chapter 6

Transmit Cyclic Delay Diversity and Receive Antenna Selection in Relay Systems

6.1 Introduction

Relay systems are attractive schemes to extend the range of wireless communications or save unnecessary transmission power from the source [1]. There are mainly two groups of relay systems. The first is described as a regenerative relay which employs a decode-and-forward (DF) scheme; while the other is called a non-regenerative delay which only includes a amplify-and-forward (AF) scheme. Comparisons of these two schemes have been presented in [1] and [2]. It is observed that the AF scheme provides a better diversity gain than the DF scheme while maintaining the same multiplexing gain. Moreover, as the AF scheme does not need to demodulate the received signals, its complexity is lower than the DF scheme and therefore exhibits less delay than the DF scheme. In addition, the AF scheme offers greater security. Relay scheme has been included in many standards, such as the WLAN standard IEEE 802.11s, the WPAN standard IEEE 802.15.5, the WMAN standard IEEE 802.16j and the Mobile Broadband Wireless Access (MBWA) standard IEEE 802.20 [3, 4, 5, 6].

In this chapter, the aforementioned TCDD/RAS scheme is embedded into a relay system in order to increase the transmission reliability of the wireless links, thereby to extend the transmission range and increase the information throughput. Two approaches are proposed here which combine the TCDD/RAS scheme with the relay system. The first one is to apply the TCDD/RAS scheme in a MIMO relay system. In this case, cyclic delay diversity is integrated into the relay station with multiple transmit antennas and antenna selection into the destination terminal. However, in some scenarios, multiple antennas are inapplicable for the relay nodes, especially for distributed relay diversity schemes, where the relay nodes are mobile units. Therefore single antenna relay stations have been used cooperatively to form distributed virtual multiple-input multiple-output (MIMO) systems. This is reported in many previous papers [7, 8, 9, 10]. Cooperative relaying based on Alamouti diversity has been investigated in [11, 12]. Distributed cyclic delay diversity relay has been described in [13, 14]. The difference between these two diversity schemes has already been discussed in Chapter 2 and 3. In a cooperative relay system, the advantage of CDD is even more valuable because of the limitation of complexity and energy in the relay stations. With this virtual multiple-antenna transmitter coded by cyclic delay diversity, the antenna selection scheme which has been derived in the last two chapters can be employed in the destination station to further improve the robustness of the wireless links.

6.2 System Model

In this section, two system models are presented. The first one is a MIMO relay system with cyclic delay diversity in the relay station and an antenna selection scheme at the

destination. The second system model is a cooperative relay system with distributed cyclic delay diversity and antenna selection scheme at the destination.

6.2.1 MIMO Relay System

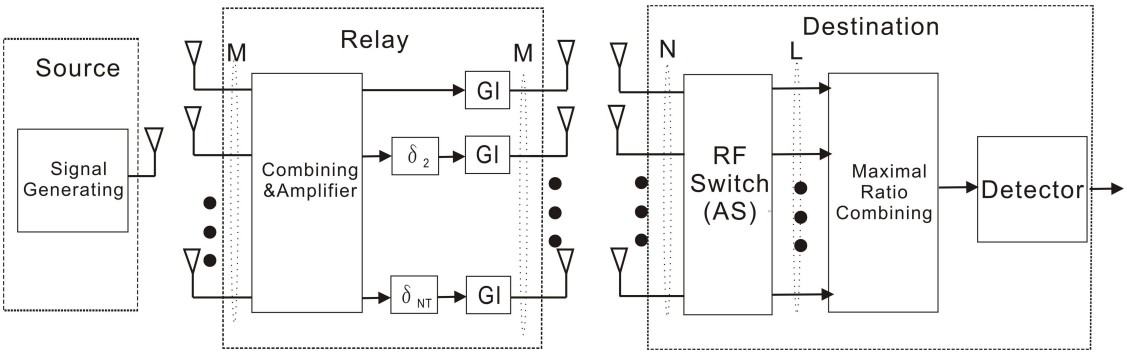

Figure 6.1 The structure of a MIMO relay system with cyclic delay diversity in the relay station and antenna selection at the destination

The MIMO relay system with cyclic delay diversity in the relay station and antenna selection at the destination is shown in Figure 6.1. A two-hop MIMO relay system model with multiple antennas in the relay station can be found in [15], where MRC is used as a receive diversity scheme. In Figure 6.1, the signal was transmitted from the source to the destination with the assistance of the relay. This diagram only illustrates the baseband structure and eliminates the up/down converter blocks. We assume there was no direct link from source to the destination. The number of antennas on source, relay and destination were 1, M, N respectively. The transmission was a non-regenerative two-hop link. In the first hop the signal was transmitted from the source to the relay, and then in the second hop the relay retransmitted the signal to the destination after amplification without decoding of the signal, while the source kept silent. In addition we assume i.i.d. quasi-static Rayleigh flat fading channels between the source, relay and the destination.

Cyclic delay diversity (CDD) was applied in the relay with fixed delay shifts. At the destination, antenna selection was applied to reduce the number of the radio frequency (RF) chains and to obtain a diversity gain directly proportional to the number of the available receive antennas. The selection criterion named maximum minimum post-processing signal to noise ratio (MMP-SNR) was employed at the destination to optimize the joint performance of CDD and antenna selection [16].

The received signal at the *m*th antenna on the relay node in the frequency domain can be written as

$$R_R^m = H_{SR}^m S_S + w_{SR}^m , \tag{6.1}$$

where R_R^m denotes the received signal at the *m*th antenna on the relay node, H_{SR}^m denotes the channel between the source and the *m*th antenna on the relay node, $S_S \in \mathbb{C}^{1\times 1}$ denotes the transmitted signal from the source, w_{SR}^m denotes the additive white Gaussian noise at the *m*th antenna on the relay node. If the channel status information is available at the relay, maximal ratio combining can be applied in the receiver side of the relay station. The combined signal can be written as

$$R_c = \sum_{m=1}^{M} \left| H_{SR}^m \right|^2 S_S + \sum_{m=1}^{M} w_{SR}^m H_{SR}^{m\,*} \ . \tag{6.2}$$

However, limited by the complexity of the relay node, the channel status information is normally absent in the relay node. Therefore a simple summation of the received signals or just a single antenna receiving scheme can be deployed at the receiver side of the relay node. The summation of the received signals can be denoted as:

$$R_s = \sum_{m=1}^{M} H_{SR}^{m} S_S + \sum_{m=1}^{M} w_{SR}^{m} . \tag{6.3}$$

The average effective E_s/N_o can be calculated as

$$\gamma_s = \frac{\mathrm{E}\left(\left| \sum_{m=1}^{M} H_{SR}^{m} \right|^2 \right) E_0}{MN_o} = \frac{M\,\mathrm{E}\left(\left| H_{SR}^{m} \right|^2 \right) E_0}{MN_o} = \frac{E_0}{N_o}, \tag{6.4}$$

where $\mathrm{E}(\bullet)$ denotes the expectation operator, E_0 denotes the energy of the transmitted signal from the source per symbol, and N_o denotes the power density of the additive white Gaussian noise. H_{SR}^{m} is Rayleigh distributed with variance of 1, therefore $\mathrm{E}\left(\left| H_{SR}^{m} \right|^2 \right) = 1$.

If only one antenna is used in the relay node for receiving the signal from the source, then the received signal can be rewritten as

$$R_R = H_{SR}^{m} S_S + w_{SR}^{m} . \tag{6.5}$$

Then there is no need for combination. The average effective E_s/N_o can be written as

$$\gamma_R = \frac{\mathrm{E}\left(\left| H_{SR}^{m} \right|^2 \right) E_0}{N_o} = \frac{E_0}{N_o} . \tag{6.6}$$

Although these two schemes achieve the same effective SNR, the summation scheme has more SNR fluctuation. As there is no blockwise diversity technique in this system, this fluctuation can not be taken advantage of. Consequently it is detrimental for further detection. Therefore, in this chapter we adopt the single receive antenna scheme, and the index can be ignored for simplification.

Let F denote the gain provided by the amplifier in the relay node and D^m denote the generating factor of cyclic delay diversity on the *m*th transmit antenna. Then the signal transmitted by the relay node is

$$S_R^m = D^m F H_{SR} S_S + D^m F w_{SR}. \tag{6.7}$$

Let $H_{RD}^{m,n}$ denote the channel between *m*th the transmit antenna in the relay station and *n*th receive antenna in the destination station. The received signal at the destination can be presented as

$$R_D^n = \sum_{m=1}^{M} H_{RD}^{m,n} D^m F H_{SR} S_S + \sum_{m=1}^{M} H_{RD}^{m,n} D^m F w_{SR} + w_{RD}^n, \tag{6.8}$$

where w_{RD}^n denotes the additive white Gaussian noise at *n*th the receiver antenna on the destination.

As given in (3.3), the multiple-input multiple-output channel between the relay node and the destination can be substituted with a single-input multiple-output channel which can be represented as $\mathrm{H}_{equ}(k) = \left\{ H_{equ}^n(k) \right\}$, $H_{equ}^n(k) = \sum_{m=1}^{M} H_{RD}^{m,n}(k) e^{j2\pi \frac{\delta_m}{N_s}(k-1)}$, where δ_m is the relative cyclic delay time on the *m*th transmit antenna of the relay node, while *k* is the carrier order (which has been ignored in the previous statement). Therefore the received signal at the destination can be written as

$$R_D^n(k) = H_{equ}^n(k) F H_{SR} S_S(k) + H_{equ}^n(k) F w_{SR}(k) + w_{RD}^n(k). \tag{6.9}$$

The quantitative performance of this scheme will be presented in Section 6.3.

6.2.2 Cooperative Relay System

The system structure of a cooperative relay system with distributed cyclic delay diversity in the relay nodes and antenna selection at the destination is shown in Figure 6.2.

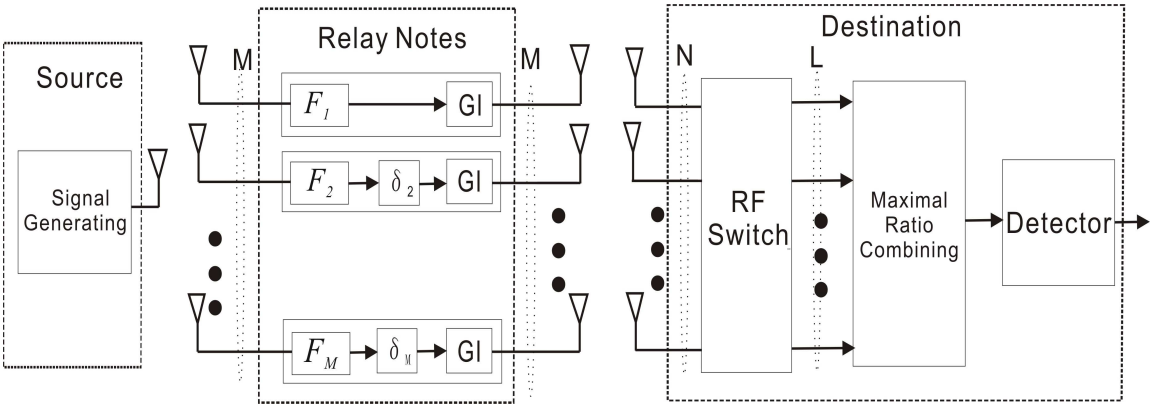

Figure 6.2 The structure of the cooperative relay system with distributed cyclic delay diversity in the relay nodes and antenna selection at the destination

Again, this diagram only illustrates the baseband structure and eliminates the up/down converter blocks. And there is no direct link from source to the destination. The source only has one antenna. There are *M* relay nodes, each of which has one antenna used for both transmitting and receiving. The destination has *N* receive antennas, from which *L* antennas are selected for further detection. This transmission is a non-regenerative two-hop link as introduced in the MIMO relay system. Distributed cyclic delay diversity is applied in the relay nodes with fixed delay shifts. At the destination, antenna selection is applied. The MMP-SNR selection criterion is employed at the destination to optimize the joint performance of CDD and antenna selection [16].

The received signals at the relay nodes in the frequency domain can be written as

$$\mathrm{R}_R = \mathrm{H}_{SR}\, S_S + \mathrm{w}_{SR}, \tag{6.10}$$

where $\mathrm{R}_R = (R_R^1,\ R_R^2,\ \cdots,\ R_R^M)'$ denotes the receive signal at relay nodes, $\mathrm{H}_{SR} = \left(H_{SR}^1,\ H_{SR}^2,\ \cdots,\ H_{SR}^M\right)'$ denotes the channel between the source and the relay nodes, $S_S \in \mathbb{C}^{1\times 1}$ denotes the transmitted signal from the source, and $\mathrm{w}_{SR} = \left(w_{SR}^1,\ w_{SR}^2,\ \cdots,\ w_{SR}^M\right)$ denotes the additive white Gaussian noise at the relay nodes.

Let $\mathrm{F} = diag\left(F_1,\ F_2,\ \cdots,\ F_M\right)$ denote the gain matrix provided by the amplifiers in the relay nodes and $\mathrm{D} \in \mathbb{C}^{M\times M}$ denote the generating matrix for cyclic delay diversity. Then the signal transmitted by the relay node is

$$\mathrm{S}_R = \mathrm{DFH}_{SR} S_S + \mathrm{DFw}_{SR}, \tag{6.11}$$

Let $\mathrm{H}_{RD} \in \mathbb{C}^{N\times M}$ denote the MIMO channel between the relay node and the destination. The receive signal at the destination can be written as

$$\mathrm{R}_D = \mathrm{H}_{RD}\,\mathrm{DFH}_{SR} S_S + \mathrm{H}_{RD}\,\mathrm{DFw}_{SR} + \mathrm{w}_{RD}, \tag{6.12}$$

where w_{RD} denotes the additive white Gaussian noise at the receiver side of the destination.

As given in (3.3), the multiple-input multiple-output channel between the relay node and the destination can be substituted with a single-input multiple-output channel where $\mathrm{H}_{RD}\mathrm{D}$ can be represented as $\mathrm{H}_{equ}(k) = \left\{H_{equ}^{n,m}(k)\right\}$, $H_{equ}^{n,m}(k) = e^{j2\pi\frac{\delta_m}{N_s}(k-1)} H^{n,m}(k)$. Therefore the received signal at the destination can be written as

$$\mathrm{R}_D = \mathrm{H}_{equ}(k)\,\mathrm{FH}_{SR} S_S(k) + \mathrm{H}_{equ}(k)\,\mathrm{Fw}_{SR}(k) + \mathrm{w}_{RD}(k). \tag{6.13}$$

The numerical simulation results of this cooperative relay system with cyclic delay diversity among the relay nodes and the antenna selection scheme at the destination will be given in the next section.

6.3 Numerical Results

In this section, a performance comparison of the MIMO relay system and the cooperative relay system is presented in numerical results based on Monte Carlo simulations in Matlab.

6.3.1 MIMO Relay System

The simulation results of the MIMO relay system are presented in this section. Figure 6.3 shows the simulation results of the MIMO relay system with different channel codes. The MMP-SNR selection criterion is employed as the antenna selection rule at the destination. There are three convolutional codes deployed with the constraint length varying as 3, 5 and 7. For a convolutional code with a constraint length of 3, although the slope of the BER curve of the MIMO relay system is steeper than the BER curve of a relay system without CDD, its error probability is larger than the later system when the E_b/N_o is smaller than 20dB. As the constraint length of the convolutional code increases, the performance of the MIMO relay system improves. When E_b/N_o is larger than a certain threshold, the BER performance of the MIMO relay system is lower than the relay system without CDD. For a convolutional code with a constraint length of 5, the crossing point is at 19dB, while for a convolutional code with a constraint length of 7, the crossing point is at 14dB. The simulation results verify again that the performance of CDD

depends significantly on the design of the channel coding. Simple convolutional coding, e.g. with a constraint length equal to 3, renders less coding gain even when a diversity gain is achieved, for the reason that the trace back spreading of the convolutional code is not broad enough to explore the frequency diversity provided by CDD.

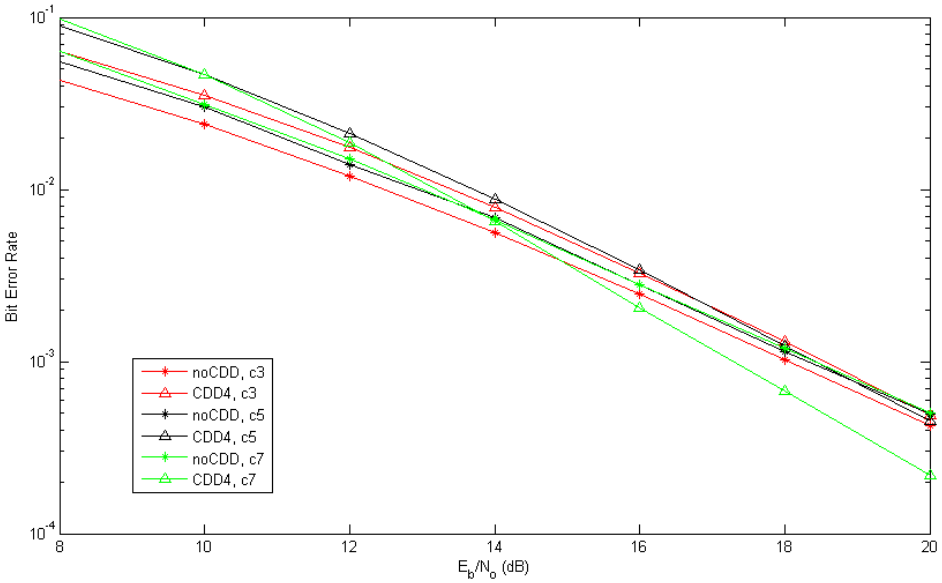

Figure 6.3 Performance comparison of MIMO relay systems with different convolutional codes. There are 4 antennas in the relay station and 1 antenna is selected from 2 at the destination. The MMP-SNR selection criterion is used as the antenna selection rule.

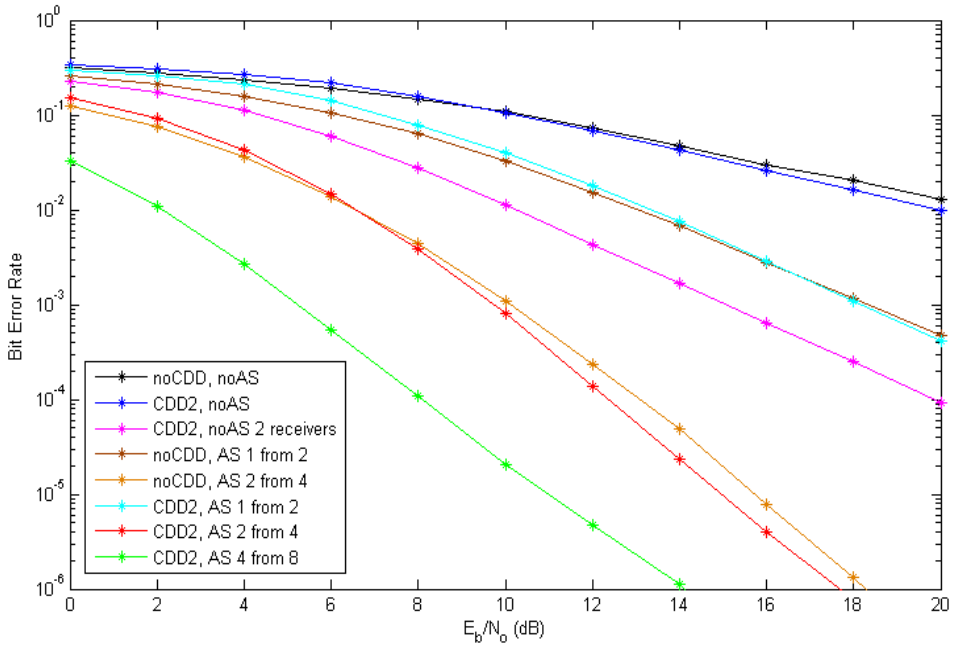

Figure 6.4 Performance comparison of MIMO relay systems with and without CDD of 2 antennas in the relay station and antenna selection of varying antenna number at the destination, the MMP-SNR selection criterion is applied as the antenna selection rule. The constraint length of the convolutional code is 7.

Figure 6.4 shows the simulation results of the relay system with 2 antennas in the relay station. The constraint length of the convolutional code is 7. The performance of the MIMO relay system with cyclic delay diversity scheme in the relay node and antenna selection at the destination is obviously much better than the system without any spatial diversity scheme or with single diversity scheme (only CDD in the relay station or only antenna selection at the destination). The MIMO relay system with CDD performs 0.2dB better than the system without CDD at a BER of 10^{-3} when the antenna selection scheme chooses 1 antenna from 2 for both systems. While the MIMO relay system with antenna

selection at the destination performs 5dB better than the relay system without antenna selection at a BER of 10^{-2} when the antenna numbers of CDD for both systems are 2 and 2 receive antennas are used at the destination, which means that 2 RF chains are required. From the slopes of BER simulation curves of the only CDD system with 2 antennas in the relay and the only antenna selection system with 2 available antennas at the destination, it can be observed that the CDD in the relay station brings less diversity gain than the antenna selection scheme at the destination.

It is also observed that the diversity gain (indicated by the slope of the BER curve) increases when the number of available antennas is larger at the destination. When the number of the available antennas at the destination is larger, the diversity gain increases more slowly with increasing E_b/N_o. When the number of the antennas is larger than 4, the diversity gain barely increases. It means that the channel diversity property has been mostly exploited and the channel is very close to an AWGN channel without fading. From the performance comparison of the MIMO relay system with antenna selection choosing 1 receive antenna from 2 available antennas for detection and the MIMO relay system which employs 2 receive antennas without selection, it can be seen that the MMP-SNR selection criterion achieves the same diversity gain as if all of the receive antennas are used for detection. In addition, the coding gain (indicated by the horizontal shift) increases when the number of selected antennas increases.

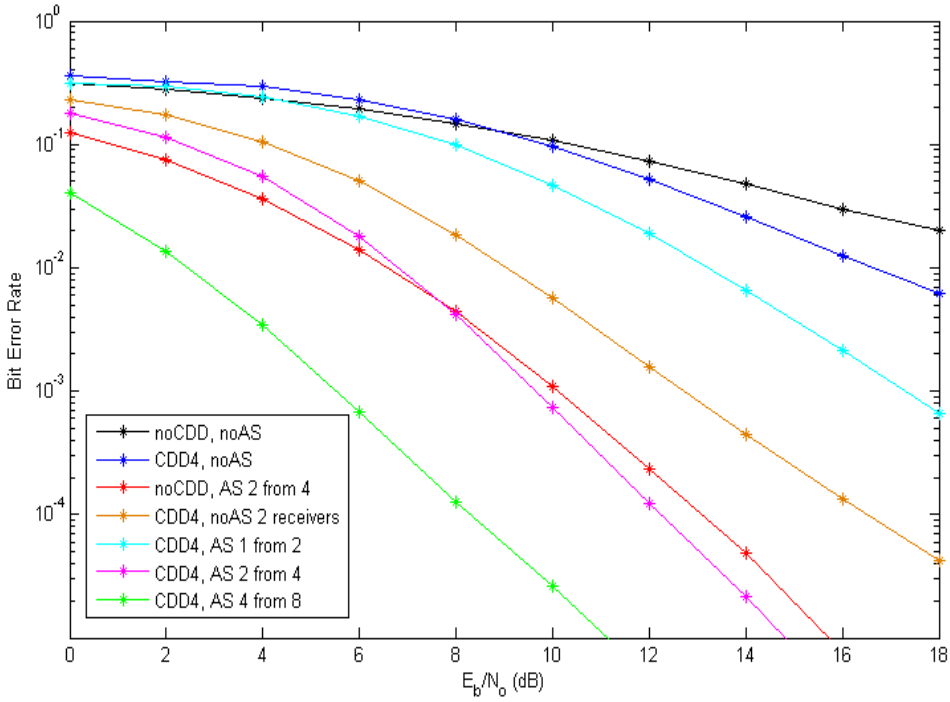

Figure 6.5 Performance comparison of MIMO relay systems with and without CDD of 4 antennas in the relay station and antenna selection with varying antenna number at the destination, the MMP-SNR selection criterion is applied as the antenna selection rule. The constraint length of the convolutional code is 7.

Figure 6.5 shows the simulation results of the relay system with 4 antennas in the relay station and the constraint length of the convolutional code is 7. The relay system with CDD performs 1dB better than the system without CDD at a BER of 10^{-5} when the antenna selection scheme chooses 2 antennas from 4 for both systems. While the MIMO relay system with antenna selection at the destination performs 10dB better than the relay system without antenna selection at a BER of 10^{-2} when the same number of antennas in the relay station for CDD is applied and the same number of antennas at the destination is used, which means the same number of RF chains. From the slopes of simulation result curves of the only CDD system with 4 antennas in the relay station and the only antenna

selection system with 4 available antennas at the destination, it can be observed that the CDD in the relay station brings less diversity gain than the antenna selection at the destination.

6.3.2 Cooperative Relay System

The simulation results of the cooperative relay system are discussed in this section. From Figure 6.6, it is observed that when the number of relay nodes which work cooperatively increases, the diversity gain becomes larger. Figure 6.7 shows the diversity gain variation with the number of relay nodes increasing. The diversity gains are calculated according to (2.12) and normalized by the diversity gain of the single antenna system with a single relay station and single antenna at the destination. The diversity gain of the single antenna system is assumed to be 1 unit. It can be seen that the diversity gain increases more slowly when the number of the relay nodes is larger. This feature is similar to the MIMO relay system.

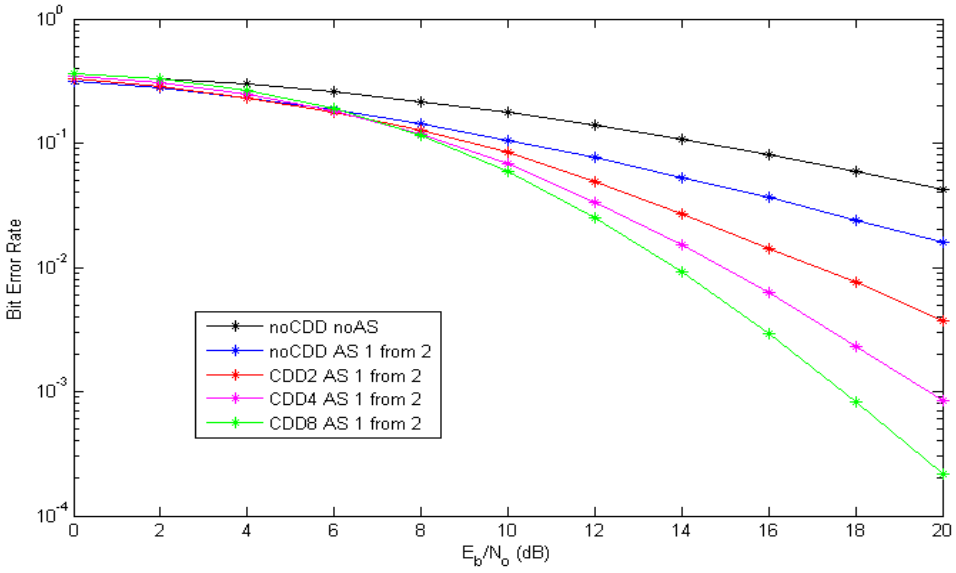

Figure 6.6 Performance comparison of cooperative relay systems with different numbers of relay nodes. Antenna selection is employed at the destination, 1 antenna is selected from 2 using the MMP-SNR selection criterion. The constraint length of the convolutional code is 7.

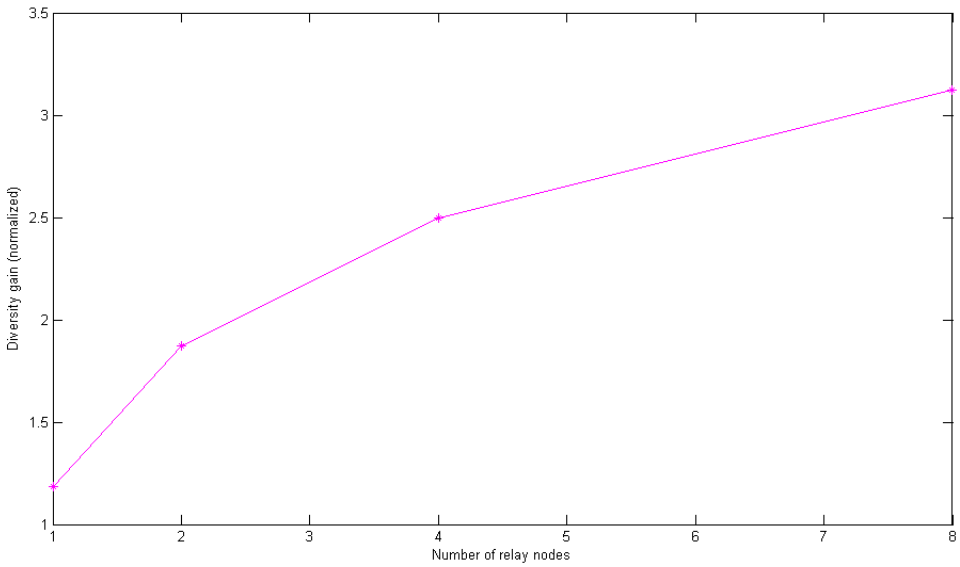

Figure 6.7 Diversity gains of cooperative relay systems with different numbers of relay nodes. Antenna selection is employed at the destination, 1 antenna is selected from 2 using the MMP-SNR selection criterion. The constraint length of the convolutional code is 7.

Figure 6.8 shows a performance comparison of the cooperative relay system with varying antenna number at the receiver of the destination. There are 2 relay nodes which employ a cyclic delay shift of half of the OFDM frame length. Similar to the results in Figure 6.4 , the diversity gain increases with the number of the available antennas for selection while the coding gain depends on the number of the selected antennas for further detection. The BER curves of the cooperative relay system with 2 receive antennas used without antenna selection at the destination and the cooperative relay system which select 1 antenna from 2 with the MMP-SNR selection criterion at the destination have the same slope, which indicates that the MMP-SNR selection criterion achieves the same diversity gain as if all of the receive antennas are used for detection. The normalized diversity gains are shown in Figure 6.9. Comparing Figure 6.7 and Figure 6.9, it can be observed that the multiple relay nodes achieve larger diversity gain than the multiple receive antennas at the destination with the same numbers of antennas. This is because the multiple relay nodes provide not only multiple independent channels between the relay stations and the destination, but also multiple channels between the source and the relay stations. However the multiple antennas at the destination only receive independent copies of the signals transmitted from the relay nodes, with a fixed number of channels between the source and the relay nodes.

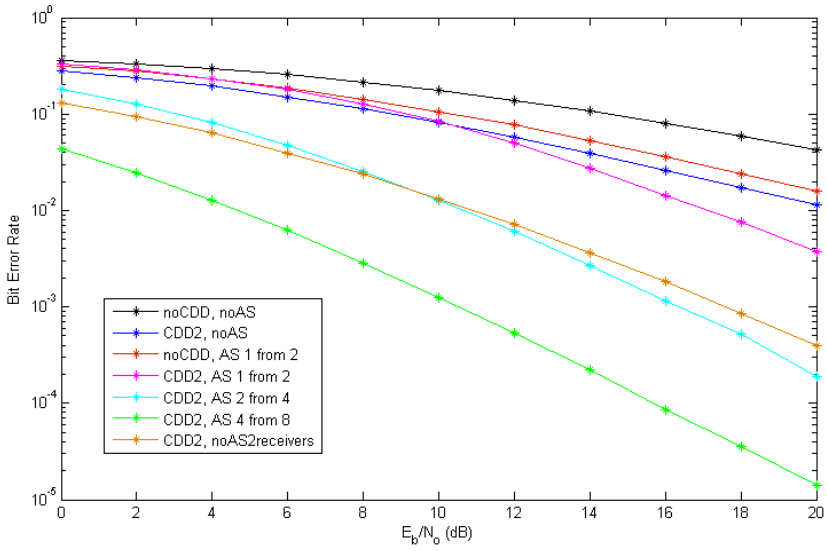

Figure 6.8 Performance of a cooperative relay system with varying receive antenna number at the destination. 2 relays work cooperatively with cyclic delay diversity. The MMP-SNR selection criterion is adopted as the antenna selection rule at the destination. The constraint length of the convolutional code is 7.

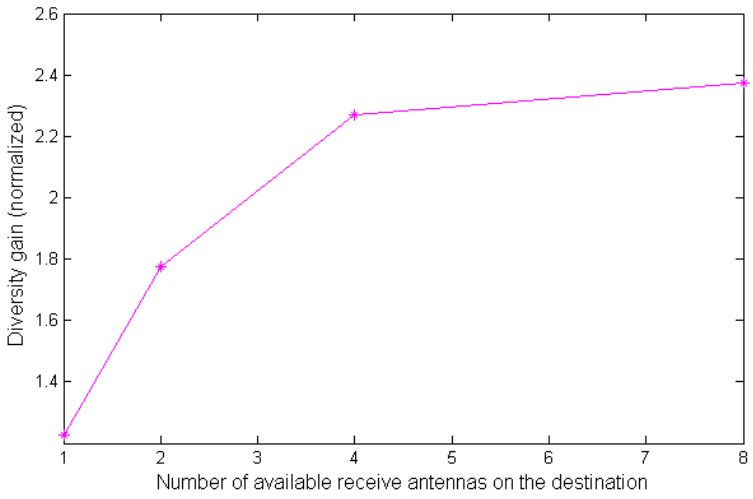

Figure 6.9 Diversity gains of a cooperative relay system with varying receive antenna number at the destination. 2 relays work cooperatively with cyclic delay diversity. The MMP-SNR selection criterion is adopted as the antenna selection rule at the destination. The constraint length of the convolutional code is 7.

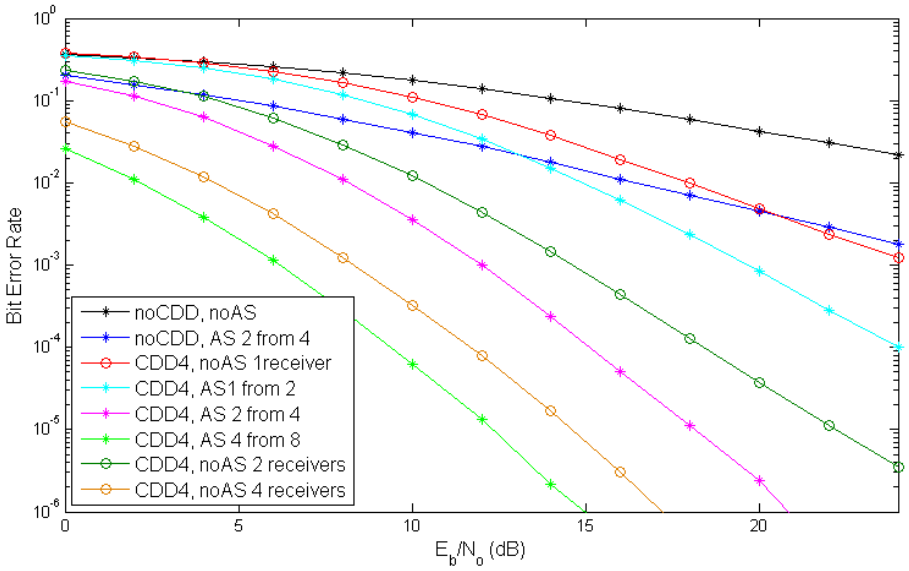

Figure 6.10 Performance of a cooperative relay system with varying receive antenna number at the destination. 4 relays work cooperatively with cyclic delay diversity. The MMP-SNR selection criterion is adopted as the antenna selection rule at the destination. The constraint length of the convolutional code is 7.

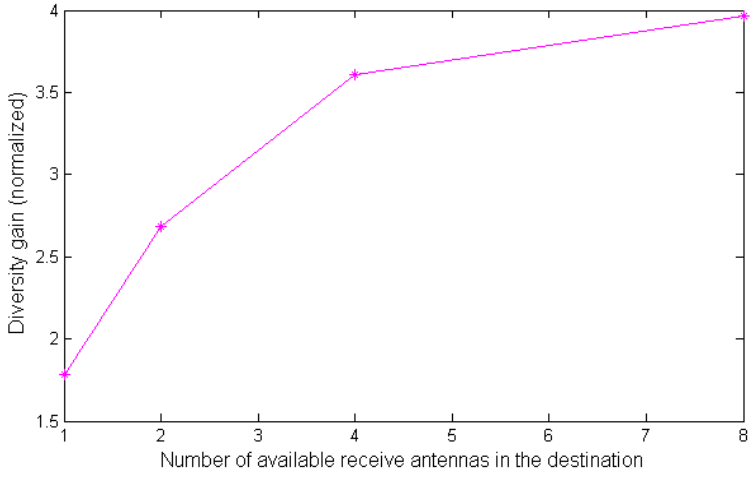

Figure 6.11 Diversity gains of a cooperative relay system with varying receive antenna number at the destination. 4 relays work cooperatively with cyclic delay diversity. The MMP-SNR selection criterion is adopted as the antenna selection rule at the destination. The constraint length of the convolutional code is 7.

Figure 6.10 shows the performance of cooperative relay system with 4 relay nodes. The cooperative relay system with CDD and a receive antenna selection scheme that chooses 2 antennas from 4 achieves a diversity gain of 3.6 compared to a diversity gain of 0.3 for the system without CDD but having the same antenna selection scheme and a diversity gain of 1.9 for the system without antenna selection but having the same CDD scheme. The diversity gain increases when number of the available receive antennas for selection is increased until the total number of the receive antennas is larger than 4, which means the diversity property of the wireless channels is saturated. The normalized diversity gains are given in Figure 6.11.

6.3.3 Comparison

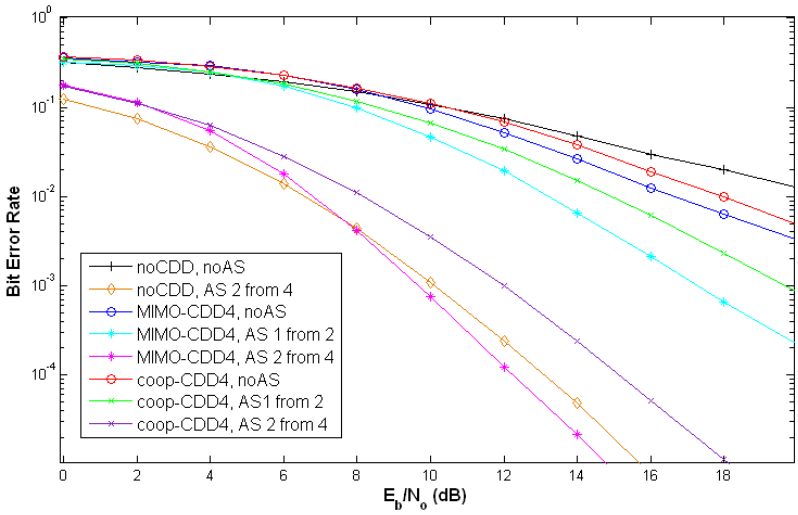

Figure 6.12 Performance comparison of a MIMO relay system and a cooperative relay system with varying receive antenna number at the destination. The MMP-SNR selection criterion is adopted as the antenna selection rule at the destination. The constraint length of the convolutional code is 7.

Figure 6.12 shows a comparison of the performance of a MIMO relay system and a cooperative relay system. The constraint length of the convolutional code is 7. It can be observed that the MIMO relay system with 4 antennas in the relay station performs 1.5 dB better than the cooperative system without antenna selection. Meanwhile, with a receive antenna selection scheme that chooses 1 antenna from 2, the MIMO relay system performance is 2.5dB better than the cooperative relay system. With a receive antenna selection scheme that chooses 2 antennas from 4, the MIMO relay system performance is 3.5dB better than the cooperative relay system.

6.4 Conclusions

This chapter proposes two new non-regenerative relay systems with joint diversity schemes both in the relay station and the destination. In the MIMO relay system cyclic delay diversity is applied on multiple transmit antennas in the relay station. Meanwhile in the cooperative relay system, distributed cyclic delay diversity is employed in separated relay nodes which work cooperatively. Antenna selection is adopted at the destination for both systems with a selection criterion named the maximum minimum post-processing signal to noise ratio selection rule.

From the numerical results, it can be observed that both two relay systems achieve high diversity gains, which depend on the number of the antennas in the relay stations and the number of the available antennas at the destination. These relay systems perform much better than the systems with only one diversity scheme (only cyclic delay diversity in the relay stations or only antenna selection scheme at the destination). Comparing the

simulation results of the MIMO relay system and the cooperative relay system, it is observed that the MIMO relay system achieves better a BER performance compared with the cooperative relay system. This is due to that in the cooperative relay system, the fluctuation feature of the multiple channel transfer functions is amplified by the diversity between the source station and relay nodes. This fluctuation renders an unequal power allocation between the relay nodes which work cooperatively with CDD scheme, and therefore leads to a BER performance loss.

The simulation results also show that when the multiplication of number of the antennas in the relay stations and the number of the available antennas at the destination is larger than 16 (which can be obtained with 4 antennas in the relay station and 4 antennas available at the destination), the diversity gain rarely increases with larger antenna number. This is due to there being significant diversity in the channel to mitigate the fading. In this case, after combination and equalization, the channel is close to an AWGN channel. In addition, the MMP-SNR antenna selection criterion achieves the same diversity gain as if all of the receive antennas are used at the destination. The coding gain depends on the number of the selected antennas for the maximal ratio combining at the destination.

References

[1] N. Laneman, *Cooperative Diversity in Wireless Networks: Algorithms and Architechtures*, Ph.D. dissertation, MIT, Cambridge, MA, Aug. 2002.

[2] R. U. Nabar, H. Bolcskei, and F. W. Kneubuhler, “Fading relay channels: performance limits and space-time signal design,” *IEEE J. Sel. Areas Commun.*, vol.22, no. 6, pp. 1099-1109, Aug. 2004.

[3] J. D. Camp and E. W. Knightly, “The IEEE 802.11s extended service set mesh networking standard,” *Communications Magazine, IEEE*, pp. 120-126, Aug. 2008.

[4] S. Max, Y. Liu and M. Sim, “Tutorial IEEE 802.15.5 - high-rate mesh WPANs”, in *IEEE LMSC Meeting*, Dallas, TX, USA, pp. 27, Nov, 2006.

[5] *IEEE 802.16's Relay Task Group*, http://ieee802.org/16/relay/.

[6] *IEEE 802.20 Mobile Broadband Wireless Access* (MBWA), http://ieee802.org/20/.

[7] C. Akcaba, P. Kuppinger and H. Bolcskei, “Distributed transmit diversity in relay networks,” *IEEE Inform. Theory Workshop (ITW)*, Bergen, Norway, pp. 233-237, Jul. 2007.

[8] A. Osserran, A. Logothetis and S. B. Slimane, “Distributed relay diversity system for OFDM-based networks,” *I. J. Commun., Network and System Science*, no. 3, pp. 207-283, 2008.

[9] S. Wei, D. Goeckel, and M. Valenti, “Asynchronous cooperative diversity,” *IEEE Transactions on Wireless Communications*, vol. 5, no. 6, pp. 1547-1557, June 2006.

[10] S. B. Slimane and A. Osseiran, “Relay communication with delay diversity for future communication systems,” in *Proc. IEEE Veh. Technol. Conf.,* Fall, Montreal, Canada, pp. 1-5, Sep. 2006.

[11] P. Anghel and M. Kaveh, “On the performance of distributed space-time coding systems with one and two non-regenerative relays,” *IEEE Trans. on Wireless Commun.*, Vol. 5, No. 2, pp. 682–692, Mar. 2006.

[12] H. Rong, Z. Zhang and P. Larsson, “Cooperative relaying based on Alamouti diversity under aggregate relay power constraints,” in *Proc. IEEE Veh. Technol. Conf.*, Spring, Melbroune, Australia, pp. 2563-2567, May 2006.

[13] A. Osseiran, A. Logothetis, P. Larsso and S. B. Slimane, “Relay Cyclic Delay Diversity: Modeling and System Performance for Future Wireless System,” *IEEE J. Sel. Areas Commun.*, pp. 25-28, Feb. 2006.

[14] S. B. Slimane, B. Zhou and X. Li, “Delay optimization in cooperative relaying with cyclic delay diversity,” in *Proc. of ICC '08, IEEE Inter. Conf.*, *pp*. 3553-3557, 2008.

[15] T. Unger, A. Klein, “Applying relay stations with multiple antennas in the one- and two-way relay channel,” in *Proc of IEEE 18th International Symposium on Personal, Indoor and Mobile Radio Communications, PIMRC*, pp. 1-5, 2007.

[16] F. Zhang, Y. Zhang, W. Q. Malik, B. Allen and D. J. Edwards, “Optimum receive antenna selection for transmit cyclic delay diversity,” *Commun., 2008. ICC '08. IEEE Int. Conf.*, pp. 3829 – 3833, May 2008.

Chapter 7

Conclusions and Future Work

7.1 Conclusions

Radio signals are corrupted by reflection, diffraction, refraction, scattering, shadowing and attenuation while being transmitted through wireless channels. This corruption, termed fading, makes the wireless communication systems unpredictable and unstable. The demand for high fidelity and high speed (a bit error rate as low as 10^{-8} and a data rate as high as 100Mbps) requires current wireless communication systems to be reliable and robust. In addition, limited by the size, power and cost of the remote unit, the intended systems should be of very low complexity and power consumption. Therefore many techniques have been derived to combat the fading effect and provide a guaranteed transmission quality.

The fading properties of wireless channels were introduced in Chapter 2. Then several statistical models describing the multipath fading channels were presented, which were used for the performance analysis and the system design of the wireless communications system in the following chapters. Two key technologies, MIMO and OFDM were included here as two basic components for the systems constructed in this thesis. OFDM was introduced to combat the multipath fading in broadband communication links, while MIMO had been developed to improve the signal transmission reliability or the data rate. For improving the link reliability, spatial diversity schemes were employed to enhance

the system performance in the perspective of error probability. Cyclic delay diversity was suggested for its low additional complexity, high flexibility and spectrum efficiency as well as the compatibility with many existing standards compared with the orthogonal space time block coding. While antenna selection was proposed to cut down the number of the expensive RF chains and also has the features of high flexibility and compatibility.

In chapter 3, a new exact bit error rate bound for a cyclic delay diversity system combined with OFDM and convolutional coding in multipath Rayleigh fading channels was developed. An approximation method is introduced to reduce the computational complexity. This performance analysis result also can be readily extend to other classes of channel codes and statistical fading channel models. From the numerical results presented in Section 3.5 it can be observed that performance bounds provide a valuable prediction of the BER performance of the CDD system with varying cyclic delay shift. This performance analysis renders a fundamental understanding of the mechanism of CDD systems and is instructive for CDD system design in Chapter 4 and Chapter 5. Compared to the exhaustive simulation or experimental search, this performance analysis saves a significant amount of time and is less computationally complex.

In Chapter 4, a original system with joint cyclic delay diversity in the transmitter and antenna selection scheme in the receiver, named as a TCDD/RAS system, was proposed to provide significant performance improvement with very low additional complexity, high compatibility and no data rate reduction compared to the TOSTBC/RAS (transmit orthogonal space-time coding and receive antenna selection) system. Another new

TCDD-OSTBC/RAS system was also derived to avoid the disadvantages of OSTBC and utilize the high flexibility of CDD to provide a balanced BER performance without sacrificing the complexity and data rate.

Based on the performance analysis bounds generated in Chapter 3, a new receive antenna selection criterion was generated for the TCDD/RAS system. However, this rule demands high computational complexity. Therefore a further new maximum minimum post-processing SNR (MMP-SNR) antenna selection criterion, which is much simpler and faster, was derived for the proposed TCDD/RAS system in flat fading Rayleigh channel. The MMP-SNR rule achieves a better BER performance than the norm selection rule and the capacity criterion with even lower additional complexity. Using the MMP-SNR rule, the TCDD/RAS system achieves a similar diversity order compared to the corresponding transmit orthogonal space-time block coding diversity scheme combined with optimum receive antenna selection of the same number of antennas, but the TCDD/RAS systems requires much lower additional complexity, suffers no data rate loss and offers compatibility with many existing standards. Diversity gain is retained by the antenna selection scheme with the MMP-SNR criterion in the TCDD/RAS system as if all the available receive antennas are used. In addition, with another new selection principle, the MMP-norm criterion, the TCDD-OSTBC/RAS system achieves a BER performance which is better than the TCDD/RAS system and the punctured TOSTBC/RAS system. Even its performance is still slightly inferior to the TOSTBC/RAS system, it suffers no spectral efficiency reduction and is of much lower complexity.

In Chapter 5, the TCDD/RAS was analyzed and estimated by simulation in frequency selective channels. A new selection rule, named maximum group minimum post-processing SNR (MGMP-SNR) selection criterion, was proposed for the receive antenna selection. The optimum selection parameter for the MGMP-SNR criterion was demonstrated to be irrelevant to the channel coding but dependent on the numbers of the antennas. The MGMP-SNR selection rule performs better than the traditional norm selection, the capacity selection rules, and even the principle based on the error probability, with much lower computational complexity.

Chapter 6 proposed two new non-regenerative relay systems with joint diversity schemes both in the relay stations and the destination in order to increase the transmission reliability of the wireless links, thereby to extend the transmission range and increase the information throughput. In the MIMO relay system cyclic delay diversity was applied on multiple transmit antennas in the relay station. Meanwhile in the cooperative relay system, distributed cyclic delay diversity was employed in separated relay nodes which work cooperatively. From the numerical results, it can be observed that both two relay systems achieve high diversity gain which depends on the multiplication of antenna number in relay stations and the number of the available antennas at the destination. These relay systems with joint diversity schemes achieve much better performance gains compared with the systems with single diversity scheme (only cyclic delay diversity in the relay stations or only antenna selection scheme at the destination). The numerical results show that the BER performance of the MIMO relay system is better than the cooperative relay system. This is due to that the fluctuations, which are generated by the multiple channels

between the source station and the relay nodes in the cooperative relay system, cannot be utilized by CDD and even become a burden for the system as they enlarge the differences of the power allocation among different relay nodes. The simulation results also show that when the multiplication of antenna number in the relay stations and the number of the available antennas at the destination is larger than 16, the diversity gain rarely increases with larger antenna numbers. This is due to there being significant diversity in the channel to mitigate the fading. In this case, after combination and equalization, the channel is close to an AWGN channel. The diversity schemes introduced in this thesis are mainly concerned with the channel fading but not the additive white Gaussian noise.

7.2 Future Work

Cyclic delay diversity has already been applied in the 802.11n standard which published in Oct. 2009. And it will be used widely in future wireless mobile, wireless broadband networks, digital audio and video broadcasting networks. It may also be applied in sensor networks as well. Due to the high flexibility of CDD, it can be combined with various other technologies. In this thesis, we consider OFDM as a necessary block which turns the space diversity, which is provided by CDD, to frequency diversity, which can be used by the error correction coding. However, CDD can also be applied in non-OFDM systems, such as the multicarrier-CDMA system introduced in [8], the KR coding system (which has been developed by Riqing Chen in our group) and other frequency spreading coding systems. Similarly, the convolutional codes can be replaced by other error correction codes, such as the Low-density parity-check codes and turbo codes.

Although the performance analysis of cyclic delay diversity system is based on a simple mathematical model with PSK signals or QAM signals modulated by OFDM and coded by convolutional code in a multipath Rayleigh fading channel, the statistical model can be generated to more practical and complicated scenarios. The channel model can be extended to other channel models such as the Nakagami model [1] [2], the Saleh-Valenzuela model [3], the log-normal model [4] and also real channel data. Alternative channel models can be directly introduced to equation (3.10) for the calculation of the expectation with respect to specific channel coefficient distributions. Moreover, the exact performance analysis for convolutional codes or more complex channel codes, such as the turbo codes [5] [6] and other concatenated channel codes [7], which are more commonly used in current wireless communication standards compared to a single channel coding scheme, needs to be developed for future wireless system design.

This thesis proposed a transmit cyclic delay diversity and receive antenna selection scheme. Mathematical performance analysis of CDD is provided here for a thorough understanding of the system mechanism and the optimum system design. The performance gains brought by the diversity schemes are verified by numerical simulation results with a Monte Carlo method. However either the performance analysis or the simulation is conducted based on a number of ideal assumptions and mathematical simplifications. Therefore extensive experimental demonstration has to be implemented for a practical estimation of the diversity gain obtained by the TCDD/RAS system as well as the TCDD/RAS embedded relay systems. The trade-off between complexity and link reliability should be investigated by experiments for the comparison of the TCDD/RAS

system, the TOSTBC/RAS as well as the TCDD-OSTBC/RAS system. Particularly, the performance of the diversity schemes highly depends on the wireless channel conditions as verified in this thesis. The performance of the TCDD/RAS system has to be exploited in variant channel conditions, such as the typical rural area, the typical urban area as well as the typical indoor environment. This estimation can specify the practical utilizations of the TCDD/RAS scheme in different environments.

In addition, relay systems, which are investigated in Chapter 6, are two-hop non-regenerative relay systems where it is assumed that there is no direct link between the source and the destination. However in real cases there may be a weak connection between the source and the destination. Meanwhile, the two-hop transmission model is of low spectrum efficiency and thereby leads to data rate degradation. Modifications should be made for the joint diversity schemes to adjust to the practical environments and guarantee a maximum performance gain with a combination of all received signals from both the source and the relay nodes. Further more, both of the MIMO relay system model and the cooperative relay system model are extreme cases: the MIMO relay system only employs a single relay station while the cooperative relay system only has a single antenna on each relay node. For practical implementation, a combination of these two systems has to be considered to balance the complexity of multiple antennas on the relay stations and the performance gain promised by the cooperative spatial diversity scheme.

A considerable amount of further research can be undertaken from this work. The performance analysis proposed in this thesis can be used as a basis for the cyclic delay

diversity system design and is hoped to be used in other CDD systems. The TCDD/RAS scheme can be applied to numerous other systems due to its high flexibility and compatibility. Experimental work needs to be undertaken to demonstrate the performance of this scheme in a variety of real-world environments.

References

[1] M. Nakagami, "The m-distribution - A general formula of intensity distribution of rapid fading," in *Statisitcal methods in Radio Wave propagation*, W. C. Hoffman, Oxford, UK, Pergamon, pp. 3-36, 1960.

[2] M. D. Yacoub, J. E. V. Bautista and L. G. R. Guedes, "On higher order statistics of the Nakagami-m distribution," *IEEE Transactions on Vehicular Technology*, vol. 48, pp. 790-794, 1999.

[3] A. A. M. Saleh and R. A. Valenzuela, "A statistical model for indoor multipath propagation," *IEEE Journal on Selected Areas in Communications*, vol. JSAC-5, pp. 128-137, Feb. 1987.

[4] H. Suzuki, "A statistical model for urban radio propagation," *IEEE Transactions on Communications*, vol. COM-25, pp. 673-680, 1977.

[5] C. Berrou, A. Glavieux and P. Thitimajshima, "Near Shannon limit error-correcting coding and decoding: Turbo-codes," in *Proc. of the IEEE International Conference on Communications*, vol. 2, Geneva, Switzerland, pp. 1064-1070, May 1993.

[6] C. Berrou and A. Glavieux, "Near optimum error correcting coding and decoding: Turbo-codes," *IEEE Transactions on Commununications*, vol. 44, pp. 1261-1271, 1996.

[7] N. Nyirongo, W. Q. Malik, and D. J. Edwards, “Concatenated RS-convolutional codes for ultrawideband multiband-OFDM,” in *Proc. of the 2006 IEEE International Conference on Ultra-Wideband*, Waltham, MA, USA., pp. 137-142, Sep. 2006.

Appendix A

Performance Analysis for BPSK Signals with Convolutional Coding in AWGN Channels

In this section, a simple performance analysis of a single antenna system without any diversity scheme in AWGN channel is investigated to provide the theory basic for the analysis of the CDD system in multipath fading channel. BPSK signal is assumed to be generated after the convolutional coding. The performance analysis can be produced based on the derivation in [1].

A bit of BPSK signal can be denoted as

$$x = \sqrt{E_c}(2C_l - 1), \tag{A.1}$$

where $C_l = 0$ or 1, is the original information bit and E_c is the transmitted signal energy for each code bit. If we assume an AWGN channel, for convolutional coding, the received signal can be denoted as

$$r_{j,m} = \sqrt{E_c}(2C_{j,m}^{(i)} - 1) + n_{j,m}^{(i)}, \tag{A.2}$$

where $n_{j,m}^{(i)}$ represents the additive Gaussian noise, which has zero mean and variance of $\sigma_n^2 = \frac{1}{2}N_0$, index *i* denotes the *i*th path in a convolutional coding trellis, index j indicates the *j*th branch and the index *m* denotes the *m*th bit in that branch. According to the distribution of $n_{j,m}^{(i)}$, the probability distribution function of the random variable $r_{j,m}$ conditioned on the transmitted signal $x_{j,m}^{(i)} = \sqrt{E_c}(2C_{j,m}^{(i)} - 1)$ is

$$P(r_{j,m}\left|C_{j,m}^{(i)}\right.) = \frac{1}{\sqrt{\pi N_0}} e^{-\frac{[r_{j,m}-\sqrt{E_c}(2C_{j,m}^{(i)}-1)]^2}{N_0}} = \frac{1}{\sqrt{\pi N_0}} e^{-\frac{r_{j,m}^2+E_c(2C_{j,m}^{(i)}-1)^2-2r_{j,m}\sqrt{E_c}(2C_{j,m}^{(i)}-1)}{N_0}}. \quad \text{(A.3)}$$

As $n_{j,m}^{(i)}$ is independent identically distributed (i.i.d.) on each bit, the joint distribution probability function for the signal array of the whole path conditioned on the transmitted sequence $\left\{C_{jm}^{(i)}\right\}$ for the *i*th path is:

$$P(r\left|C^{(i)}\right.) = \prod_{j,m} \frac{1}{\sqrt{\pi N_0}} e^{-\frac{[r_{j,m}-\sqrt{E_c}(2C_{j,m}^{(i)}-1)]^2}{N_0}} = \prod_{j,m} \frac{1}{\sqrt{\pi N_0}} e^{-\frac{r_{j,m}^2+E_c(2C_{j,m}^{(i)}-1)^2-2r_{j,m}\sqrt{E_c}(2C_{j,m}^{(i)}-1)}{N_0}}. \quad \text{(A.4)}$$

In order to simplify the calculation, a metric can be defined for the joint probability of the *i*th path through the coding trellis [1]

$$\mu^{(i)} = \log P(r\left|C^{(i)}\right.). \quad \text{(A.5)}$$

In this case, if we neglect the terms that are common to all paths, the metric for the *i*th path can be expressed as

$$\mu^{(i)} = \sum_j \sum_m r_{j,m}(2C_{j,m}^2 - 1). \quad \text{(A.6)}$$

If we assume the *0*th path is the original path for the transmitted signal, and *e*th path is the error path that the Viterbi decoder considered. Then the probability of erroneously decoding the *e*th path as the transmitted path, which is identical as the pairwise error probability for the first bit on that signal path, is

$$\begin{aligned} P_2(d) &= P(\mu^{(e)} \geq \mu^{(0)}) \\ &= P(\mu^{(e)} - \mu^{(0)} \geq 0) \\ &= P\left[\sum_j \sum_m r_{j,m}(C^e_{j,m} - C^0_{j,m}) \geq 0\right] \end{aligned} \quad . \tag{A.7}$$

As path *i=0* and path *i=e* are identical expect *d* positions, the equation above can be represented in a simpler form:

$$P_2(d) = P\left[\sum_{l=1}^{d} r_l(C^e_l - C^0_l) \geq 0\right]. \tag{A.8}$$

Substituting (A.2) into (A.8), the error probability can be denoted as

$$P_2(d) = P\left\{\sum_{l=1}^{d}\left[\sqrt{E_c}(2C^0_l - 1)(C^e_l - C^0_l) + n_l(C^e_l - C^0_l)\right] \geq 0\right\}. \tag{A.9}$$

Because n_l is a random variable of Gaussian distribution with 0 mean, $n_l\left(C^e_l - C^0_l\right)$ has the same distribution as n_l. Therefore it can be substituted directly with n_l. (A.9) can be expressed as

$$P_2(d) = P\left\{\sum_{l=1}^{d}\left[\sqrt{E_c}(2C^0_l - 1)(C^e_l - C^0_l) + n_l\right] \geq 0\right\}. \tag{A.10}$$

As BPSK signals are transmitted here, $C_l = 0$ or 1, we can calculate (A.10) as following.

a. If $C^0_l = 0$, then $C^e_l = 1$,

$(2C^0_l - 1)(C^e_l - C^0_l) = (-1)\times 1 = -1$

b. If $C^0_l = 1$, then $C^e_l = 0$

$(2C^0_l - 1)(C^e_l - C^0_l) = 1\times(-1) = -1$

Therefore whether $C_l = 0$ or 1, the pairwise error probability can be written as

$$\begin{aligned} P_2(d) &= P\left[\sum_{l=1}^{d}\left(-\sqrt{E_c}+n_l\right)\geq 0\right] \\ &= P\left[\sum_{l=1}^{d} y_l \geq 0\right] \\ &= P\left[y \geq 0\right] \end{aligned} \quad . \tag{A.11}$$

As $\{y_l\}$ are i.i.d Gaussian distributed with mean $-\sqrt{E_c}$ and variance $\frac{1}{2}N_0$, y are Gaussian distributed with mean $-d\sqrt{E_c}$ and variance $\frac{1}{2}dN_0$. Therefore the probability distribution function for y can be denoted as

$$P(y) = \frac{1}{\sqrt{\pi d N_0}} \mathrm{e}^{-\frac{[y-d\sqrt{E_c})]^2}{dN_0}} . \tag{A.12}$$

Therefore the error probability of the pairwise comparison of these two paths which differ in d bits is

$$\begin{aligned} P_2(d) &= \int_0^{\infty} \frac{1}{\sqrt{\pi d N_0}} \mathrm{e}^{-\frac{[y-d\sqrt{E_c})]^2}{dN_0}} dy \\ &= Q\left(\sqrt{\frac{2E_c}{N_0}d}\right) \\ &= Q\left(2\gamma_b R_c d\right) \end{aligned} \quad . \tag{A.13}$$

where $\gamma_b = E_b / N_0$ is the received signal energy per bit to noise ratio, R_c is the code rate of the convolutional coding and the Q-function is

$$Q(x) = \frac{1}{\sqrt{2\pi}} \int_x^{\infty} e^{-\frac{x^2}{2}} dx . \tag{A.14}$$

As derived in [1], the bit error probability for convolutionally coded signals can be denoted as

$$\begin{aligned} P_b &< \sum_{d=d_{free}}^{\infty} \beta_d P_2(d) \\ &< \sum_{d=d_{free}}^{\infty} \beta_d Q\left(\sqrt{2\gamma_b R_c d}\right) \end{aligned} . \qquad \text{(A.15)}$$

where d_{free} is the free distance of the convolutional trellis code and β_d weight of each $P_2(d)$. Here β_d is the number of paths which differ with the correct path on *d* positions.

This performance analysis of a single antenna system without any diversity scheme in AWGN channel is basic for the analysis of the CDD system in multipath fading channels.

Reference

[1] J. G. Proakis, *Digital Communications* , McGraw-Hill, 4th Edition, 2000.

Appendix B

Pairwise Error Probability for 16QAM Signals in AWGN Channels

Assume that the received signal for a simple 16QAM system in AWGN channel can be presented as

$$R = S + n \tag{B.1}$$

where S denotes the signal transmitted, while n is the additive Gaussian noise and R denotes the received signal.

For a typical 16QAM scheme, the corresponding codewords are shown in Figure B.1:

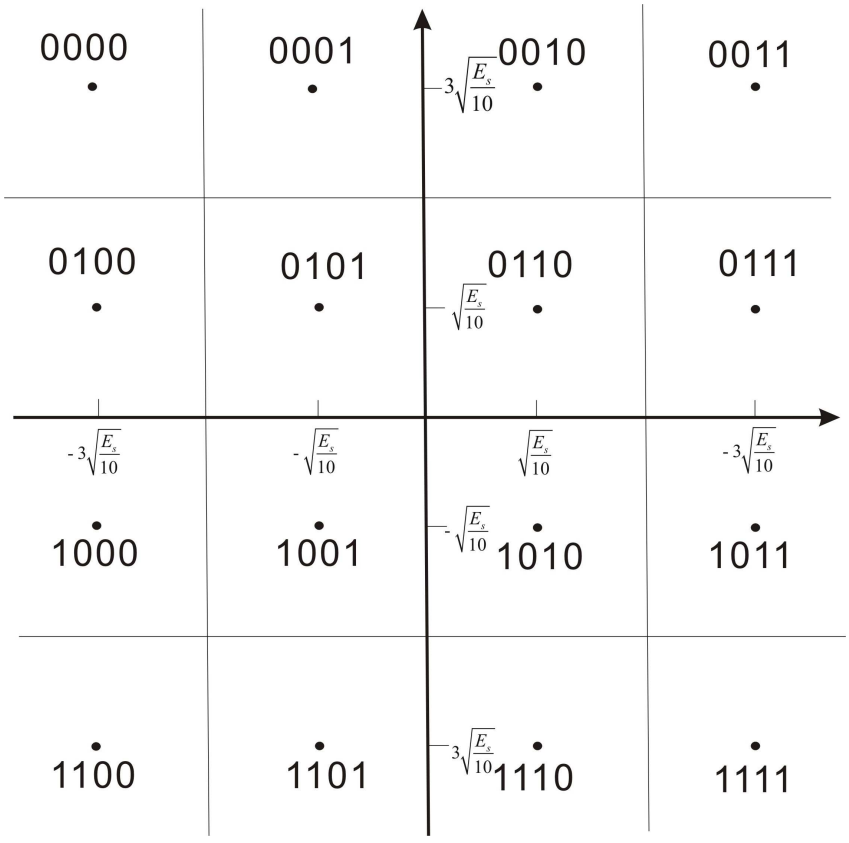

Figure B.1 16QAM codeword constellation

As described in Section 5.3.1, there are three cases in the constellation. One in the corner, such as S_0; one in the middle, such as S_5; one for the rest of the symbols, such as S_1. Symbols in one case have the same error probability expression provided by the symmetric characteristics of the four quadrants in the constellation. Meanwhile the pairwise error probability for different cases should be calculated differently.

According to Section 5.3.1, for the first case, assuming S_0 is transmitted, the probability that S_0 is detected correctly can be written as

$$P_2\left(S_0|S_0\right) = p\left(real\left(R\right) \le -2\sqrt{\frac{E_s}{10}}|S_0\right) p\left(imag\left(R\right) > 2\sqrt{\frac{E_s}{10}}\right), \tag{B.2}$$

where $real\left(\bullet\right)$ denotes the operation of taking the real part of a complex number and $imag\left(\bullet\right)$ denotes taking the imaginary part. As the noise is Gaussian distributed with zero mean and a variance of $\frac{N_0}{2}$. Therefore, the real part of *R* obeys the following distribution function:

$$p\left(real\left(R\right)|S_0\right) = \frac{1}{\sqrt{\pi N_0}} e^{-\frac{\left(real(R)+3\sqrt{\frac{E_s}{10}}\right)}{N_0}}. \tag{B.3}$$

While the imaginary part of *R* follows the distribution function:

$$p\left(imag\left(R\right)|S_0\right) = \frac{1}{\sqrt{\pi N_0}} e^{-\frac{\left(imag(R)-3\sqrt{\frac{E_s}{10}}\right)}{N_0}}. \tag{B.4}$$

Therefore, the probability that S_0 is detected correctly (B.2) can be represented as

$$P_2\left(S_0\middle|S_0\right) = \frac{1}{\sqrt{\pi N_0}}\int_{-\infty}^{-2\sqrt{\frac{E_s}{10}}} e^{-\frac{\left(r+3\sqrt{\frac{E_s}{10}}\right)}{N_0}} dr \times \frac{1}{\sqrt{\pi N_0}}\int_{2\sqrt{\frac{E_s}{10}}}^{+\infty} e^{-\frac{\left(I+3\sqrt{\frac{E_s}{10}}\right)}{N_0}} dI \quad . \quad \text{(B.5)}$$

$$= \left(1-\frac{1}{2}erfc\left(\sqrt{\frac{E_s}{10N_0}}\right)\right)^2$$

Meanwhile, the probability that S_1 is erroneously detected can be written as

$$P_2\left(S_1\middle|S_0\right) = p\left(real\left(R\right)\le -2\sqrt{\frac{E_s}{10}}\middle|S_0\right)p\left(0<imag\left(R\right)\le 2\sqrt{\frac{E_s}{10}}\middle|S_0\right)$$

$$= \left(1-\frac{1}{2}erfc\left(\sqrt{\frac{E_s}{10N_0}}\right)\right)\left(\frac{1}{2}erfc\left(\sqrt{\frac{E_s}{10N_0}}\right)-\frac{1}{2}erfc\left(3\sqrt{\frac{E_s}{10N_0}}\right)\right) \quad . \quad \text{(B.6)}$$

Therefore the pairwise probability that S_y is detected while S_x was transmitted can be presented in the following table:

Assuming S_0 is transmitted:

S_y	$P\left(S_y\middle\|S_0\right)$
S_0	$\left(1-\frac{1}{2}erfc\left(\sqrt{\frac{E_s}{10N_0}}\right)\right)^2$
S_1	$\left(1-\frac{1}{2}erfc\left(\sqrt{\frac{E_s}{10N_0}}\right)\right)\left(\frac{1}{2}erfc\left(\sqrt{\frac{E_s}{10N_0}}\right)-\frac{1}{2}erfc\left(3\sqrt{\frac{E_s}{10N_0}}\right)\right)$
S_2	$\left(1-\frac{1}{2}erfc\left(\sqrt{\frac{E_s}{10N_0}}\right)\right)\left(\frac{1}{2}erfc\left(3\sqrt{\frac{E_s}{10N_0}}\right)-\frac{1}{2}erfc\left(5\sqrt{\frac{E_s}{10N_0}}\right)\right)$

S_3	$\left(1-\frac{1}{2}erfc\left(\sqrt{\frac{E_s}{10N_0}}\right)\right)\frac{1}{2}erfc\left(5\sqrt{\frac{E_s}{10N_0}}\right)$
S_4	$\left(\frac{1}{2}erfc\left(\sqrt{\frac{E_s}{10N_0}}\right)-\frac{1}{2}erfc\left(3\sqrt{\frac{E_s}{10N_0}}\right)\right)\left(1-\frac{1}{2}erfc\left(\sqrt{\frac{E_s}{10N_0}}\right)\right)$
S_5	$\left(\frac{1}{2}erfc\left(\sqrt{\frac{E_s}{10N_0}}\right)-\frac{1}{2}erfc\left(3\sqrt{\frac{E_s}{10N_0}}\right)\right)^2$
S_6	$\left(\frac{1}{2}erfc\left(\sqrt{\frac{E_s}{10N_0}}\right)-\frac{1}{2}erfc\left(3\sqrt{\frac{E_s}{10N_0}}\right)\right)\left(\frac{1}{2}erfc\left(3\sqrt{\frac{E_s}{10N_0}}\right)-\frac{1}{2}erfc\left(5\sqrt{\frac{E_s}{10N_0}}\right)\right)$
S_7	$\left(\frac{1}{2}erfc\left(\sqrt{\frac{E_s}{10N_0}}\right)-\frac{1}{2}erfc\left(3\sqrt{\frac{E_s}{10N_0}}\right)\right)\frac{1}{2}erfc\left(5\sqrt{\frac{E_s}{10N_0}}\right)$
S_8	$\left(\frac{1}{2}erfc\left(3\sqrt{\frac{E_s}{10N_0}}\right)-\frac{1}{2}erfc\left(5\sqrt{\frac{E_s}{10N_0}}\right)\right)\left(1-\frac{1}{2}erfc\left(\sqrt{\frac{E_s}{10N_0}}\right)\right)$
S_9	$\left(\frac{1}{2}erfc\left(3\sqrt{\frac{E_s}{10N_0}}\right)-\frac{1}{2}erfc\left(5\sqrt{\frac{E_s}{10N_0}}\right)\right)\left(\frac{1}{2}erfc\left(\sqrt{\frac{E_s}{10N_0}}\right)-\frac{1}{2}erfc\left(3\sqrt{\frac{E_s}{10N_0}}\right)\right)$
S_{10}	$\left(\frac{1}{2}erfc\left(3\sqrt{\frac{E_s}{10N_0}}\right)-\frac{1}{2}erfc\left(5\sqrt{\frac{E_s}{10N_0}}\right)\right)^2$
S_{11}	$\left(\frac{1}{2}erfc\left(3\sqrt{\frac{E_s}{10N_0}}\right)-\frac{1}{2}erfc\left(5\sqrt{\frac{E_s}{10N_0}}\right)\right)\frac{1}{2}erfc\left(5\sqrt{\frac{E_s}{10N_0}}\right)$
S_{12}	$\frac{1}{2}erfc\left(5\sqrt{\frac{E_s}{10N_0}}\right)\left(1-\frac{1}{2}erfc\left(\sqrt{\frac{E_s}{10N_0}}\right)\right)$
S_{13}	$\frac{1}{2}erfc\left(5\sqrt{\frac{E_s}{10N_0}}\right)\left(\frac{1}{2}erfc\left(\sqrt{\frac{E_s}{10N_0}}\right)-\frac{1}{2}erfc\left(3\sqrt{\frac{E_s}{10N_0}}\right)\right)$

S_{14}	$\frac{1}{2}erfc\left(5\sqrt{\frac{E_s}{10N_0}}\right)\left(\frac{1}{2}erfc\left(3\sqrt{\frac{E_s}{10N_0}}\right)-\frac{1}{2}erfc\left(5\sqrt{\frac{E_s}{10N_0}}\right)\right)$
S_{15}	$\left[\frac{1}{2}erfc\left(5\sqrt{\frac{E_s}{10N_0}}\right)\right]^2$

Assuming S_5 is transmitted:

S_y	$P\left(S_y \middle\| S_5\right)$
S_0	$\left(\frac{1}{2}erfc\left(\sqrt{\frac{E_s}{10N_0}}\right)\right)^2$
S_1	$\frac{1}{2}erfc\left(\sqrt{\frac{E_s}{10N_0}}\right)\left(1-erfc\left(\sqrt{\frac{E_s}{10N_0}}\right)\right)$
S_2	$\frac{1}{2}erfc\left(\sqrt{\frac{E_s}{10N_0}}\right)\left(\frac{1}{2}erfc\left(\sqrt{\frac{E_s}{10N_0}}\right)-\frac{1}{2}erfc\left(3\sqrt{\frac{E_s}{10N_0}}\right)\right)$
S_3	$\frac{1}{2}erfc\left(\sqrt{\frac{E_s}{10N_0}}\right)\frac{1}{2}erfc\left(3\sqrt{\frac{E_s}{10N_0}}\right)$
S_4	$\left(1-\frac{1}{2}erfc\left(\sqrt{\frac{E_s}{10N_0}}\right)\right)\frac{1}{2}erfc\left(\sqrt{\frac{E_s}{10N_0}}\right)$
S_5	$\left(1-\frac{1}{2}erfc\left(\sqrt{\frac{E_s}{10N_0}}\right)\right)^2$
S_6	$\left(1-erfc\left(\sqrt{\frac{E_s}{10N_0}}\right)\right)\left(\frac{1}{2}erfc\left(\sqrt{\frac{E_s}{10N_0}}\right)-\frac{1}{2}erfc\left(3\sqrt{\frac{E_s}{10N_0}}\right)\right)$
S_7	$\left(1-erfc\left(\sqrt{\frac{E_s}{10N_0}}\right)\right)\frac{1}{2}erfc\left(3\sqrt{\frac{E_s}{10N_0}}\right)$

S_8	$\left(\frac{1}{2}erfc\left(\sqrt{\frac{E_s}{10N_0}}\right)-\frac{1}{2}erfc\left(3\sqrt{\frac{E_s}{10N_0}}\right)\right)\frac{1}{2}erfc\left(\sqrt{\frac{E_s}{10N_0}}\right)$
S_9	$\left(\frac{1}{2}erfc\left(\sqrt{\frac{E_s}{10N_0}}\right)-\frac{1}{2}erfc\left(3\sqrt{\frac{E_s}{10N_0}}\right)\right)\left(1-erfc\left(\sqrt{\frac{E_s}{10N_0}}\right)\right)$
S_{10}	$\left(\frac{1}{2}erfc\left(\sqrt{\frac{E_s}{10N_0}}\right)-\frac{1}{2}erfc\left(3\sqrt{\frac{E_s}{10N_0}}\right)\right)^2$
S_{11}	$\left(\frac{1}{2}erfc\left(\sqrt{\frac{E_s}{10N_0}}\right)-\frac{1}{2}erfc\left(3\sqrt{\frac{E_s}{10N_0}}\right)\right)\frac{1}{2}erfc\left(3\sqrt{\frac{E_s}{10N_0}}\right)$
S_{12}	$\frac{1}{2}erfc\left(3\sqrt{\frac{E_s}{10N_0}}\right)\frac{1}{2}erfc\left(\sqrt{\frac{E_s}{10N_0}}\right)$
S_{13}	$\frac{1}{2}erfc\left(3\sqrt{\frac{E_s}{10N_0}}\right)\left(1-erfc\left(\sqrt{\frac{E_s}{10N_0}}\right)\right)$
S_{14}	$\frac{1}{2}erfc\left(3\sqrt{\frac{E_s}{10N_0}}\right)\left(\frac{1}{2}erfc\left(\sqrt{\frac{E_s}{10N_0}}\right)-\frac{1}{2}erfc\left(3\sqrt{\frac{E_s}{10N_0}}\right)\right)$
S_{15}	$\frac{1}{2}erfc\left(3\sqrt{\frac{E_s}{10N_0}}\right)^2$

Assuming S_1 is transmitted:

S_y	$P\left(S_y \middle\| S_5\right)$
S_0	$\left(1-\frac{1}{2}erfc\left(\sqrt{\frac{E_s}{10N_0}}\right)\right)\frac{1}{2}erfc\left(\sqrt{\frac{E_s}{10N_0}}\right)$
S_1	$\left(1-\frac{1}{2}erfc\left(\sqrt{\frac{E_s}{10N_0}}\right)\right)\left(1-erfc\left(\sqrt{\frac{E_s}{10N_0}}\right)\right)$

S_2	$\left(1-\frac{1}{2}erfc\left(\sqrt{\frac{E_s}{10N_0}}\right)\right)\left(\frac{1}{2}erfc\left(\sqrt{\frac{E_s}{10N_0}}\right)-\frac{1}{2}erfc\left(3\sqrt{\frac{E_s}{10N_0}}\right)\right)$
S_3	$\left(1-\frac{1}{2}erfc\left(\sqrt{\frac{E_s}{10N_0}}\right)\right)\frac{1}{2}erfc\left(3\sqrt{\frac{E_s}{10N_0}}\right)$
S_4	$\left(\frac{1}{2}erfc\left(\sqrt{\frac{E_s}{10N_0}}\right)-\frac{1}{2}erfc\left(3\sqrt{\frac{E_s}{10N_0}}\right)\right)\frac{1}{2}erfc\left(\sqrt{\frac{E_s}{10N_0}}\right)$
S_5	$\left(\frac{1}{2}erfc\left(\sqrt{\frac{E_s}{10N_0}}\right)-\frac{1}{2}erfc\left(3\sqrt{\frac{E_s}{10N_0}}\right)\right)\left(1-erfc\left(\sqrt{\frac{E_s}{10N_0}}\right)\right)$
S_6	$\left(\frac{1}{2}erfc\left(\sqrt{\frac{E_s}{10N_0}}\right)-\frac{1}{2}erfc\left(3\sqrt{\frac{E_s}{10N_0}}\right)\right)^2$
S_7	$\left(\frac{1}{2}erfc\left(\sqrt{\frac{E_s}{10N_0}}\right)-\frac{1}{2}erfc\left(3\sqrt{\frac{E_s}{10N_0}}\right)\right)\frac{1}{2}erfc\left(3\sqrt{\frac{E_s}{10N_0}}\right)$
S_8	$\left(\frac{1}{2}erfc\left(3\sqrt{\frac{E_s}{10N_0}}\right)-\frac{1}{2}erfc\left(5\sqrt{\frac{E_s}{10N_0}}\right)\right)\frac{1}{2}erfc\left(\sqrt{\frac{E_s}{10N_0}}\right)$
S_9	$\left(\frac{1}{2}erfc\left(3\sqrt{\frac{E_s}{10N_0}}\right)-\frac{1}{2}erfc\left(5\sqrt{\frac{E_s}{10N_0}}\right)\right)\left(1-erfc\left(\sqrt{\frac{E_s}{10N_0}}\right)\right)$
S_{10}	$\left(\frac{1}{2}erfc\left(3\sqrt{\frac{E_s}{10N_0}}\right)-\frac{1}{2}erfc\left(5\sqrt{\frac{E_s}{10N_0}}\right)\right)\left(\frac{1}{2}erfc\left(\sqrt{\frac{E_s}{10N_0}}\right)-\frac{1}{2}erfc\left(3\sqrt{\frac{E_s}{10N_0}}\right)\right)$
S_{11}	$\left(\frac{1}{2}erfc\left(3\sqrt{\frac{E_s}{10N_0}}\right)-\frac{1}{2}erfc\left(5\sqrt{\frac{E_s}{10N_0}}\right)\right)\frac{1}{2}erfc\left(3\sqrt{\frac{E_s}{10N_0}}\right)$
S_{12}	$\frac{1}{2}erfc\left(5\sqrt{\frac{E_s}{10N_0}}\right)\frac{1}{2}erfc\left(\sqrt{\frac{E_s}{10N_0}}\right)$

S_{13}	$\frac{1}{2}erfc\left(5\sqrt{\frac{E_s}{10N_0}}\right)\left(1-erfc\left(\sqrt{\frac{E_s}{10N_0}}\right)\right)$
S_{14}	$\frac{1}{2}erfc\left(5\sqrt{\frac{E_s}{10N_0}}\right)\left(\frac{1}{2}erfc\left(\sqrt{\frac{E_s}{10N_0}}\right)-\frac{1}{2}erfc\left(3\sqrt{\frac{E_s}{10N_0}}\right)\right)$
S_{15}	$\frac{1}{2}erfc\left(5\sqrt{\frac{E_s}{10N_0}}\right)\frac{1}{2}erfc\left(3\sqrt{\frac{E_s}{10N_0}}\right)$

Table B.1 Pairwise error probability for 16QAM modulated signals

Assuming all the symbols are distributed with equal likelihood, therefore the pairwise error probability of 16QAM can be denoted as

$$P_2 = \frac{1}{16}\left(4\times P\left(S_e\left|S_0\right.\right)+4\times P\left(S_e\left|S_5\right.\right)+8\times P\left(S_e\left|S_1\right.\right)\right) \tag{B.7}$$

where S_e is the probably erroneously detected symbol.